



**University of Venda**

**Formulation and characterisation of *banana rachis*  
derived composites and its application in adsorption of  
dyes**

**A thesis submitted in fulfilment of the requirement for the degree of**

**MASTER OF SCIENCE IN BIOCHEMISTRY**

**SCHOOL OF MATHEMATICAL AND NATURAL SCIENCES**

**UNIVERSITY OF VENDA**

**by**

**PHUNGO MATODZI**

**11584858**

**Supervisor: Dr B van Driessel**

**Co - Supervisor: Dr MA Legodi**

**March 2020**

## Abstract

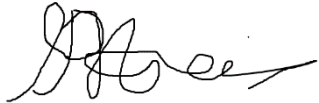
Adsorption of Coomassie brilliant blue (CBB G-250) from aqueous solutions on the adsorbents chitosan, alpha cellulose, banana rachis fibre, banana rachis fibre/chitosan composite, alpha cellulose/chitosan composite, and activated carbon were studied experimentally. The removal efficiency of the adsorbents was also tested using a concentration of dye from 50 to 800 mg/l. The absorbed amount increases as the adsorbents mass increases (1, 1.5, 2, 2.5, and 3 g/l) from alpha cellulose (9.4 to 50%), chitosan (15.6 to 56.3%), banana rachis fibre (21.9 to 65.5%), alpha cellulose/chitosan composite (6.3% to 84.4%), activated carbon (31.6 to 84.4%), and banana rachis fibre/chitosan composite (37.5% to 93.8%), for the initial concentration (50 mg/l) after 80 minutes. The absorbed amount increases as the adsorbents mass increases from banana rachis fibre (6.6 to 19.5%), alpha cellulose (5.3 to 28.1%), chitosan (21.0 to 33.7%), alpha cellulose/chitosan composite (38.2 to 44.8%), banana rachis fibre/chitosan composite (45.3 to 51.2%), and activated carbon (66.8 to 79.8%), for the high concentration (800 mg/l) after 80 minutes. Two isotherm models namely Freundlich and Langmuir models were tested. The equilibrium data for alpha cellulose/chitosan composite, activated carbon, alpha cellulose, banana rachis fibre/chitosan composite, banana rachis fibre, and chitosan fitted well to the Langmuir model, correlation coefficient  $R^2$  (0.9999, 0.9984, 0.998, 0.994, 0.9661, and 0.9474 respectively) were bigger than the corresponding Freundlich correlation coefficient  $R^2$ . Composites as well as components of composites were further characterized by x-ray diffraction (XRD). The (%)  $Cl_{XRD}$  of chitosan, alpha cellulose/chitosan composite, alpha cellulose, banana rachis fibre/chitosan composite, and banana rachis fibre readings values in this study ranges from 94.28%, 91.54%, 82.75%, 60.77%, and 37.69%, respectively. The present study results suggest the possible use of a waste such as banana rachis fibre waste combined with chitosan for the development of a new cheap and efficient adsorbent that could be used in dyes removal from wastewater. Adsorption of Coomassie brilliant blue (CBB G-250) from aqueous solutions was absorbed better by banana rachis fibre/chitosan composite, followed by activated carbon and then the banana rachis fibre.

**Key words:** Adsorption, Banana rachis fibre, composites, ATR-IR, X-ray diffraction, Isotherm, Coomassie Brilliant Blue.

## Declaration

I, Matodzi Phungo, declare that this thesis submitted to the University of Venda for a Master of Science degree in Biochemistry under the department of Biochemistry in the School of Mathematics and Natural Sciences is my own unaided work, with the exception of citations, and that this work has not been submitted to any other institution for award of any degree.

Signature:



Date: 08/09/2020

## Dedication

This dissertation is dedicated to my mom (Maureen Sarah Munengiwa Phungo), dad (Solomon Namadzavho Phungo), sisters (Rolivhuwa and Zwivhuya Phungo) and brothers (Fhumulani, Rendani, Rotondwa, Zwonaka, Unarine, and Hakundwi Phungo).

## Acknowledgements

It was a blessing doing this research. I would like to thank God for his grace that sustained me throughout my research, all glory to Him. I would like to thank Dr B van Driessel my supervisor and Dr MA Legodi my co – supervisor for helping me with the research project.

I would also like to thank my supervisor for his support to my research work. I would like to thank the University of Venda for providing financial support through the work study program and the RPC money. And I give thanks to my family and friends for their support and love.

## Table of Contents

<b>Abstract.....</b>	<b>i</b>
<b>Declaration.....</b>	<b>ii</b>
<b>Dedication.....</b>	<b>iii</b>
<b>Acknowledgements.....</b>	<b>iv</b>
<b>List of Symbols and Abbreviations .....</b>	<b>vii-viii</b>
<b>List of Figures.....</b>	<b>ix-xii</b>
<b>List of Tables.....</b>	<b>xiii-xiv</b>
<b>General introduction.....</b>	<b>xv</b>
<b>CHAPTER 1.....</b>	<b>1-13</b>
<b>1. Introduction.....</b>	<b>1-13</b>
<b>1.1. National Water Act of South Africa.....</b>	<b>1</b>
<b>1.2. Environmental problems caused by dyes.....</b>	<b>1-2</b>
<b>1.3. Formulation of the different composites with graphene.....</b>	<b>2</b>
<b>1.4. Coomassie brilliant blue G-250 dye.....</b>	<b>2-3</b>
<b>1.5. Banana plants and rachis banana fibre.....</b>	<b>4</b>
<b>1.6. Lignocellulose.....</b>	<b>4</b>
<b>1.7. Cellulose.....</b>	<b>5</b>
<b>1.8. Holocellulose.....</b>	<b>6-7</b>
<b>1.9. Chitosan.....</b>	<b>7-9</b>
<b>1.10. Attenuated total reflection infra-red spectromerty.....</b>	<b>9</b>
<b>1.11. Isotherm studies.....</b>	<b>9</b>
<b>1.12. Activated carbon, agricultural waste and bio-sorbents.....</b>	<b>10</b>
<b>1.13. Hypothesis.....</b>	<b>10</b>
<b>1.14. Aim.....</b>	<b>10-11</b>
<b>1.15. Rationale for study.....</b>	<b>11-12</b>
<b>1.16. Conclusion.....</b>	<b>13</b>

<b>CHAPTER 2.....</b>	<b>14-26</b>
<b>2. Characterisation of banana rachis fibres by chemical analysis.....</b>	<b>14</b>
2.1. Chapter summary.....	14
2.2. Introduction.....	14-15
2.3. Materials and Methods.....	15-17
2.4. Results and Discussions.....	17-25
2.5. Conclusion.....	26
<b>CHAPTER 3.....</b>	<b>27-54</b>
<b>3. Equilibrium and isotherm studies for different adsorbents (banana rachis fibre, chitosan, alpha cellulose, and activated carbon).....</b>	<b>27</b>
3.1. Chapter summary.....	27
3.2. Introduction.....	28
3.3. Materials and Methods.....	28-31
3.4. Results and Discussions.....	31-52
3.5. Conclusion.....	53-54
<b>CHAPTER 4.....</b>	<b>55-113</b>
<b>4. Formulation and chemical analysis of composites (banana rachis fibre/chitosan composite and alpha cellulose/chitosan composite).....</b>	<b>55</b>
4.1. Chapter summary.....	55
4.2. Introduction.....	56-57
4.3. Materials and Methods.....	57-63
4.4. Results and Discussions.....	64-111
4.5. Conclusion.....	112-113
<b>CHAPTER 5.....</b>	<b>114-116</b>
<b>Conclusion.....</b>	<b>114-116</b>
<b>Reference.....</b>	<b>117-133</b>
<b>Appendix.....</b>	<b>134-158</b>

## List of Symbols and Abbreviations

<b><u>Abbreviations of units</u></b>	<b><u>Symbol Interpretation</u></b>
<b>°C</b>	Degree Celsius
<b>%</b>	Percent
<b>ml</b>	Milliliter
<b>rpm</b>	Revolutions per minute
<b>mg/l</b>	Milligram per gram
<b>g</b>	Gram
<b>nm</b>	Nanometer ( $10^{-9}$ )
<b>hrs</b>	Hours
<b>mg/g</b>	Milligrams per gram
<b>°F</b>	Fahrenheit
<b>m<sup>-1</sup></b>	Per meter
<b>cm<sup>-1</sup></b>	Per centimetre
<b>pH</b>	Potential of hydrogen
<b>β</b>	Beta
<b>α</b>	Alpha
<b>V/W</b>	Volume per weight
<b>C<sub>0</sub></b>	Initial dye concentration
<b>C<sub>e</sub></b>	Equilibrium dye concentration
<b>q<sub>e</sub></b>	Capacity of sorbent
<b>R<sup>2</sup></b>	Correlation Coefficient
<b>v/v</b>	Volume per Volume
<b>w/w</b>	Mass per Mass
<b>mg</b>	Milligram
<b>Min</b>	Minutes
<b>l/g</b>	Litre per gram
<b>A<sub>i</sub></b>	Initial absorbance of the dye
<b>A<sub>t</sub></b>	Absorbance of the dye at any interval
<b>-OH</b>	Hydroxyl
<b>C=O</b>	Carbonyl
<b>CO<sub>2</sub>H</b>	Carboxyl
<b>kV</b>	Kilovolt
<b>mA</b>	Milliampere
<b>Ni</b>	Nickel



<b>CuK</b>	Copper Potassium
<b>Å</b>	Angstrom
<b>NaOH</b>	Sodium Hydroxide
<b>N</b>	Moles
<b>Na<sub>2</sub>CO<sub>3</sub></b>	Sodium Carbonate
<b>HCl</b>	Hydrochloric Acid
<b>µg</b>	Microgram
<b>mm</b>	Millimetre
<b>CBB G-250</b>	Coomassie Brilliant Blue G-250
<b>CBB</b>	Coomassie Brilliant Blue
<b>ATR-IR</b>	Attenuated Total Reflection Infrared Spectrophotometry
<b>XRD</b>	X-Ray Diffraction
<b>H<sub>2</sub>SO<sub>4</sub></b>	Sulphuric acid

## List of Figures

Figure 1.1: Structure of Coomassie brilliant blue G-250	3
Figure 1.2: Structure of a, banana plant rachis fibre pointed and b, harvested rachis	4
Figure 1.3: Structure of lignocellulose	5
Figure 1.4: Structure of cellulose	6
Figure 1.5: Chemical formula of holocellulose	7
Figure 1.6: Structure of chitosan	9
Figure 2.1: Banana rachis extractive free material obtained after soxhlet extraction (2.92 g)	19
Figure 2.2: Cellulose obtained from banana rachis after cellulose extraction (0.31 g)	21
Figure 2.3: Holocellulose obtained from banana rachis fibre after holocellulose extraction (1.04 g)	22
Figure 2.4: Lignin containing material from the banana rachis fibre after the klason treatment method (0.03 g)	24
Figure 3.1: The standard curve of CBB G-250 dye at a concentration of 800 mg/l	32
Figure 3.2: Effect of adsorbent dosage on decolourisation of CBB G-250 dye (%) using various adsorbents	33
Figure 3.3: Effect of contact time on adsorption of the CBB G-250 dye using various adsorbents	38
Figure 3.4: Adsorption isotherm of CBB G-250 dye, $q_e$ (capacity of sorbent) versus $C_e$ (equilibrium dye concentration) using various adsorbents A. Chitosan B. Alpha cellulose C. Banana rachis fibre D. Activated carbon	43
Figure 3.5: Linearised version of Langmuir isotherm of various adsorbents A. Chitosa B. Alpha cellulose C. Banana rachis fibre D. Activated carbon	45
Figure 3.6: Freundlich isotherm of various adsorbents A. Chitosan B. Alpha cellulose C. Banana rachis fibre D. Activated carbon	47
Figure 4.1: Schematic of methodology employed for the <i>in situ</i> precipitation of composites	60

Figure 4.2: A. Alpha cellulose/chitosan composite (6.07 g), B. Banana rachis fibre/chitosan composite (6.18 g)	64
Figure 4.3: ATR-IR spectrum of banana rachis fibre	66
Figure 4.4: ATR-IR spectrum of cellulose fraction extracted from banana rachis fibre	67
Figure 4.5: ATR-IR spectrum of chitosan	68
Figure 4.6: ATR-IR spectrum of alpha cellulose regenerated	69
Figure 4.7: ATR-IR spectrum of holocellulose obtained from banana rachis fibre	70
Figure 4.8: ATR-IR spectrum of rachis fibre control	71
Figure 4.9: ATR-IR spectrum of alpha cellulose control	72
Figure 4.10: ATR-IR spectrum of regenerated chitosan	73
Figure 4.11: ATR-IR spectrum of rachis fibre/chitosan composite pellet (0.5 g of rachis fibre used to produce composite)	75
Figure 4.12: ATR-IR spectrum of banana rachis fibre/chitosan composite supernatant(0.5 g)	76
Figure 4.13: ATR-IR spectrum of banana rachis fibre/chitosan composite pellet (5.0 g rachis fibre used during composite formation.)	77
Figure 4.14: ATR-IR spectrum of banana rachis fibre/chitosan composite supernatant (5 g)	78
Figure 4.15: ATR-IR spectrum of alpha cellulose/chitosan composite pellet (0.5 g)	79
Figure 4.16: ATR-IR spectrum of alpha cellulose/chitosan composite supernatant (0.5 g)	79
Figure 4.17: ATR-IR spectrum of alpha cellulose/chitosan composite pellet (5 g)	81
Figure 4.18: ATR-IR spectrum of alpha cellulose/chitosan composite supernatant (5 g)	82
Figure 4.19: X-ray diffraction spectra of banana rachis fibre	85
Figure 4.20: X-ray diffraction spectra of chitosan	86
Figure 4.21: X-ray diffraction spectra of alpha cellulose	87
Figure 4.22: X-ray diffraction spectra of banana rachis fibre/chitosan composite	88
Figure 4.23: X-ray diffraction spectra of alpha cellulose/chitosan composite	89
Figure 4.24: Effect of adsorbent dosage on decolourisation of CBB G-250 dye (%) using various A. Alpha cellulose/chitosan composite B. Banana rachis fibre/chitosan composite	94

Figure 4.25: Effect of contact time on adsorption of the CBB G-250 dye using various composites at different concentrations A. 50 mg/l B. 800 mg/l	97
Figure 4.26: Adsorption isotherm of CBB G-250 dye ( $q_e$ versus $C_e$ ) using various composites A. Alpha cellulose/chitosan composite B. Banana rachis fibre/chitosan composite	100
Figure 4.27: Linearised version of Langmuir isotherm of various composites A. Alpha cellulose/chitosan composite B. Banana rachis fibre/chitosan composite	102
Figure 4.28: Freundlich isotherm of various composites A. Alpha cellulose/chitosan composite and B. Banana rachis fibre/chitosan composite	102
Figure 4.29: Standard curve depicting absorbance as a function of glucose content	106
Figure 4.30: Above shows the different volumes (0.1, 0.2, and 0.5 ml) of glucose solutions after the addition of anthrone reagent it were for the standard curve of glucose	152
Figure 4.31: Above shows the different volumes (0.1, 0.2, and 0.5 ml) of distilled water after the addition of anthrone reagent	152
Figure 4.32: Above shows the different volumes (0.1, 0.2, and 0.5 ml) of chitosan hydrolysate solutions after the addition of anthrone reagent	153
Figure 4.33: Above shows the different volumes (0.1, 0.2, and 0.5 ml) of alpha cellulose hydrolysate solutions after the addition of anthrone reagent	153
Figure 4.34: Above shows the different volumes (0.1, 0.2, and 0.5 ml) of banana rachis fibre hydrolysate solutions after the addition of anthrone reagent	154
Figure 4.35: Above shows the different volumes (0.1, 0.2, and 0.5 ml) of alpha cellulose/chitosan composite hydrolysate solutions after the addition of anthrone reagent	154
Figure 4.36: Above shows the different volumes (0.1, 0.2, and 0.5 ml) of banana rachis fibre/chitosan composite hydrolysate solutions after the addition of anthrone reagent	155
Figure 4.37: Standard curve depicting absorbance as a function of hexosamine content	109
Figure 4.38: Above shows different concentration (20, 30, 40, 50, and 70 $\mu$ l) of glucosamine solutions after the addition of Ehrlich reagent for the standard curve of glucosamine	156

Figure 4.39: Above shows different concentration (20, 30, 40, 50, and 70 $\mu$ l) of alpha cellulose hydrolysate solutions after the addition of Ehrlich reagent	156
Figure 4.40: Above shows different concentration (20, 30, 40, 50, and 70 $\mu$ l) of chitosan hydrolysate solutions after the addition of Ehrlich reagent	157
Figure 4.41: Above shows different concentration (20, 30, 40, 50, and 70 $\mu$ l) of banana rachis fibre hydrolysate solutions after the addition of Ehrlich reagent	157
Figure 4.42: Above shows different concentration (20, 30, 40, 50, and 70 $\mu$ l) of alpha cellulose/chitosan composite hydrolysate solutions after the addition of Ehrlich reagent	158
Figure 4.43: Above shows different concentration (20, 30, 40, 50, and 70 $\mu$ l) of banana rachis fibre/chitosan composite hydrolysate solutions after the addition of Ehrlich reagent	158

## List of Tables

Table 2.1: Chemical composition of banana rachis fibre (The percentage of the dry weight of the banana rachis fibre)	25
Table 3.1: The equilibrium models equations	31
Table 3.2: The percentage of decolourisation of different adsorbents of different concentrations	37
Table 3.3: Percentage of sorption activity and equilibrium concentration ( $C_e$ ) of adsorbents at the lowest and highest CBB dye concentrations used	41
Table 3.4: The capacity of adsorption of CBB G-250 dye using different adsorbents at an equilibrium concentration	44
Table 3.5: Langmuir and Freundlich adsorption isotherm constants of the adsorption of CBB G-250 dye of various adsorbents	50
Table 4.1: The major ATR-IR bands in banana rachis fibre, alpha cellulose, chitosan, banana rachis fibre/chitosan composite, and alpha cellulose/chitosan composite (regenerated and non-regenerated samples)	84-85
Table 4.2: The $Cl_{XRD}$ (%) of samples	93
Table 4.3: The percentage of decolourisation of different adsorbents at different concentrations	96
Table 4.4: Percentage sorption activity and equilibrium concentration ( $C_e$ ) of composites observed at the lowest and highest CBB dye concentrations of CBB dye	99
Table 4.5: The capacity of adsorption of CBB G-250 dye using different adsorbents at an equilibrium concentration	104
Table 4.6: Langmuir and Freundlich adsorption isotherm constants for the adsorption of CBB G-250 dye on various composites	103
Table 4.7: Total carbohydrate (excluding hexosamine) content of various adsorbents determined with the Anthrone method after acid hydrolysis	108
Table 4.8: The percentage of hexosamine present in various adsorbents after acid hydrolysis	



## General introduction

In this study the title of the research is formulation and characterisation of banana rachis derived composites and its application in sorption of dyes. The thesis is divided into five chapters and then the references. Chapter 1 deals with the literature review, hypothesis and the specific objectives of the study. The study will further determine the capacity of the banana rachis fibre, cellulose, chitosan, activated carbon and banana rachis fibre-based adsorbents composites for the dye using isotherm studies.

Chapter 2 deals with characterisation of banana rachis fibre by chemical analysis such as; sampling, determination of water and fiber content, homogenization, determination of the extractives, cellulose, and holocellulose, Klason method for estimation of lignin present in banana rachis fibre. Chapter 3 deals with equilibrium and isotherm studies, the dye stock solution and construction of a standard CBB G-250 dye curve, the dye adsorption assessment methodology, the equilibrium time sorption experiments, the equilibrium studies, and then lastly the Langmuir and Freundlich isotherms of the various adsorbents (banana rachis fibre, chitosan, alpha cellulose, and activated carbon).

Chapter 4 deals with formulation and chemical analysis of composites such as; the preparation of chitosan/alpha cellulose and chitosan/banana rachis fibre composites by *in situ* precipitation, the characterisation of different adsorbents using ATR-IR, the powdered x-ray diffraction analysis, the dye adsorption assessment methodology, the equilibrium time sorption experiments, the equilibrium studies, and then lastly the Langmuir and Freundlich isotherms of the various adsorbents (alpha cellulose/chitosan composite and banana rachis fibre/chitosan composite), the acid hydrolysis of various adsorbents (chitosan, banana rachis fibre, alpha cellulose, alpha cellulose/chitosan composite, and banana rachis fibre/chitosan composite), the total sugar estimation of acid hydrolysates using the Anthrone method, and then the glucosamine estimation of acid hydrolysate using the hexosamine method. Chapter 5 deals with the overall conclusion.



# CHAPTER 1

## Literature review

### 1. Introduction

#### 1.1. National Water Act of South Africa

The Department of Water Affairs under the National Water Act of South Africa announced the integrated coastal management Act in 2008 (Act No. 24 of 2008) (Department of Environmental Affairs, 2014). One example of an industrial sector that uses high volumes of water, and generates polluted and coloured effluents in South Africa is the pulp and paper industry (eQ Insight, 2012). Effluent treatment is required to meet environmental regulations and decrease environmental impacts to aquatic ecosystems (eQ Insight, 2012). The textile industry is one of the greatest polluters in the world with 20% of global industrial water pollution coming from the treatment and dyeing of textiles, as is estimated by the World Bank (Kant, 2012). The discharge of dyes in open water streams is worrying for both toxicological and esthetical reasons (Tahir and Alam, 2014). The law mentioned above was promulgated to assist in regulating discharges from the water used by industries into the environment and compels industry to reduce their pollution of water resources.

#### 1.2. Environmental problems caused by dyes

Dyes are used in many industrial outlets such as food, paper, carpets, rubbers, plastics, cosmetics and textiles industries to colour their products. Effluents discharged from above mentioned industries, contain hazardous elements and causes environmental problems (Gupta and Ali, 2002). The presence of dyes in the industrial wastewaters causes toxicity to aquatic life and mutagenicity to humans (Boyter, 2007). Adsorbents can alleviate these problems by efficient removal of pollutants with the option of controlled incineration or even reclamation of valuable adsorbents and reuse in further treatment regiments (Kulkarni and Kawave, 2014). Commercial adsorbents used for domestic water treatment include ion-exchange resins in combination with activated carbon (Arnold and Larsen, 2006). However, these products are relatively expensive and are only generally suitable for small scale treatment of municipal home water sources (Arnold and Larsen, 2006). Larger scale, economic treatment of industrial effluent requires readily available and cheaper adsorbents,

which have not been investigated sufficiently to lead to practical industrial application in general.

### 1.3 Formulation of the different composites with graphene

Graphene is a polymer composed of single layers of planar carbon atoms that is packed into honeycomb assemblies and based on the graphite structure that has attracted much interest (Fitzer *et al.*, 1995). Graphene nanocomposites with polysaccharides are easily synthesized bio-based polymers. Polysaccharides include: cellulose, chitosan, starch, and alginates, each group with unique properties (Fitzer *et al.*, 1995). Graphene is used as adsorbents for the removal of various pollutants from effluents, according to a review article about the special use of graphene derivate as materials for the removal of environmental pollutants (Kyzas *et al.*, 2014). Graphene nanocomposites have been produced with chitosan and used for the removal of dyes and heavy metal ions, (Terzopoulou *et al.*, 2015).

Adsorption activity might be present in composite materials-derived from two or more original sources/materials. Adsorption interactions are the result of surface forces (hydrogen bonding, electrostatic interactions, and van der Waals forces), hence the final adsorption capacity of composite materials could almost be considered as the sum of the capacities of its origin sources (Terzopoulou *et al.*, 2015).

The reinforcement effect of graphene on polysaccharides is due to the improved interactions between the reactive groups including: carboxyl and hydroxyl groups with the carboxyl, amino or hydroxyl groups of polysaccharides (Terzopoulou *et al.*, 2015). The difference between graphene and polysaccharides groups is graphene does not have oxygen functional groups, which can result in the reduction of surface area and compromise the electrochemical performance. Formulation of the different composites with graphene serves as an example on what holds the composites together.

### 1.4. Coomassie brilliant blue G-250 dye

Coomassie brilliant blue dye (CBB) is the name given to two similar triphenylmethane dyes that were developed for use in the textile industry but are now used for staining proteins in analytical biochemistry (Chiral *et al.*, 1993). The chemical structure of CBB G-250 is shown in Figure 1.1. The colour of the dye depends on the acidity of the solution (Fox, 1987). CBB is an organic compound that can be used for colourisation of fibers. It is highly light resistant and is also used in copying papers, in hectograph- and printing inks, as well as in textile

applications. Dyes represent a major class of organic pollutants present in wastewater. The discharge of industrial wastewater containing dyes is considered as one of the highest environmental problems.

It is actually difficult to estimate the actual global production and consumption of dyes, but it is estimated that worldwide production of dyes and pigments would reach 9.0 million tons by volume of US\$ 30.0 billion by the 2020. However, according to one estimates there was an annual production of  $>7.5 \times 10^5$  metric tons of different dyes and nearly 280,000 tons (i.e. 2-50%) of textiles dyes are discharged into the effluents (Madamwar *et al.*, 2019). The presence of even very low concentrations of dyes in water reduces light penetration through the water surface, precluding photosynthesis of the aqueous flora. Many of these dyes are carcinogenic, mutagenic, and teratogenic and also toxic to human beings, fish species and microorganisms.

Therefore, the removal of dyes from wastewater effluents is of great concern. It is applied by different techniques, but it also belongs to the basic class of dyes which is adsorbed from solution by silk or wood and has little affinity for cotton (Tahir and Alam, 2014). Dyes used in various industries have harmful effects on living organisms within short exposure periods. Generally, the possible mechanisms of cationic dye adsorption onto biosorbents are as follows: (1) electrostatic attraction, (2) hydrogen bonding, and (3) n-p interactions (or n-p electron donor-acceptor interactions) (Tran *et al.*, 2017).

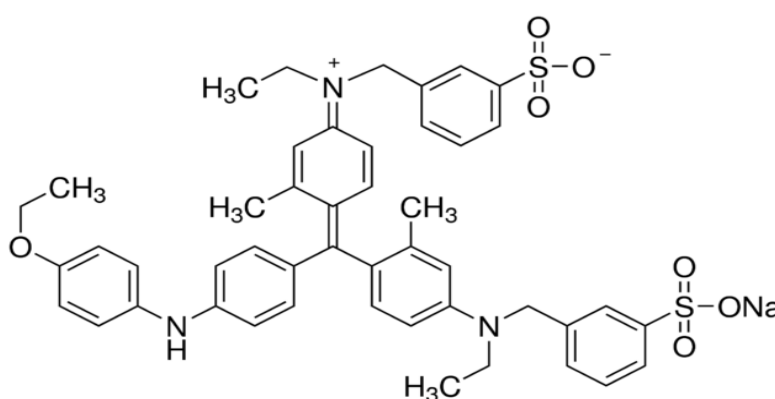


Figure 1.1: Structure of Coomassie brilliant blue G-250 (Syrový and Hodný, 1991)

## 1.5. Banana plants and rachis banana fibre

The interest in natural fibre reinforced composite materials is growing rapidly in industrial application as well as fundamental research. Plants such as flax, cotton, hemp, jute, sisal, kenaf, bamboo, banana are used as the source of lignocellulosic fibers are more applied as reinforcement in composites (Rohit and Dixit, 2016). The availability, renewability, low density and low price have made them economical alternative to glass and carbon fibres. The natural fibre composites are not only environmentally friendly, but they also provide satisfactory mechanical strength (Ashik and Sharma, 2015).

Composites are being used in transportation and construction sector. They are generally lignocellulosic, consisting of helically wound cellulose microfibrils in amorphous matrix of lignin and hemicellulose (Mukhopadhyay *et al.*, 2008). Banana and plantains are planted in every humid tropical region and constitute the 4<sup>th</sup> largest fruit crop of the world (Morton, 1987). Rachis is the stalk of the inflorescence from the first fruit to the male part (Robinson and Galan, 2010).

The rachis is a waste material left after the harvesting of bananas, it is abundantly found on natural growing banana plants and is freely available after harvesting is completed. It is potentially of no cost since it is a waste material and easy to process because it is a relative pliable material. The rachis is one of the banana plant constituents that contain the largest amount of fibrous material (Velasquez-Arredondo *et al.*, 2010). Banana plant rachis (a) and harvested rachis (b) is indicated in Figure 1.2.



Figure 1.2: Structure of a, banana plant rachis pointed b, harvested rachis ([www.eclipseproject.eu/waste-based-nanofillers](http://www.eclipseproject.eu/waste-based-nanofillers))

## 1.6. Lignocellulose

Banana rachis fibre is rachis, pseudo stem, leaf sheath and peel of the banana plant, which are cellulose-rich sources, are currently also being tested for fibrous material because they are considered to be potentially the best components for use in manufacturing composites materials (Arsene *et al.*, 2013). Lignocellulose structure is indicated in Figure 1.3. Banana fibre, a lignocellulosic fibre, is a bast fibre with relatively good mechanical properties. High cellulosic content and low micro-fibril angle are desirable to obtain the desired mechanical properties (Verma *et al.*, 2016). Lignins are composed of nine carbon units derived from substituted cinnamyl alcohol; that is, coumaryl, coniferyl, and syringyl alcohols (Mukhopadhyay *et al.*, 2008).

Lignin as a natural recalcitrant kind of material plays an important role in natural decay resistance are associated with the easily degradable hemicelluloses (Mohanty *et al.*, 2001; Verma *et al.*, 2016). Banana pseudo stem's outer covering is a cellulosic material while the core or pith is rich in polysaccharides and other trace elements but lower in lignin content (Cordeiro *et al.*, 2004). Banana pseudo stem fibres have high potential in absorbing spilled oils in refineries (Hubbe *et al.*, 2013). Lignocellulosic materials are inexpensive and ecofriendly biosorbents (Lee *et al.*, 2014). Lignocelluloses usually contain around 40% cellulose, 20% hemicellulose and 20 - 30% lignin (Tuomela *et al.*, 2000).

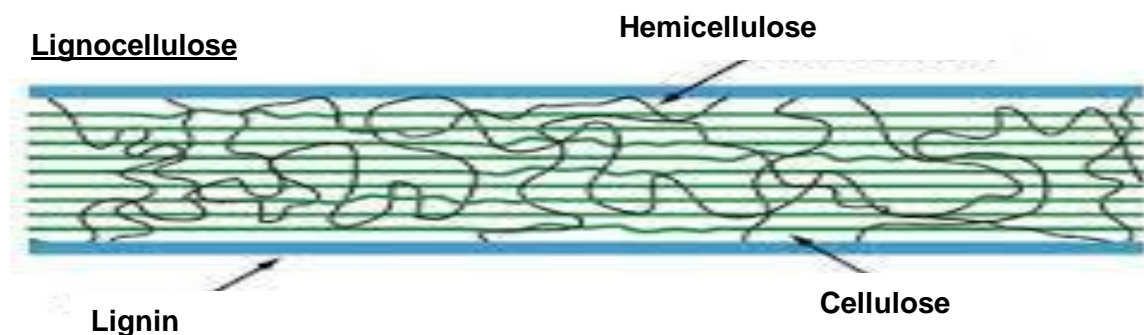


Figure 1.3: Structure of lignocellulose ([www.Sfi.mtu.edu](http://www.Sfi.mtu.edu))

## 1.7. Cellulose

Cellulose is an organic compound with the formula  $(C_6H_{10}O_5)_n$ . It is a polysaccharide comprised of a linear chains of several hundred to many thousands of  $\beta(1\rightarrow4)$  linked d-glucose units (Updegraff, 1969). The chemical structure of cellulose is indicated in Figure 1.4. The multiple hydroxyl groups on the glucose from one chain form hydrogen bonds with other

chains. Various forms of crystalline structures of cellulose are known, corresponding to the occurrence of hydrogen bonds between and within its carbohydrate strands (Bishop, 2007).

Ionic liquids combining 1-butyl-3-methyl imidazolium cation with different anions were investigated as potential solvents for cellulose (Li *et al.*, 2004). The ability to dissolve cellulose has resulted in unique processing technologies being developed leading to novel cellulose derivative products including blends, composites, ionic gels and fibres. These materials are environmentally friendly and can replace petroleum-based products associated with negative impacts on the environment (Isik *et al.*, 2014). Cellulosic fibers are naturally anionic in charge and cationic polymers are absorbed onto fibers by electrostatic attraction (Li *et al.*, 2004). This can facilitate its interaction with other biopolymers.

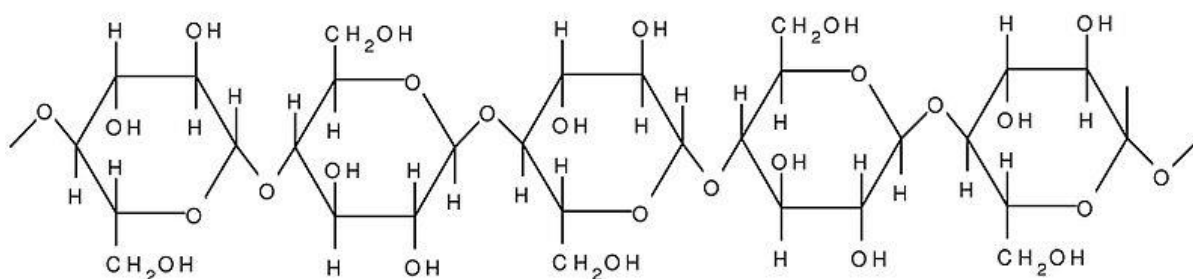


**Figure 1.4: Structure of cellulose (www.easychem.com.au/production - of - materials/biomass - research/cellulose/)**

### 1.8. Holocellulose

The combination of cellulose (40 - 45%) and the hemicelluloses (15 - 25%) are called holocellulose and usually accounts for 65 - 70% of the wood dry weight (Rowell *et al.*, 2013). The holocellulose, which constitutes 70 - 80 percent of wood tissue is a linear polysaccharide made up of glucose units (Robertson and Wood, 1979). The chemical formula of holocellulose is indicated in Figure 1.5. These polymers (cellulose and hemicelluloses) are made up of simple sugars, mainly, d-glucose, d-mannose, d-galactose, d-xylose, l-arabinose, l-glucuronic acid, and lesser amounts of other sugars such as l-rhamnose and d-fucose. The polymers (cellulose and hemicelluloses) are rich in hydroxyl groups that are responsible for moisture sorption through hydrogen bonding (Rowell *et al.*, 2013).

Delignification is a critical process towards the successful characterization of cellulose and hemicelluloses from lignocellulosic biomass (Hubbel and Ragauskas, 2010). The presence of lignin in biomass reduces accessibility to the cellulose microfibrils. Lignin can also hinder or



mask molecular details from spectroscopic techniques (Hubbell and Ragauskas, 2010). For these reasons, it is essential to remove all or majority of the incorporated lignin prior to analysis. The most popular and established laboratory method for the removal of lignin from biomass is acid-chlorite delignification utilizing an aqueous solution of acetic acid and sodium chlorite (Hubbell and Ragauskas, 2010). This method effectively bleaches and then solubilizes lignin at moderate temperatures (Hubbell and Ragauskas, 2010). The major carbohydrate portion of wood is composed of cellulose and hemicellulose polymers with minor amounts of other sugar polymers such as starch and pectin (Stamm, 1964).

A complex mixture of polysaccharides remains after the removal of lignin from tree-wood following treatment with sodium chlorite solution ([www.oxfordreference.com](http://www.oxfordreference.com)). Holocelluloses are major energy sources available to decomposer organisms, constituting 70 - 80% of fresh organic material (Swift *et al.*, 1979). Holocellulose is one of the main components of organic matter. Holocellulose is the main polymeric component of the plant cell wall, the most abundant polysaccharide and an important renewable resource (Jarwanto and Tachibana, 2009).

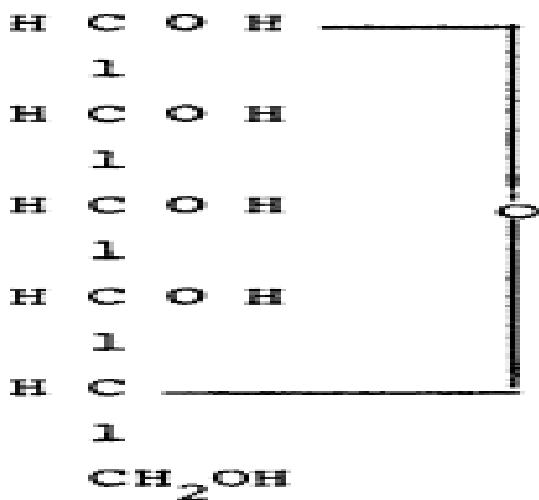


Figure 1.5: Chemical formula of holocellulose (Robertson and Wood, 1979)

such as

Chitosan is a linear polysaccharide composed of  $\beta$ -(1, 4)-linked d-glucosamine (deacetylated unit) and N-acetyl-d-glucosamine (acetylated unit) (Shahidi and Synowiecki, 1991). The structure of chitosan is shown in Figure 1.6. The shells of shrimp and sea crustaceans contain chitin that is extracted and converted to chitosan using an alkaline treatment. This method is

used to obtain commercial chitosan (Shahidi and Synowiecki, 1991). Chitosan is used in water processing engineering in the filtration process. It is further used to remove phosphorus, heavy metals, and oils from water (Woodmansey, 2002).

Composites of chitosan with bentonite, gelatin, silica gel, or other fining agents, are utilised to clarify wine, mead, and beer (Rayner, 2006). Chitosan can be dissolved in ionic liquids. An ionic liquid, 1-butyl-3-methylimidazolium chloride can dissolve up to 10 (w/v) % chitin or chitosan (Xie *et al.*, 2005). The advantages of using fungal polysaccharides such as chitosan-glucan complexes from various fungi (*A niger* and *Mucor rouxii*) in the removal of metal ions have been studied previously (Muzzarelli, 2011).

Chitosan is a principal component of cell walls of certain fungi such as *Gongronella* spp., *Absidia* spp., *Aspergillus* spp., *Rhizopus* spp. These fungi belong to the class of Zygomycetes (Tamura *et al.*, 2011). It was discovered that chitosan-glucan from fungi had a higher adsorption capacity compared to chitosan derived from crustaceans, in collecting transition metal ions from aqueous solutions (Muzzarelli, 2011). Chitin is the most abundant amino polysaccharide polymer occurring in nature and is the building material that gives strength to the exoskeletons of crustaceans, insects, and the cell walls of fungi.

The main natural sources of chitin are shrimp and crab shells, which are an abundant byproduct of the food-processing industry, that provides large quantities of this biopolymer to be used in biomedical applications. Because the fungal chitosan–glucan complex is less crystalline and more expanded, which means that it is more accessible to chemicals (Muzzarelli, 2011). The amount of chitin resources indicates approximately 0.7, 1.4, and 29.9 million tons of chitin are annually recovered from squid, oyster, and shellfish, respectively (Das *et al.*, 2016). The seafood industry generates  $\sim 10^6$  tonnes of chitin annually as a waste stream, much of which is composted or converted to low-value products such as fertilizers, pet foods and fishmeal (Schmitz *et al.*, 2019). In the biosphere, over 1 billion tons of chitin are synthesized each year by organisms ([biologydictionary.net/chitin](http://biologydictionary.net/chitin)).



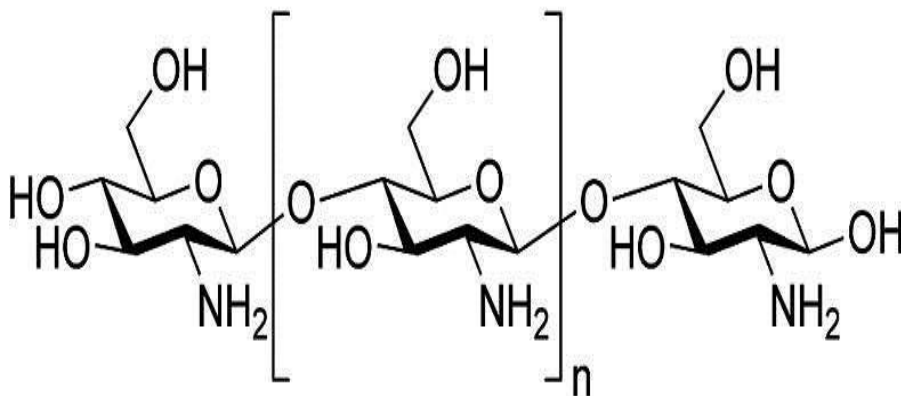


Figure 1.6: Structure of Chitosan (Shahidi and Synowiecki, 1991)

### 1.10. Attenuated total reflection infra-red spectrometry

Attenuated total reflection (ATR) is used in conjunction with infrared spectroscopy which permits samples to be observed directly in the solid or liquid state without further sample preparation as opposed to conventional infra-red measurement techniques (transmission method). The energy of each peak in an absorption spectrum corresponds to the frequency of the vibration of a molecule, therefore permitting qualitative identification of certain bond types in the sample. Infra-red spectroscopy is also used to observe the changes occurring in the crystallinity and polymorphic nature of chitin/chitosan as a function of the N-deacetylation level (Kumirska *et al.*, 2010). Hydrogen bonding occurs whenever a hydrogen atom serves as a carrier between two electronegative atoms by a covalent bond to the one and to the other by an electrostatic bond (Kuzmina *et al.*, 2012).

### 1.11. Isotherm studies

Isotherm studies resolve the distribution of adsorbate solute between the liquid and solid phases at different equilibrium concentrations (Ng *et al.*, 2002). There are many isotherm models described in literature but many studies refer to Freundlich and Langmuir types of adsorption isotherms which are used preferentially over others (Dada *et al.*, 2012). Langmuir and Freundlich adsorption isotherms are used for the determination of sorption capacity of adsorbents for dyes. Porosity is a measure of the void (i.e. ("empty") spaces in a material, and is a fraction of the volume of voids over the total volume (Gholizadeh *et al.*, 2013). Isotherm can show whether the pores are microporous and whether the exposed surface residues are located almost exclusively within the micro-pores (Lowell and Shields, 1984).

### 1.12. Activated carbon, agricultural wastes and bio-sorbents

Activated carbon is the most important adsorbent used on an industrial scale (Menéndez-Diaz and Gullon, 2006). Various physical forms of activated carbon are manufactured depending on their application: granular to be used in adsorption columns and power forms for use in batch adsorption followed by filtration (Rajagopal, 1991). Activated carbon is used as an adsorbent due to its high adsorption abilities in removing organic pollutants from wastes water. The high adsorption capacity of activated carbon is due to its high surface area. Activated carbon is a form of carbon processed to have small, low-volume pores that increase the surface area available for adsorption or chemical reactions.

Due to its high degree of microporosity, one gram of activated carbon has a surface area in excess of 3,000 m<sup>2</sup> (32,000 sq ft) (Dillon *et al.*, 1989) as determined by gas adsorption (Jhadhav, 2015). An activation level sufficient for useful application may be attained solely from high surface area. However, the cost of activated carbon is relatively high and regeneration is difficult, which limits its usage in dye waste treatments (Waranusantigui *et al.*, 2003). As a result, many researchers have investigated low-cost, agricultural wastes {bagasse pitch, maize cob, coconut shell, rice husk, etc. (Annadurai *et al.*, 2002) and bio-sorbents such as yeast, fungi, bacteria, chitin, chitosan, algae and peat mass (Crini, 2006).

### 1.13. Hypothesis

It is hypothesized that banana rachis fibres when combined with biopolymer such as chitosan will yield adsorbent with higher capacity compared to activated carbon. Furthermore, rachis fibres might contain materials/functional groups that could interact with functional groups of chitosan to facilitate adsorption of dyes. Furthermore, interaction between chitosan and banana rachis will alter the physiochemical characteristics of these materials to facilitate dye binding. It is speculated that either physical/structural (surface area/porosity and changes in crystallinity) and/or chemical changes (hydrogen bond formation/disintegration) might enhance adsorption ability of rachis fibres when combined with chitosan.

### 1.14. Aim

The primary aim of this study was to test the possibility of using banana rachis fibre, cellulose, chitosan, activated carbon and banana rachis fibre based adsorbents composites, for removal of a dye (Coomassie brilliant blue G-250) dissolved in water. The study will further determined the capacity of the banana rachis fibre, cellulose, chitosan, activated carbon and banana rachis fibre-based adsorbents composites for the dye using isotherm studies.

The specific aims in this study are:

- 1) To determine sorption capability of a cellulose-based waste primary banana rachis fibres, as well as composite of rachis fibres in combination with biopolymer such as chitosan to obtain highly adsorbent materials for adsorption of dye solutions. To obtain equilibrium time for dye adsorption to each adsorbent.
- 2) To quantify adsorption capacity using isotherm studies, with activated carbon as reference adsorbent.
- 3) To determine basic mechanisms of absorption involved and to measure crystallinity index values.
- 4) To chemically characterized banana rachis fibres and composites by conventional techniques.
- 5) To investigate change in hydrogen-bond formation (by ATR-IR) in the various adsorbents and to determine its effects on sorption of dyes.
- 6) To study crystallinity of the products by a powdered x-ray diffraction method.

### **1.15. Rationale for study**

During this study banana rachis was selected as a renewable agricultural waste material. The rachis material was first chemically characterised to determine the nature thereof. Various potential adsorbents were studied in terms of effect of dosages and colour intensities on the adsorbance of the dye CBB. Activated carbon was included for bench marking purposes. The equilibrium times were determined using preselected criteria and subsequently used in isotherm studies. The isotherm studies were conducted to quantify the adsorbent capacity for CBB dye and two models, namely, Freundlich and Langmuir were used for this purpose. Composites were prepared using commercial cellulose and banana rachis, in combination with chitosan.

Cellulose was used as it is the major constituent in banana rachis fibre, it represents a relative less complex biopolymer compared to lignocellulose and a lot of research has been done on the use of cellulose in composites over the years. The use of rachis fibre in composites as far as known has, not been attempted previously. Chitosan was included since it apparently improves the durability of fibres when used in composites. It also exhibits an antimicrobial effect that could be useful if fibres are to be used over long periods as adsorbents on an industrial scale. The composites were characterised by XRD and ATR-IR studies.

The latter was used to examine functional groups and also to ascertain the interactions between the components following composite formation. XRD was used to study mainly crystallinity of composites and their constituents. The composites was also hydrolysed and the total carbohydrates estimated, this was followed by hexosamine determinations. Hexosamine is the building block of chitosan and analysis thereof gives an indication of the amount of chitosan present in the composites.

The same strategy was followed to determine the isotherms of the composites during CBB dye adsorption as were conducted with the adsorbents mentioned above. The various isotherms were compared to determine the effect of composite formation on the capacity of composites relative to the dye adsorption capacities of constituents from which the composites were made. Isotherms were also used to gain information of the basic mechanisms of dye adsorption, whether it occurs by the monolayer or by a multilayer approach.

## 1.16. Conclusion

From this literature review the following can be conclude:

1. Dyes are used in many products such as food, paper, carpets, rubbers, plastics, cosmetics and textiles to colour their products. Effluents discharged from above mentioned industries, hazardous elements and causes environmental problems.
2. Coomassie brilliant blue dye (CBB) is the name given to two similar triphenylmethane dyes that were developed for use in the textile industry but are now used for staining proteins in analytical biochemistry. It is a basic dye which is adsorbed from solution by silk or wood and has little affinity for cotton.
3. The rachis is a waste material left after the harvesting of bananas and is readily available after harvesting is completed. It is potentially of no cost since it is a waste material and easy to process because it is a relative pliable material.
4. Activated carbon is used as an adsorbent due to its high adsorption abilities in removing organic pollutants from wastes water. However, the cost of activated carbon is relatively high and the regeneration is difficult, which limits its usage in dye waste treatments.

## CHAPTER 2

### 2. Characterisation of banana rachis fibres by chemical analysis

#### 2.1. Chapter Summary

The banana rachis fibre was prepared as adsorbent for the adsorption of CBB dye from aqueous solution. Before such studies were conducted however it was important to examine the chemical makeup of the biosorbent material. Locally available banana rachis fibre had a water content of 92.21% and the fibre yield percentage of 8.4%. The content of extractives in banana rachis fibre was 2.7%. The cellulose levels present in banana rachis fibre was 30.3%. The hemicellulose was 23.2%. The Klason lignin obtained from the banana rachis fibre was 15%. These results suggest banana rachis fibre is a potential low-cost adsorbent for the dye removal from industrial wastewater.

*Key words:* Banana rachis fibre, Extractives, Cellulose, Hemicellulose, Klason lignin.

#### 2.2. Introduction

This experimental section involves the chemical analysis of the banana rachis fibre. This is important since the chemical make-up has an important bearing on the nature of the material. Banana farming generates huge quantity of biomass all of which goes to waste and the above ground parts like pseudostem and peduncle are the major sources of fibre. Banana fibre can be used as raw material by various industries for production of a range of products like paper, cardboards, tea bags, currency notes and high quality dress materials. Banana rachis fibres are known to be good source of cellulose, hemicellulose, and lignin (Preethi and Balakrishna, 2013). In this chapter there was sampling of banana rachis fibre wastes, determination of water and fibre content of banana rachis fibre, and homogenization of rachis fibres.

The First samples were treated to remove lipid extractives using a soxhlet extraction method. Soxhlet extraction is a continuous solid-liquid extraction where a desired compound is extracted from solid material (containing unwanted products) using a solvent. The solid is placed in a filter paper thimble which is then placed into the main chamber of the soxhlet extractor (Santos *et al.*, 2011). The solvent (heated to reflux) travels into the main chamber and the partially soluble components are slowly transferred to the solvent. The extractives

have low or medium molecular weight and can be extracted by specific solvents such as acetone, toluene, alcohol and water (Silverio *et al.*, 2006).

Extractives are sugars, starches, waxes, fats, fatty acids, phenolic substances, terpenoids, and resin acids (Sjostrom, 1993). The cellulose content was determined using the Kurscher-Hoffner approach that entails the treatment of banana rachis fibre with nitric acid solution under reflux (Li *et al.*, 2010). Holocellulose content was determined following a method using sodium chlorite as oxidizing agent to remove lignin, the treatment of lignocellulose from banana rachis fibre leads to a white delignified product (Willis and Scott, 1988). During the Klason treatment method, the banana rachis fiber was treated with sulphuric acid to obtain a lignin containing material (Willis and Scott, 1988). All the analyses performed are based on gravimetric measurements of at least duplicate samples.

## **2.3. Materials and Methods**

### **2.3.1. Sampling**

The banana rachis wastes, obtained from farms in Limpopo province, in the Levubu area, was used. After harvesting of the fruit, the rachis was processed shortly after collection.

### **2.3.2. Determination of water and fibre content of banana rachis fibre**

The banana rachis was cut into smaller pieces and the wet weight of the rachis pieces were measured. From the material, the fibres were subsequently removed by scrubbing and the fibres were extracted by using a knife (Zuluaga *et al.*, 2007). The banana rachis fibres were washed several times with distilled water and were filtered using a Buchner funnel equipped with filter paper and a vacuum pump. After the fibres were dried in an oven overnight at 70 °C. The dry weight of the fibres were measured using a electronic balance and afterwards stored in a desiccator. All analysis reported here and below were performed in duplicate and averages calculated.

### **2.3.3. Homogenization of rachis fibres**

The dried fibres were ground several times using a homogenizer, 37 000 rpm, 15 minutes. Fibres, in a fine powdery form, was obtained following sieving using a commercial sieve.

#### **2.3.4. Determination of the extractive, cellulose and holocellulose present in banana rachis fibre**

##### **2.3.4.1. Extractive removal**

A 3 g sample of banana rachis fibre was first submitted to soxhlet extraction with ethanol/toluene (1:2 v/v) mixture in a fume cardboard for 8 hours. The soxhlet was heated using a heating mantle during the extraction process (Li *et al.*, 2010). A rotary evaporator was subsequently used to remove the organic phase from the extractives and the dry weight of the extractives were determined after placement in an oven at 60 °C overnight (Li *et al.*, 2010).

##### **2.3.4.2. Cellulose extraction**

The cellulose content was determined using the Kurscher-Hoffner approach which consists of treating 1 g of extractives-free sample with (12.31 M) 30 ml of nitric acid solution under reflux during four cycles of 1 hour. After each cycle the solution was removed and replaced by a fresh volume of nitric acid solution. The nitric acid solution was prepared by mixing one volume of 55% (w/w) solution of nitric acid with four volume of 99% purity ethanol (Li *et al.*, 2010). The material left after the treatment was washed with distilled water then dried at 60 °C overnight in an oven. The dry weight was determined following the procedure as indicated below in Chapter 2, Section 2.4.1.2.

##### **2.3.4.3. Holocellulose extraction**

Holocellulose was determined following a method using sodium chlorite to remove lignin. An amount of 2 g of extractives-free banana rachis fractions was mixed with 65 ml distilled water, 0.5 ml acetic acid, and 0.6 g pure sodium chlorite during 1 hour treatment at 75 °C. This treatment was repeated three times until the sample became white, indicating complete bleaching. The sample was filtered through filter paper and washed with distilled water. The sample was dried at 60 °C overnight and cooled in a desiccator and the mass was recorded after weighing with an electronic balance (Li *et al.*, 2010).

##### **2.3.5. Klason method for estimation of lignin present in rachis fibres**

Approximately 0.2 g of the sample of rachis fibres were accurately weighed to the nearest 0.1 mg using an analytical electronic balance into a small beakers. One milliliter (ml) of 72% H<sub>2</sub>SO<sub>4</sub> was added per 100 mg of sample. The mixture is placed in a water bath at 30 °C and is stirred



frequently to assure complete mixing of the components. This constitute the primary hydrolyses step. After exactly 1 hour, it is diluted and transferred to an Erlenmeyer flask, using 28 ml of water for each 1 ml of acid. Secondary hydrolysis is then conducted in an autoclave at 120 °C for 1 hour. The hot solution is filtered through a filter paper, and the Klason lignin residue is washed with hot water to remove the acid. The crucibles containing the banana rachis samples are then dried to constant weight at 105 °C in an oven and are weighed to the nearest 0.1 mg. Before weighing the samples are allowed to cool down in a desiccator. Lignin is expressed as a percentage of the original sample mass (Willis and Scott, 1988).

## 2.4. Results and Discussions

### 2.4.1. Chemical analysis of rachis fibre

#### 2.4.1.1. Determination of water content of the rachis

The water content of the rachis was determined using the mass of the wet weight (291.22 g) of the two parts of banana rachis collected and dry weight (22.68 g) which gives the calculated results below:

$$\begin{aligned}
 \text{Water content} &= \frac{\text{wet weight} - \text{dry weight}}{\text{wet weight}} \times 100 \\
 &= \frac{291.22 - 22.68}{291.22} \times 100 \\
 &= 92.21\% \text{ water is present in the banana rachis fibre}
 \end{aligned}$$

The 92.21% water content obtained, was higher than the 64.8% of moisture content of banana pseudo-stem obtained by Baloyi (2012), higher than the 9.74% moisture level of banana stem recorded by Mukhopadhyay *et al.* (2008), lower than the 96% of moisture content of banana pseudo-stem obtained by Li *et al.* (2010).

### 2.4.1.2. Fibre yield

Fibre yield percentage refers to the percentage of lignocellulosic material, mainly consisting of polysaccharides, cellulose micro-fibrils, hemicelluloses, lignin, pectin and water-soluble components (Gopinathan *et al.*, 2017).

$$\begin{aligned} \text{Fibre yield (\%)} &= \frac{\text{weight of the dried fibre (gm)}}{\text{weight of the fibre after decortified (gm)}} \times 100 \\ &= \frac{22.68}{270.80} \times 100 \\ &= 8.4\% \end{aligned}$$

The % yield of fibres was 8.4%. This means that the fibres obtained were marginally higher than the 0.8% obtained by Phungo (2014), higher than the peduncle of Nendran (0.283%) presented by Preethi and Balakrishna (2013), higher than 1.0% values by Uma *et al.* (2005), higher than the pseudostem of Nendran (2.30%), and higher than pseudostem of Poovan (2.71%) values by Preethi and Balakrishna (2013). Values of yields evidently depended on the plant cultivar used and method of extraction employed.

### 2.4.2. Extractives determination of banana rachis fibre

#### 2.4.2.1. Contents of extractives in banana rachis fibre

The amount of extractives obtained from 3 g banana rachis fibre was 0.0807 g after the soxhlet extraction. Banana rachis fibre after Soxhlet extraction is shown in Figure 2.1. The %yield of the extractives obtained from banana rachis fibre was calculated as follows:

$$\begin{aligned} \% \text{Yield} &= \frac{\text{Mass of extractives obtained}}{\text{Mass of banana rachis fibre used}} \times 100\% \\ &= \frac{0.0807 \text{ g}}{3 \text{ g}} \times 100 \end{aligned}$$

= 2.7% extractives

Therefore, the extractives-free materials present were calculated as follows:

The extractives-free materials = Mass of banana rachis fibre used – Mass of extractive isolates obtained:

$$= 3 \text{ g} - 0.0807 \text{ g}$$

$$= 2.92 \text{ g}$$

Therefore, in 3 g rachis fibre there was left a total of 2.92 g extractive free materials.

A 2.7% extractive fraction was obtained from 3 g dry weight of banana rachis fibre. It was slightly lower than the 3.05% extractives obtained by Li (2010). Other workers recorded even higher values such as 4.46% by Bilba *et al.* (2007) as cited by Makhopadhyay *et al.* (2008), 10.6% obtained by Abdul Khali *et al.* (2006) and 12% by Baloyi (2012). Banana rachis extractive free material obtained after soxhlet extraction are shown in Figure 2.1.



**Figure 2.1: Banana rachis extractive free material obtained after soxhlet extraction (2.92 g)**  
After the Soxhlet extraction process, the banana rachis extractive free material indicated a brown colour, and soft texture.

### 2.4.2.2. Cellulose levels present in rachis fibre

The amount of cellulose obtained from 1 g extractives free materials was 0.31 g as shown in Figure 2.2. The total amount of extractives free materials obtain from 3 g rachis fibres was 2.92 g. Therefore, from 2.92 g extractives-free materials X g cellulose will be obtained which can be calculated as follows:

$$X \text{ g cellulose} = (\text{Total extractive free material}) \times (\text{mass of cellulose obtained})$$

$$\begin{array}{r} \text{-----} \\ 1 \text{ g extractive free materials} \\ = 2.92 \text{ g} \times 0.31 \text{ g} \\ \text{-----} \\ 1 \text{ g} \\ = 0.91 \text{ g cellulose} \end{array}$$

The % yield of cellulose was calculated as follows:

$$\% \text{ yield} = 0.91 \text{ g} \times 100$$

$$\begin{array}{r} \text{-----} \\ 3 \text{ g} \\ = 30.3\% \text{ cellulose} \end{array}$$

Therefore, the banana rachis fibre contained 30.3% cellulose which is higher than the value of 28.1% obtained by Baloyi (2012), lower than the value of cellulose, namely, 31 - 35% obtained by Bilba *et al.* (2007), lower than the value of cellulose content 60 - 82% obtained by Reddy and Yang (2005). Other cellulose values were also higher compared with the values obtained in this study for rachis fibres (56.1% and 51.5%) as was reported by Atchison (1993). Cellulose is a valuable product with many applications. The high cellulose content of banana rachis fibre compared to other agricultural residues has a potential to be a cheap source of this valuable polymer. The lower level was found in this study as compared with results reported by others might have been due to different cultivars used in the respective studies. Cellulose obtained from banana rachis after cellulose extraction are shown in Figure 2.2.



**Figure 2.2: Cellulose obtained from banana rachis after cellulose extraction, the experiments was repeated four times (0.31 g)**

After the cellulose extraction from banana rachis using the Kurscher-Hoffner approach, the cellulose indicated a light brown colour and soft texture.

#### 2.4.2.3. Holocellulose levels contained in rachis fibre

The amount of holocellulose obtained from 2 g extractives free materials was 1.35 g as in shown Figure 2.3. The total amount of extractives-free materials obtained from 3 g rachis fibre was 1.03 g. Therefore, from 1.03 g extractives-free materials X g holocellulose will be obtained which can be calculated as follows (using logic proportion):

X g holocellulose = (Total extractives-free materials) x (Mass of holocellulose obtained)

$$\begin{aligned}
 & \text{-----} \\
 & \text{Extractives-free materials} \\
 & \\
 & = 1.03 \text{ g} \times 1.35 \text{ g} \\
 & \text{-----} \\
 & \quad 2 \text{ g} \\
 & = 0.695 \text{ g holocellulose was present in 3 g banana rachis fibre}
 \end{aligned}$$

The % yield was calculated as follows:

$$\% \text{ yield} = 0.695 \text{ g} \times 100$$

-----

3 g

= 23.2 % holocellulose

Therefore, the banana rachis fibre contained 23.2% of holocellulose which was lower than the 65.2% obtained by Abdul Khali *et al.* (2006), 72.71% given by Li *et al.* (2010) and 77.6% obtained by Baloyi (2012), lower than the holocelluloses, representing 77 and 75% for rachis fibres and rachis, respectively (Cordeiro *et al.*, 2006). In comparison with the traditional raw material used in the pulp and papermaking industry, it was found that the content of holocellulose in banana pseudo-stem was much lower than wood fibres (Gong 2007), but still higher than straw, which is a typical kind of non-wood fiber (Liu *et al.*, 2003). The lower level was found in this study as compared with results reported by others might have been due to different cultivars used in the respective studies and the observed differences could be due to the extraction techniques. Holocellulose obtained from banana rachis fiber after holocellulose extraction are shown in Figure 2.3.

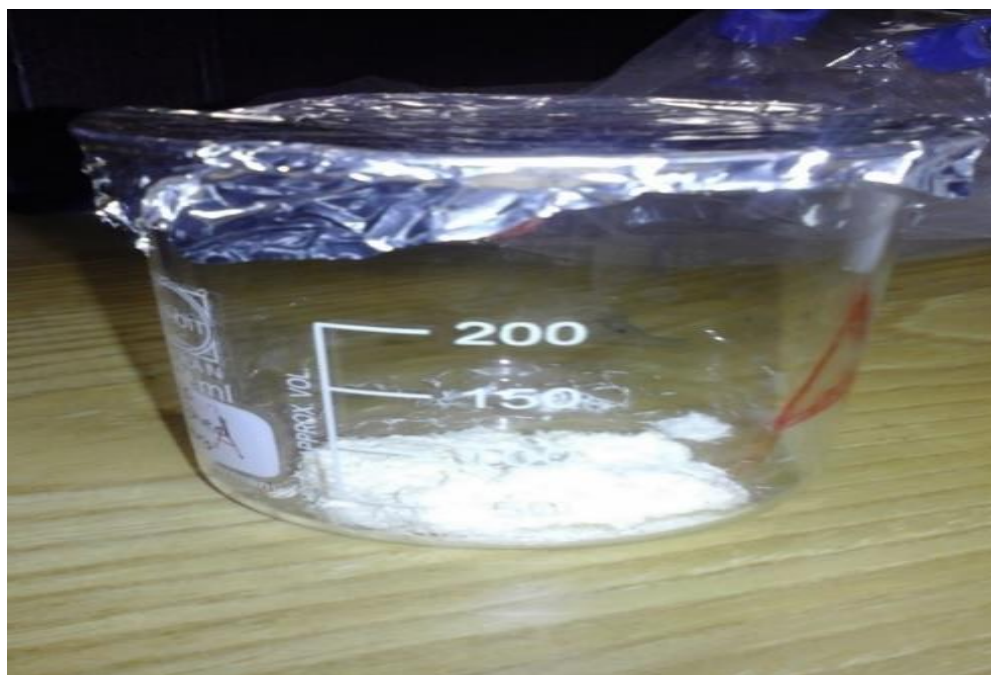


**Figure 2.3: Holocellulose obtained from banana rachis fibre after holocellulose extraction (1.35 g)**

After the holocellulose extraction from banana rachis fibre using sodium chlorite to remove lignin, the holocellulose indicated a white colour and soft texture.

#### 2.4.2.4. Klason treatment method for lignin content of rachis fibres

The lignin is expressed as a percentage of the original sample. Klason lignin obtained was 0.03 g after 0.2 g of banana rachis fibre extractive free sample was dissolved in the sulphuric acid as indicated on Figure 2.4.

$$\begin{aligned} \text{Klason lignin} &= \frac{0.03\text{g}}{0.2\text{g}} \times 100 \% \\ &= 15\% \end{aligned}$$

The Klason lignin yield was 15%, which was somewhat higher than 10 - 13% by Oliveria *et al.* (2009), similar to the Nendran pseudostem value of 14.39% by Preethi and Balakrishna (2013), higher than the lignin in rachis fibres namely 11.8% and in rachis 10.5% (Cordeiro *et al.*, 2006). Within the range for lignin (15 -16%) by Bilba *et al.* (2007). It was furthermore lower than the lignin observed in pseudostem and peduncle fibre of the Monthan cultivar 21.56% and 20.66% by Preethi and Balakrishna (2013). Therefore, generally lower amount of the Klason lignin was obtained than reported in the literature. The lignin yield of different banana plants differ significantly among the cultivars. Lignin containing material from the banana rachis fibre after the klason treatment method are shown in Figure 2.4.





**Figure 2.4: Lignin containing material from the banana rachis fibre after the klason treatment method (0.03 g)**

The lignin containing material indicated a black colour and soft texture.

The percentages for each constituent found in of banana rachis fibre are presented for each constituent in Table 2.1. As stated by Li *et al.*, 2010, the chemical composition of banana stem were moisture content 96%, cellulose 39.12%, holocellulose 72.71%, extracts 3.05%, which were higher than the results in the study, and for the klason lignin 8.88% which was lower. The hemicellulose fraction shown was estimated by calculation.



**Table 2.1: Chemical composition of banana rachis fibre (The percentage of the dry weight of the banana rachis fibre)**

<b>Constituent</b>	<b>Content (%)</b>
Water content	92.21
Fibre yield	8.4
Extractives (lipids)	2.7
Cellulose	30.3
Holocellulose	23.2
Lignin	15.0
Hemicellulose	20.4

<sup>1</sup>Hemicellulose was calculated by subtracting cellulose content from the holocellulose value

## 2.5. Conclusion

1. Locally available banana rachis fibre had a water content of 92.21% and the fibre yield percentage of 8.4%.
2. Lignocelluloses usually contain around 40% cellulose so comparing to what is obtained the cellulose is lower 30.3% but also acceptable.
3. Hemicellulose obtained was 20.4%, which is higher than 20% of hemicellulose expected to be obtained. The content of extractives in banana rachis fibre was 2.69%, which is lower and good for the adsorbent usage. The holocellulose was 23.2%.
4. The Klason lignin obtained from the banana rachis fibre was 15% which is lower than 20-30% of lignin expected to be obtained.

## CHAPTER 3

### 3. Equilibrium and isotherm studies for different adsorbents (banana rachis fibre, chitosan, alpha cellulose, and activated carbon)

#### 3.1. Chapter Summary

Adsorption is an important technique because of its simplicity and high efficiency, as well as the availability of a wide range of adsorbents. It has proven to be an effective method for removal of different dyes from waste materials. The sorption activity as determined at a low concentration of 50 mg/l CBB dye was as follows: 17.52% for alpha cellulose, 12.76% for activated carbon, 5.88% for banana rachis fibre, 0.56% for chitosan. At the higher concentration (800 mg/l), the highest sorption activity was 88.60% for activated carbon, 35.71 for alpha cellulose, 17.87% for banana rachis fibre, and 8.70% for chitosan. The effect of the adsorbents dosage (1, 1.5, 2, 2.5, and 3 g/l) on decolourization of the CBB G-250 dye at the lower concentration (50 mg/l) was tested. At the adsorbents dosage of 3 g/l, the highest level was 84.4% for activated carbon, followed by 65.5% for banana rachis fibre, 56.3% for chitosan; and lastly 50% for alpha cellulose. At the high concentration (800 mg/l), the highest activity was 79.3% for activated carbon, followed by 33.7% for chitosan, 28.1% for alpha cellulose, and lastly 19.5% for banana rachis fibre. The highest capacity of adsorption of CBB G-250 dye recorded using different adsorbents determined by isotherm studies at an equilibrium concentration at 30 °C and pH 6.59 - 6.71 were: chitosan 32.60 mg/g, banana rachis fibre 35.87 mg/g, alpha cellulose 39.13 mg/g, and activated carbon 48.07 mg/g. The adsorption isotherms with activated carbon, alpha cellulose, banana rachis fibre, and chitosan can be described better by the Langmuir model with correlation coefficients ( $R^2 = 0.9984, 0.998, 0.9661, \text{ and } 0.9474$ , respectively) than the corresponding Freundlich correlation coefficients. However, banana rachis fibre, activated carbon, alpha cellulose and chitosan were also explained by the Freundlich correlation coefficients ( $R^2 = 0.9866, 0.9542, 0.9449, \text{ and } 0.9387$ , respectively) since they did not differ much from the corresponding Langmuir values.

*Keywords:* Coomassie brilliant blue, Adsorption, Standard curve, Isotherms.

## 3.2. Introduction

Many industries outlets especially textiles, paper, plastics, leather, food, cosmetics, etc., use dyes to colour their final products. Removal of dyes from effluents is environmentally important and that is where adsorption can play a role as an efficient method for the removal of dyes. These experiments were designed to determine the concentration of the dye, the effect of concentration of dye as well as adsorbent dosages on the adsorption process, the equilibrium time for CBB dye adsorption followed by the sorption capacity determination of the materials (banana rachis fiber, alpha cellulose, chitosan, and activated carbon) for the CBB G-250 dye (Bradford Protein Assay, 2018).

The effect of the different adsorbents (chitosan, alpha cellulose, banana rachis fibre, and activated carbon) dosages (1, 1.5, 2, 2.5, and 3 g/l) on decolourization of the CBB G-250 dye were investigated. The capacity of adsorption of CBB G-250 dye using different adsorbents (chitosan, alpha cellulose, banana rachis fibre, and activated carbon) were determined by isotherm studies at an equilibrium concentration. Langmuir and Freundlich adsorption isotherms were used to investigate the relationship between the concentration of sorbed species and the sorption capacity of adsorbents (chitosan, alpha cellulose, banana rachis fibre, and activated carbon) for CBB dye after dye adsorption equilibrium was attained.

## 3.3. Materials and Methods

### 3.3.1. Dye stock solution and construction of a standard CBB G-250 dye curve

A stock solution of 800 mg/l was prepared by dissolving the required amount of dye (0.8 g) in distilled water using a one liter volumetric flask to which was added 6 drops of absolute ethanol to facilitate dissolution of the dye. Distilled water was added until the meniscus reached the mark. The solution was mixed well. A number of standards was prepared from the stock solution by accurate serial dilutions using automatic pipette. The dye stock solution was stored in a dark place and the standards were prepared fresh each time the experiment is carried out. A calibration curve was drawn by measuring the absorbance of each dilution at a wavelength of 600 nm (wavelength at which maximum adsorption was obtained) was plotted (Bradford, 1976). Adsorption as a function of known dye concentration for each dye solution using a spectrophotometer operated at 600 nm was plotted (Bradford, 1976).

### 3.3.2. Dye adsorption assessment methodology

Amount of 1, 1.5, 2, 2.5, and 3 g/l of the powdered rachis fibre, alpha cellulose, chitosan, and activated carbon were added to separate conical flasks, respectively, which contained 150 ml CBB dye. The replicate samples containing 1, 1.5, 2, 2.5, and 3 g/l of the powdered rachis fibre, alpha cellulose, chitosan, and activated carbon were prepared. Each adsorbent dosage mentioned above was tested using a concentration series of dye from 50 mg/l up to 800 mg/l. The flasks were agitated at 150 rpm at 30 °C on an incubator shaker. Samples were drawn after 80 minutes and centrifuged at 3500 rpm for 10 minutes. Samples were diluted with distilled water (2:3  $\mu$ l, sample:distilled water) and the absorption read at 600 nm. A graph of decolourisation of dye (%) against dosage of adsorbents (g/l) was constructed and used to determine the percentage of decolourisation of dye. The percentage decolourisation of dye was calculated using equation (1) (Forootanfar *et al.*, 2016):

$$\text{Percentage of decolourisation} = [(A_i - A_t) / A_i] \times 100\% \quad (1)$$

where  $A_i$  is the initial absorbance of the dye and  $A_t$  is the absorbance of the dye at any time interval in aqueous solution.

### 3.3.3. Equilibrium time sorption experiments

Amount of 3 g/l of the powdered rachis fibre, alpha cellulose, chitosan, and activated carbon were added to separate conical flasks, which contained 150 ml CBB dye. The adsorbent dosage mentioned above was tested using various concentration of dye, 50 mg/l and 800 mg/l. The flasks were agitated at 150 rpm at 30 °C on an incubator shaker. The replicate samples containing 3 g/l of the powdered rachis fibre, alpha cellulose, chitosan, and activated carbon were prepared. Samples were drawn at regular time intervals (0, 5, 10, 15, 20, 25, 30, 35, 40, 45, 50, 60, 80 minutes) and centrifuged at 3500 rpm for 10 minutes (Ata *et al.*, 2012). Samples were diluted and the absorption read at 600 nm. A graph of absorption against time was constructed and used to determine the time taken to reach equilibrium. Equilibrium was attained when no significant changes in absorbance readings were observed over time.

### 3.3.4. Adsorption Isotherm Studies

#### 3.3.4.1. Equilibrium studies

The amount of dye sorbed at equilibrium per unit mass,  $q_e$  (mg/g) was calculated as shown below:

$$q_e = (C_0 - C_e) \times V/W \quad (2)$$

where  $C_0$  and  $C_e$  (mg/l) are the liquid-phase concentrations of CBB at initial and equilibrium, respectively.  $V$  (in litres) is the volume of the solution and  $W$  (g) is the mass of dry sorbent used (Gupta *et al.*, 2004).

#### 3.3.4.2. Langmuir and Freundlich isotherms

The adsorption of Coomassie Brilliant Blue on rachis banana fibres, alpha cellulose, chitosan, and activated carbon were studied separately as a function of different CBB concentrations, 100 mg/l, 200 mg/l, 400 mg/l and 800 mg/l. All other parameters were kept constant, namely: shaking time (80 minutes) and sorbent concentration (3 g/l). A volume of 150 ml of CBB (100 mg/l, 200 mg/l, 400 mg/l and 800 mg/l) solution was agitated with 3 g/l of different samples separately until equilibrium was reached on a shaker. After equilibrium was reached, the samples were centrifuged.

The replicate samples containing 3 g/l of rachis fibres, alpha cellulose, chitosan, and activated carbon were prepared. Samples were diluted and the absorption read at 600 nm. Langmuir and Freundlich, adsorption isotherms were used to investigate the relationship between the concentration of sorbed species and the sorption capacity of banana rachis fibre, alpha cellulose, chitosan, and activated carbon for CBB dye. The experimental data were used to graph the Langmuir, and Freundlich equilibrium models. The applicability and suitability of applying the linearized isotherm models to the data were compared by evaluating the values of the Langmuir and Freundlich correlation coefficients ( $R^2$ ) in each case, (Abdel-Ghani *et al.*, 2017). The highest value of  $R^2$  indicates the more correct model. The two tested model equations are summarized in Table 3.1.

**Table 3.1: The equilibrium models equations**

Model	Equation	Parameters
Langmuir	$\frac{C_e}{q_e} = \frac{1}{b q_{max}} + \frac{C_e}{q_{max}}$	$q_{max}$ is the amount of dye adsorbed per unit mass of adsorbent (mg/g) $b$ is the Langmuir constant related to the adsorption capacity (L/g) $C_e$ is the concentration of adsorbate in the solution at equilibrium (mg/L) $q_m$ is the maximum uptake per unit mass of carbon (mg/g) (Abdel-Ghani <i>et al.</i> , 2017).
Freundlich	$\ln q_e = \ln K_f + (1/n) \ln C_e$	$C_e$ and have the same meaning as in the Langmuir isotherm $K_f$ is the Freundlich constant. $n$ is the empirical parameter representing the energetic heterogeneity of the adsorption sites (Hameed <i>et al.</i> , 2008b).

### 3.4. Results and Discussions

#### 3.4.1. Adsorption Equilibrium and Isotherm studies

##### 3.4.1.1. Standard CBB G-250 dye curve

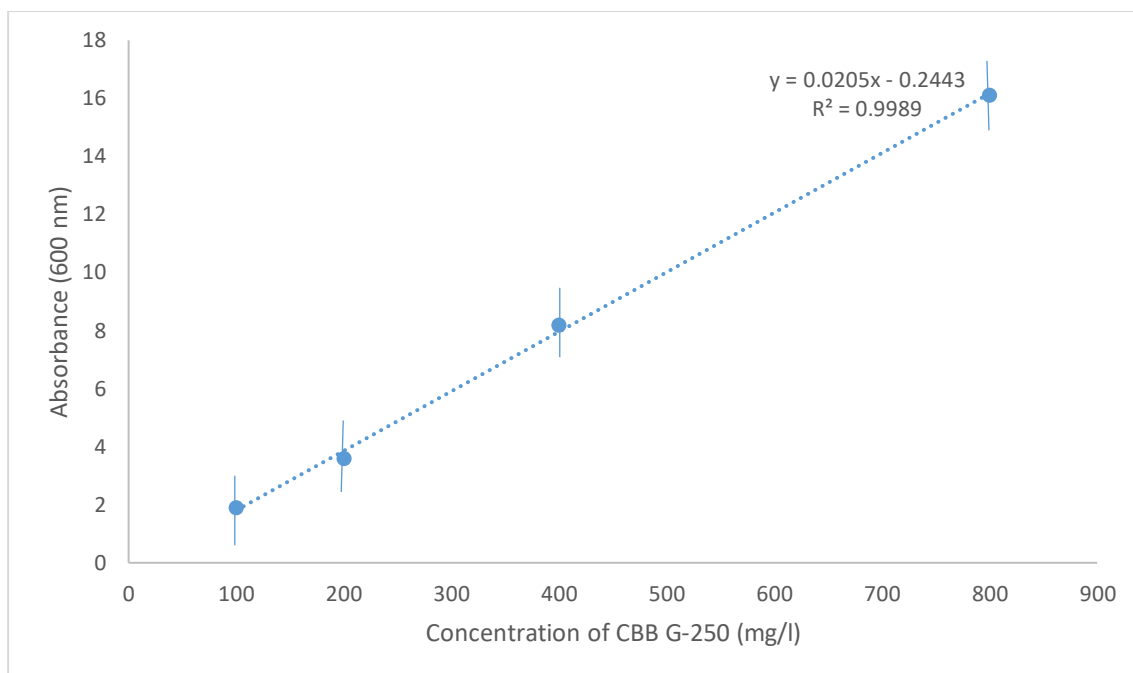


**Figure 3.1: The standard curve of CBB G-250 dye at a concentration of 800 mg/l**

A linear relationship between absorbance and concentrations (Figure 3.1). Samples were diluted 25 times before adsorption values were taken. Therefore, the absorbance is directly dependent on the concentration of the dye. The standard curve would be used to calculate the subsequent experiments. It was constructed using averages of duplicate adsorption values.

The concentration of dye was calculated using the formula obtained by linear regression analysis from the standard straight line graph above as follows:

$$Y = mx + c \text{ (straight line equation)}$$

$$Y = 0.0205x - 0.2443$$

where 'y' indicates absorbance of samples at 600 nm and 'x' indicates concentration of dye in mg/l.



### 3.4.2. Effect of the various adsorbent dosage on decolourization of the CBB G-250 dye

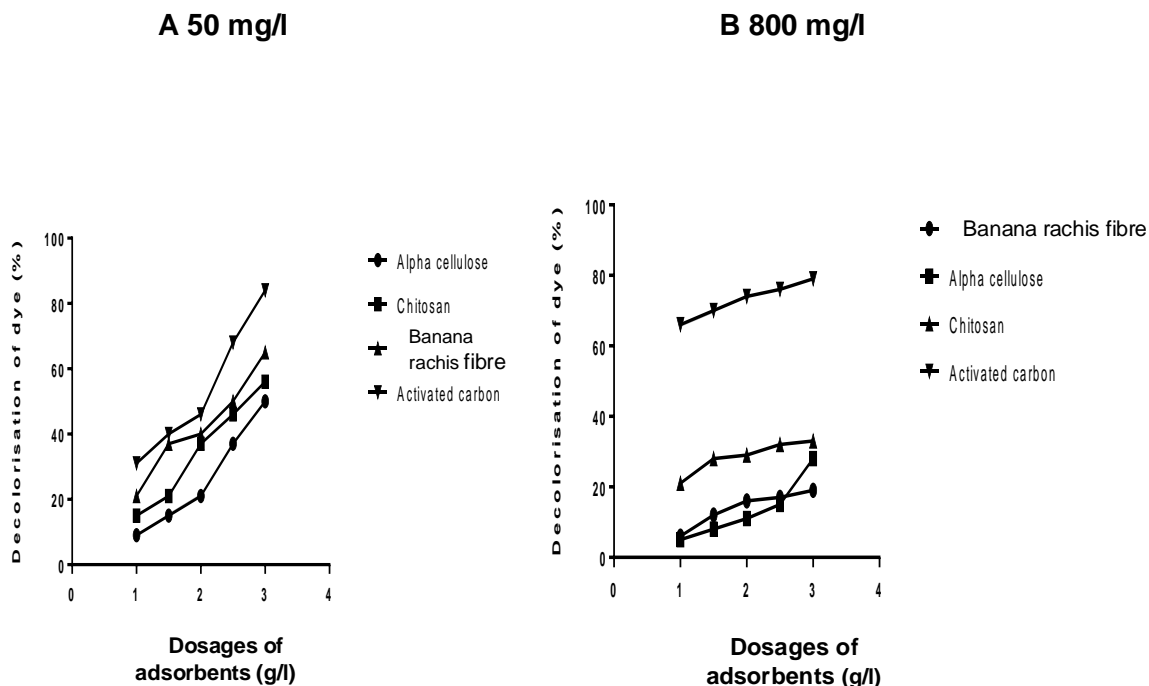


**Figure 3.2: Effect of adsorbent dosage on decolourisation of CBB G-250 dye (%) using various adsorbents A. 50 mg/l and B. 800 mg/l**

The effect of various adsorbents dosage on decolourisation of CBB G-250 dye (%), Figure A. adsorption at a low concentration of 50 mg/l. Figure B. adsorption using concentration of 800 mg/l using different adsorbents (alpha cellulose, chitosan, banana rachis fibre, and activated carbon) dosages after 80 minutes, 30 °C, and pH 6.59 - 6.71 and 1, 1.5, 2, 2.5, 3 g/l adsorbents dosages (Figure 3.2 A and B). The figure 3.2 A and B shows the adsorption of CBB G-250 dye (%) reading over (against) different dosage of adsorbents during sorption experiments as indicated above.

#### Low concentration (50 mg/l) of CBB G-250 dye

##### Percentage of the decolourisation (alpha cellulose)

The low concentration is represented by 50 mg/l.  $A_i$  represents Initial absorbance of the dye and  $A_t$  represents absorbance of the dye at any interval at the adsorbents dosages of 1, 1.5, 2, 2.5, 3 g/l.

$$\text{Decolourization (\%)} = \frac{A_i - A_t}{A_i} \times 100\%$$

$$\begin{aligned}
 & A_i \\
 &= 0.032 - 0.016 \\
 & \dots\dots\dots \times 100\% \\
 & 0.032 \\
 &= 50\%
 \end{aligned}$$

The percentage of the decolourization for alpha cellulose at a dosage of 3 g/l was 50%.

$$\begin{aligned}
 \text{Decolourization (\%)} &= A_i - A_t \\
 & \dots\dots\dots \times 100\% \\
 & A_i \\
 &= 0.032 - 0.020 \\
 & \dots\dots\dots \times 100\% \\
 & 0.032 \\
 &= 37.5\%
 \end{aligned}$$

The percentage of the decolourization for alpha cellulose at a dosage of 2.5 g/l was 37.5%.

$$\begin{aligned}
 \text{Decolourization (\%)} &= A_i - A_t \\
 & \dots\dots\dots \times 100\% \\
 & A_i \\
 &= 0.032 - 0.025 \\
 & \dots\dots\dots \times 100\% \\
 & 0.032 \\
 &= 21.9\%
 \end{aligned}$$

The percentage of the decolourization for alpha cellulose at a dosage of 2 g/l was 21.9%.

$$\text{Decolourization (\%)} = A_i - A_t$$

$$\dots\dots\dots \times 100\%$$

$$A_i$$

$$= 0.032 - 0.027$$

$$\dots\dots\dots \times 100\%$$

$$0.032$$

$$= 15.6\%$$

The percentage of the decolourization for alpha cellulose at a dosage of 1.5 g/l was 15.6%.

$$\text{Decolourization (\%)} = A_i - A_t$$

$$\dots\dots\dots \times 100\%$$

$$A_i$$

$$= 0.032 - 0.029$$

$$\dots\dots\dots \times 100\%$$

$$0.032$$

$$= 9.4\%$$

The percentage of the decolourization for alpha cellulose at a dosage of 1 g/l was 9.4%.

The equation to calculate the percentage of the decolourization of the CBB G-250 dye for the alpha cellulose at the dosages of 3, 2.5, 2, 1.5, and 1 g/l is similar to the calculations for the other adsorbents (chitosan, banana rachis fibre, and activated carbon) their calculations are found in the Appendix section, respectively, were performed similarly as shown above.

The decolourization of CBB G-250 dye by adsorption on alpha cellulose, chitosan, activated carbon and banana rachis fibre was found to increase with the adsorbent dose/charge and attained at over 80 minutes testing time period. At the lower concentration (50 mg/l) the percentage decolourization of the CBB G-250 dye increases from 9.4 to 50.0% alpha cellulose, 15.6 to 56.3% for chitosan, 21.9 to 65.6% for banana rachis fibre, and 31.6 to 84.4% for activated carbon. For the batch adsorption experiments on alpha cellulose, chitosan, activated carbon, and banana rachis fibre, the effect of adsorbent dosage on the CBB G-250

dye adsorption by alpha cellulose, chitosan, activated carbon, and banana rachis fibre were examined.

Significant variations in the uptake capacity and removal efficiency are observed at different adsorbent dosages (1, 1.5, 2, 2.5, 3 g/l) indicating that the highest concentration tested is obtained with an adsorbent dosage of (3 g/l) (Figure 3.2 A and B). The reason for the apparent systematic dip at 2g/l is to check the removal of CBB G-250 dye at different adsorbent dosages, the more the adsorbent dosages increase the more the dye is removed. This result was expected because the removal efficiency is generally increased by the fact that the more mass available, the more the contact surface offered to the adsorbent.

### **High concentration (800 mg/l) of CBB G-250 dye**

The equation to calculate the percentage of the decolourisation of the CBB G-250 dye (800 mg/l) for the alpha cellulose, chitosan, activated carbon and banana rachis fibre at the dosages of 3, 2.5, 2, 1.5, and 1 g/l is similar to the calculations for the other adsorbents (alpha cellulose, chitosan, activated carbon, and banana rachis fibre) their calculations are found in the Appendix section, respectively were performed similarly as shown on the low concentration (50 mg/l) of CBB G-250 dye above.

At a high concentration CBB G-250 dye (800 mg/l) using a adsorbent dosage of 3 g/l, the percentage decolourization at equilibrium also decreased compared to low concentration (50 mg/l) tested from 28.1 to 50.0% for alpha cellulose dosage, 33.7 to 56.3% for chitosan, 19.5 to 65.6% for banana rachis fibre, and 79.3 to 84.4% for activated carbon. As the low concentration (50 mg/l) of Coomassie Brilliant Blue dye was increased, the absorbance efficiency was decreased (Figure 3.2 A and B).

This may be due to the fact that at lower concentrations almost all the dye molecules were adsorbed very quickly on the outer surface, but further increases in the low CBB G-250 dye concentrations led to fast saturation of the adsorbents (alpha cellulose, chitosan, banana rachis fibre, and activated carbon) surface, and thus most of the dye adsorption apparently took place slowly inside the pores (Hameed and El-Khaiary, 2008; Khaleque and Roy, 2016). For the batch adsorption experiments on alpha cellulose, chitosan, banana rachis fibre, and

activated carbon, the effect of adsorbent dosage on the CBB G-250 dye adsorption were examined.

Significant variations in the uptake capacity and removal efficiency are observed at different adsorbent dosages (1 to 3 g/l). This would indicate that the highest concentration tested is obtained with an adsorbent dosage of 3 g/l (Figure 3.2 A and B). It was observed that as the dosage of adsorbent was increased, the removal efficiency became higher (Figure 3.2 A and B). Increase in the removal efficiency of Coomassie brilliant blue dye with the increased amount of adsorbent dose is due to the increased surface area and the availability of additional adsorption sites (Khaleque and Roy, 2016). The percentage of decolourisation of alpha cellulose, chitosan, banana rachis fibre, and activated carbon at an initial concentration (50 mg/l) and highest concentration (800 mg/l) are shown in Table 3.2.

**Table 3.2: The percentage of decolourisation of different adsorbents at different concentrations**

Adsorbents	Percentage decolourisation (%)									
	Initial concentration (50 mg/l)					Highest concentration (800 mg/l)				
	1	1.5	2	2.5	3	1	1.5	2	2.5	3
Dosages (g)										
Alpha cellulose	9.4	15.6	21.9	37.5	50	5.3	8.7	11.1	15.1	28.1
Chitosan	15.6	21.9	37.5	46.9	56.3	21.0	28.3	29.1	32.3	33.7
Banana rachis fibre	21.9	37.5	40.6	50	65.6	6.6	12.7	16.5	17.2	19.5
Activated carbon	31.6	40.6	46.9	68.8	84.4	66.8	70.2	74.3	76.8	79.3

### 3.4.3. Equilibrium time sorption experiments

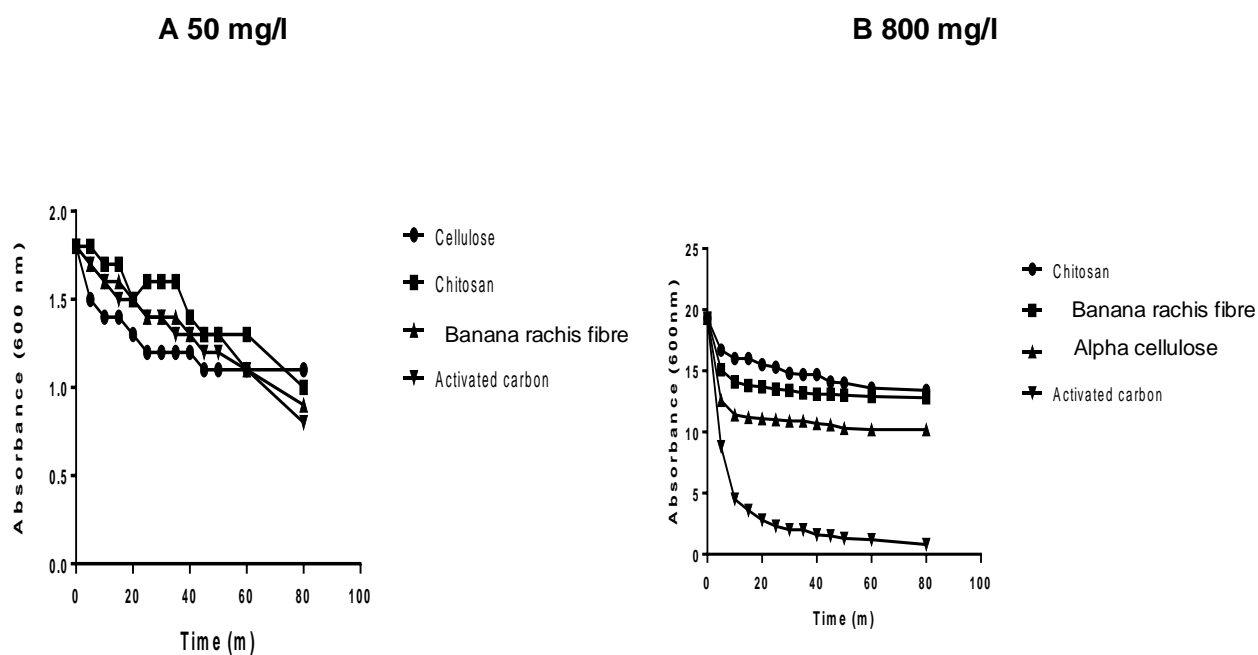


**Figure 3.3: Effect of contact time on adsorption of the CBB G-250 dye (A. 50 mg/l and B. 800 mg/l) using various adsorbents**

Figure 3.3 A. shows adsorption at an initial concentration of 50 mg/l CBB, while Figure 3.3 B. Adsorption using a concentration of 800 mg/l CBB, for various adsorbents (activated carbon, cellulose, banana rachis fibre and chitosan) after 80 minutes, 30 °C, and pH 6.59 - 6.71 and 3 g/l adsorbent dosage. The figures (3.3 A and B) below shows the absorbance reading over time obtained during sorption experiments conducted with the sorbents indicated above.

The adsorption at an initial concentration of 50 mg/l CBB using various adsorbents (cellulose, chitosan, banana rachis fiber and activated carbon) was very slow, the equilibrium was not yet reached (Figure 3.3 A). As stated by Gabelman, (2017), the adsorption process is exothermic, the temperature significantly affects the amount of adsorbate absorbed. Based on Le Chatelier's principle, operation of exothermic processes at higher temperature favors conditions that evolve less heat. The temperature 30 °C which was used here at this study was high, because at a given pressure, the amount of adsorbate adsorbed at equilibrium decreases with increasing temperature which leads to the equilibrium not yet reached. For this reason, adsorption processes are usually operated at room temperature.

### Concentration tested initially (50 mg/l)

After about 45 minutes and 50 minutes the data presented in Figure. 3.3 A. shows that equilibrium was not yet reached. Absorbance of dye after 45 minutes using alpha cellulose and banana rachis fibre and 50 minutes using chitosan and activated carbon. The sorption activity of the dye by the adsorbents is calculated below:

$$\text{Absorbance} = 0.0205x - 0.24443$$

Therefore: X (Concentration of the CBB G-250 dye) = Absorption + 0.2443

$$\begin{aligned} & \text{-----} \\ & 0.0205 \\ & = (0.022 \times 25) + 0.2443 \\ & \text{-----} \\ & 0.0205 \\ & = 38.75 \text{ mg/l} \end{aligned}$$

The concentration of dye at equilibrium ( $C_e$ ) is therefore 38.75 mg/l for the alpha cellulose.

The equation to calculate the percentage sorption activity of the alpha cellulose is:

$$\begin{aligned} \% \text{ Sorption activity} &= C_0 - C_e \\ & \text{-----} \times 100 \\ & C_0 \end{aligned}$$

where  $C_0$  is the initial dye concentration and  $C_e$  is the dye concentration at equilibrium. Therefore,

$$\begin{aligned} \% \text{ Sorption activity} &= 50 \text{ mg/l} - 38.75 \text{ mg/l} \\ & \text{-----} \times 100 \\ & 50 \text{ mg/l} \\ & = 22.5\% \end{aligned}$$

The percentage sorption activity of alpha cellulose is therefore 22.5%.

The equation to calculate the percentage sorption activity of the alpha cellulose is similar to the calculations for the other adsorbents (activated carbon, banana rachis fibre, and chitosan) their calculations are found in the Appendix section, and were performed similarly as shown above.

### Highest concentration of dye tested during adsorption experiments (800 mg/l)

After about 45 minutes (alpha cellulose and banana rachis fibre) and 50 minutes (chitosan and activated carbon), Figure 3.3 B. shows that equilibrium was reached. The value can be substituted in the equation derived from the CBB standard curve.

$$\text{Absorbance} = 0.0205x - 0.2443$$

Therefore: X (Concentration of the CBB G-250 dye) = Absorption + 0.2443

$$\begin{aligned} & \frac{\text{-----}}{0.0205} \\ & = \frac{(0.065 \times 25) + 0.2443}{0.0205} \\ & = 91.19 \text{ mg/l} \end{aligned}$$

The concentration of dye at equilibrium ( $C_e$ ) is therefore 91.19 mg/l for the activated carbon.

The equation to calculate the percentage sorption activity of activated carbon is:

$$\begin{aligned} \% \text{ Sorption activity} &= \frac{C_0 - C_e}{C_0} \times 100 \end{aligned}$$

where  $C_0$  is the initial dye concentration and  $C_e$  is the dye concentration at equilibrium.

Therefore,

$$\begin{aligned} \% \text{ Sorption activity} &= \frac{800 \text{ mg/l} - 91.18 \text{ mg/l}}{800 \text{ mg/l}} \times 100 \\ &= 88.60\% \end{aligned}$$

The percentage sorption activity of activated carbon is therefore 88.60%.



The equation to calculate the percentage sorption activity of the activated carbon is similar to the calculations for the other adsorbents (alpha cellulose, banana rachis fibre, and chitosan) their calculations are found in the Appendix section, and were performed similarly as show above.

The percentage sorption activity of CBB G-250 dye increases with time and attains a maximum value after 45 minutes and 50 minutes and thereafter, it reaches a constant value indicating that no more CBB G-250 dye is removed from the solution. Therefore, changing the initial concentration of dye from 50 to 800 mg/l, the adsorbed amount increases from 0.56% to 11.77% for chitosan, 12.76% to 17.87% for banana fibre, 22.5% to 35.71% for alpha cellulose, 17.62% to 88.60% for activated carbon.

This may be attributed to an increase in the driving force of the concentration gradient with increasing the initial basic dye concentration in order to overcome the mass transfer resistance of CBB G-250 dye between the aqueous and solid phases (Moussa *et al.*, 2015). The percentage of sorption activity (%) of different adsorbents at lowest concentration (50 mg/l) and highest concentration (800 mg/l) are shown in Table 3.3.

**Table 3.3: Percentage sorption activity and equilibrium ( $C_e$ ) of adsorbents at the lowest and highest CBB dye concentrations used**

Adsorbents	Sorption activity (%)		Equilibrium concentration $C_e$ (mg/l)	
	Low concentration	High concentration	Low concentration	High concentration
Chitosan	0.56	11.77	49.72	705.82
Banana rachis fibre	12.76	17.87	43.62	657.0
Activated carbon	17.62	88.60	41.19	91.91
Alpha cellulose	22.50	35.71	43.62	514.36

#### 3.4.4. Isotherm studies

From the results obtained following isotherm studies the capacity of adsorption of CBB G-250 dye using chitosan, were calculated as follows (for chitosan): The equation to calculate the capacity of adsorption of CBB G-250 dye at different concentrations 100, 200, 400, and 800 mg/l for the chitosan at the dosage of 3 g/l is similar to the calculations for the other adsorbents

(alpha cellulose, banana rachis fibre, and activated carbon) their calculation are found in the Appendix section, and were performed similarly as shown below.

1.  $q_e$  for 100 mg/l

$$\begin{aligned}q_e &= (C_0 - C_e) \times V/W \\&= (100 - 69) \times (2/6) \\&= 10.33 \text{ mg/g}\end{aligned}$$

2.  $q_e$  for 200 mg/l

$$\begin{aligned}q_e &= (C_0 - C_e) \times V/W \\&= (200 - 158.3) \times (0.3333) \\&= 13.90 \text{ mg/g}\end{aligned}$$

3.  $q_e$  for 400 mg/l

$$\begin{aligned}q_e &= (C_0 - C_e) \times V/W \\&= (400 - 31.0) \times (0.3333) \\&= 27.33 \text{ mg/g}\end{aligned}$$

4.  $q_e$  for 800 mg/l

$$\begin{aligned}q_e &= (C_0 - C_e) \times V/W \\&= (800 - 702.2) \times (0.3333) \\&= 32.60 \text{ mg/g}\end{aligned}$$

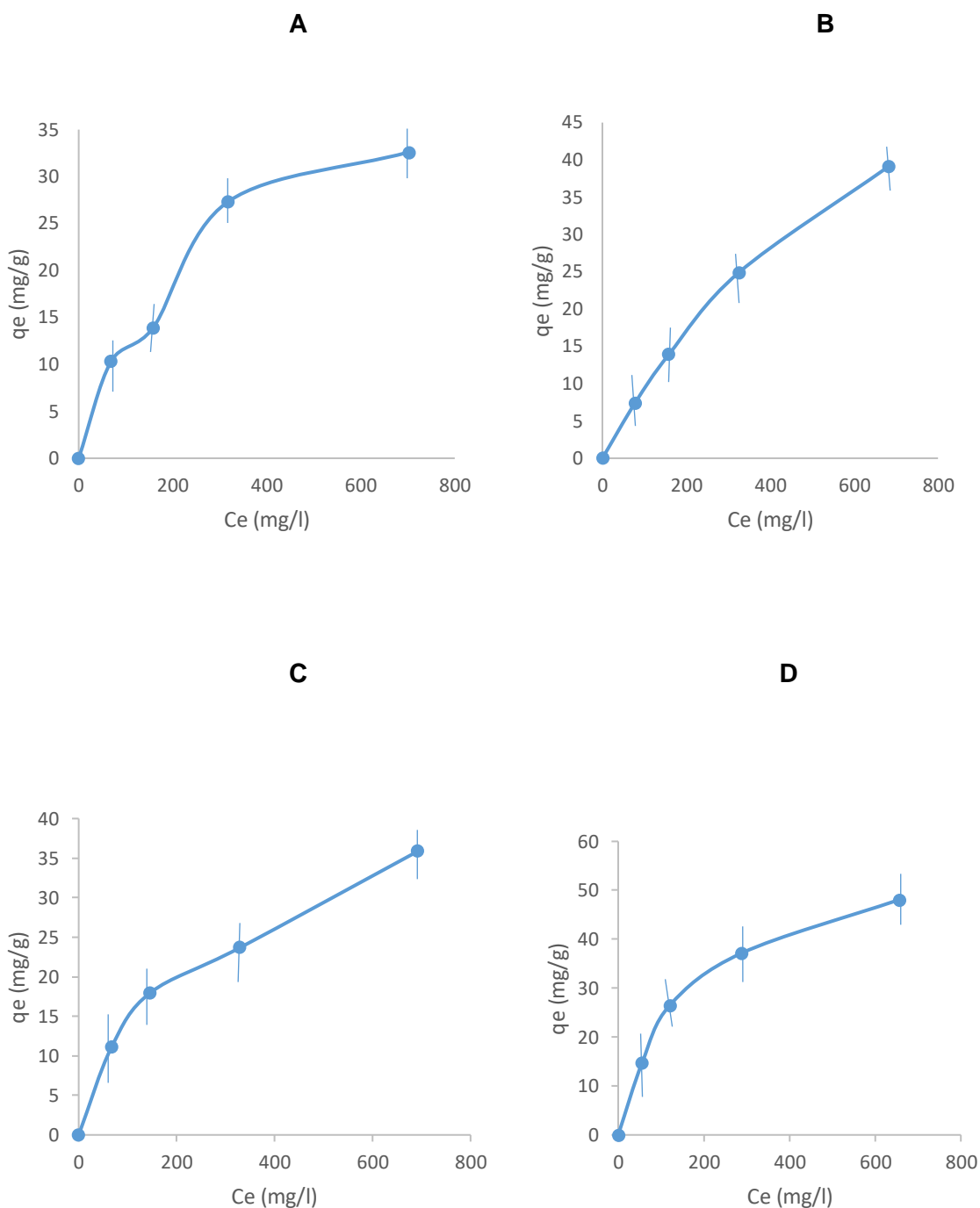


**Figure 3.4: Adsorption isotherm of CBB G-250 dye (800 mg/l),  $q_e$  (capacity of sorbent) versus  $C_e$  (Equilibrium dye concentration) using various adsorbents A. Chitosan, B. Alpha cellulose, C. Banana rachis fibre, and D. Activated carbon**

The capacity of adsorption of CBB G-250 dye (800 mg/l) using various adsorbents (chitosan and activated carbon) after 50 minutes and also for various adsorbents (alpha cellulose and banana rachis fibre) after 45 minutes, 30 °C, pH 6.59 - 6.71 and 3 g/l adsorbent dosage, when equilibrium was reached as was already determined previously (Figure 3.4 A to D). It reached saturation point at a CBB dye concentration of 702.2, 682.6, 692.4, and 655.8 mg/l for chitosan, alpha cellulose, banana rachis fibre and activated carbon, respectively, expect for the alpha cellulose it didn't reach the saturation. At this concentration (702.2, 682.6, 692.4, and 655.8 mg/l) the chitosan, alpha cellulose banana rachis fibre and activated carbon, respectively, adsorption reached the point where less and less CBB G-250 dye is further removed from the solution as initial dye concentration levels increases.

The capacity of adsorption of CBB G-250 dye using chitosan, alpha cellulose, banana rachis fibre, and activated carbon was found to increase with time and approach a constant value at 45 minutes (Figure 3.4 A to D). On changing the initial concentration of CBB G-250 dye solution from 100 to 800 mg/l, the amount adsorbed increased from 10.33 to 32.60 mg/g for chitosan, 7.40 to 39.13 mg/g for alpha cellulose, 11.07 to 35.87 mg/g for banana rachis fibre, and 14.73 to 48.07 mg/g for activated carbon. Activated carbon seems to be having a higher capacity of adsorption followed by banana rachis fibre, alpha cellulose, and chitosan (Santhi *et al.*, 2011). The capacity of adsorption of CBB G-250 dye using different adsorbents at an equilibrium concentration is shown in Table 3.4.

**Table 3.4: The capacity of adsorption of CBB G-250 dye using different adsorbents at an equilibrium concentration**

Adsorbents	Capacity of adsorption of CBB G-250 dye (mg/g)				Equilibrium concentration $C_e$ (mg/l)			
	100	200	400	800	100	200	400	800
Chitosan	10.33	13.90	27.33	32.60	69	158.3	318.0	702.2
Alpha cellulose	7.40	13.9	24.90	39.13	77.8	158.3	325.3	682.6
Banana rachis fibre	11.07	17.97	23.67	35.87	66.8	146.1	329	692.4
Activated carbon	14.73	26.50	37.17	48.07	55.8	120.5	288.5	655.8

### 3.4.5. Langmuir and Freundlich isotherms

Two isotherm equations are tested in this work. One is the Langmuir and the Freundlich equations are commonly used for the describing adsorption equilibrium of adsorbate onto the adsorbent. The Langmuir isotherm is applicable to monolayer chemisorptions while Freundlich isotherm is used to describe adsorption on surface having heterogeneous energy distribution (Gupta *et al.*, 2011) (Figure 3.5 A to D, Figure 3.6 A to D).

Under the conditions tested in this work the following results were obtained for the Langmuir model in batch experiments.

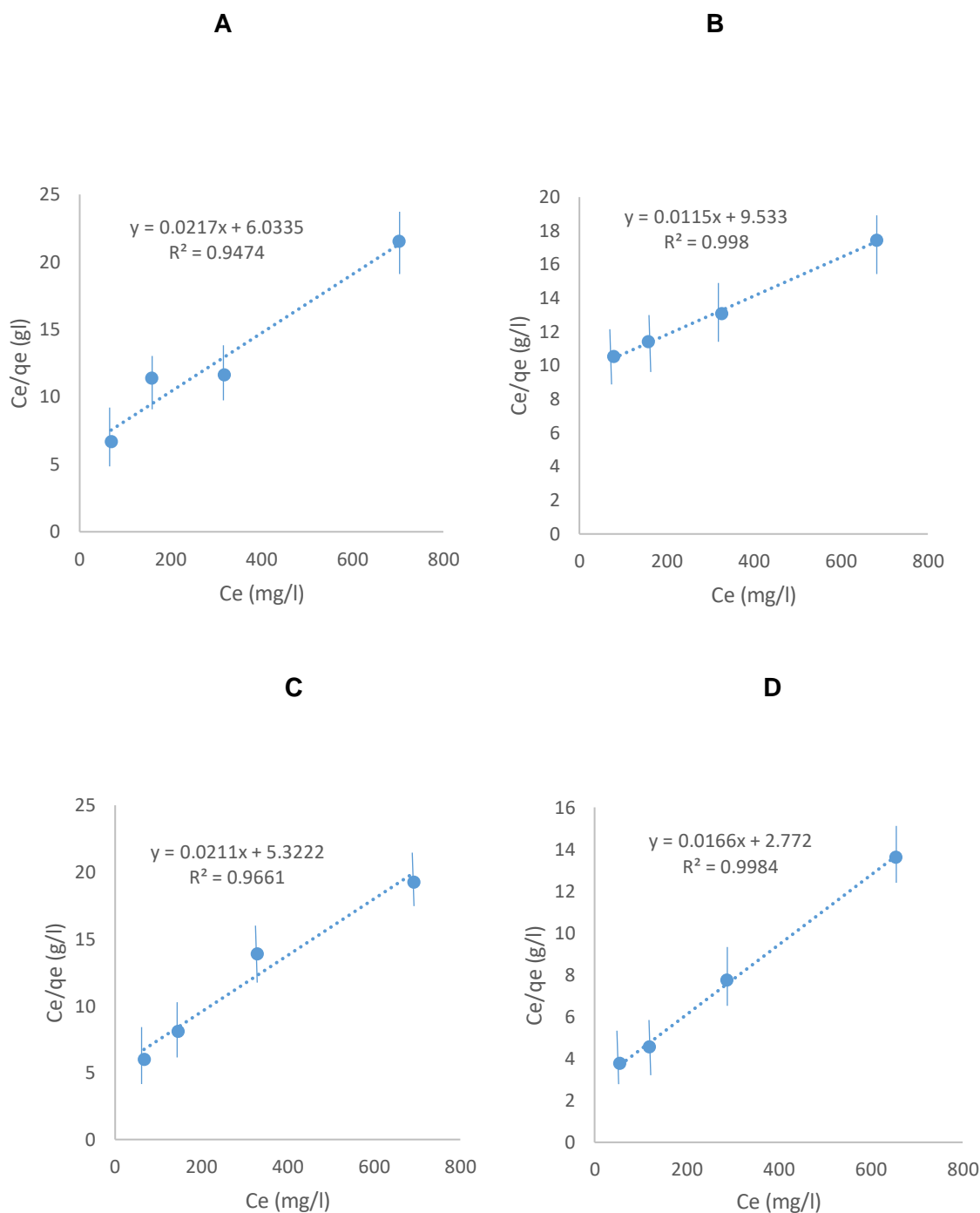


**Figure 3.5: Linearised version of Langmuir isotherm of various adsorbents A. Chitosan, B. Alpha cellulose, C. Banana rachis fibre, and D. Activated carbon**

The adsorption of CBB G-250 dye using various adsorbents (chitosan and activated carbon) after 50 minutes and also using various adsorbents (alpha cellulose and banana rachis fibre) after 45 minutes, 30 °C, pH 6.59 – 6.71 and 3 g/l adsorbent dosage (Figure 3.5 A to D).

To investigate the fitting of Langmuir model for the equilibrium data of CBB G-250 dye sorption a linearized form of the model was employed. The correlation coefficient was found to be 0.9474, 0.998, 0.9661, and 0.9984 for chitosan, alpha cellulose, banana rachis fibre and activated carbon, respectively, indicating that the data was fitted well using the Langmuir

model. It is observed that the activated carbon linearized Langmuir isotherm showed higher value of correlation coefficient ( $R^2 = 0.9984$ ) than that of the other three linearized Langmuir isotherm.

The closer the value is to 1, the better the fit, or relationship, between the two factors. The goodness of fit, or the degree of linear correlation, measures the distance between a fitted line on a graph and all the data points that are scattered around the graph. A good fit has an  $R^2$  that is close to 1 ([www.investopedia.com/terms/C/coefficient-of-determination.asp](http://www.investopedia.com/terms/C/coefficient-of-determination.asp)). From the Langmuir plot, capacity of adsorption was found to be 32.60, 39.13, 35.87, and 48.7 mg/g for chitosan, alpha cellulose, banana rachis fibre, and activated carbon, respectively. A plot of  $1/q_e$  versus  $1/C_e$  gives  $b$  and  $q_{max}$  if the isotherm follows the Langmuir equation (Annadurai *et al.*, 2002) (Figure 3.5 A to D).

Under the conditions tested in this work the following results were obtained for the Freundlich model in batch experiments.

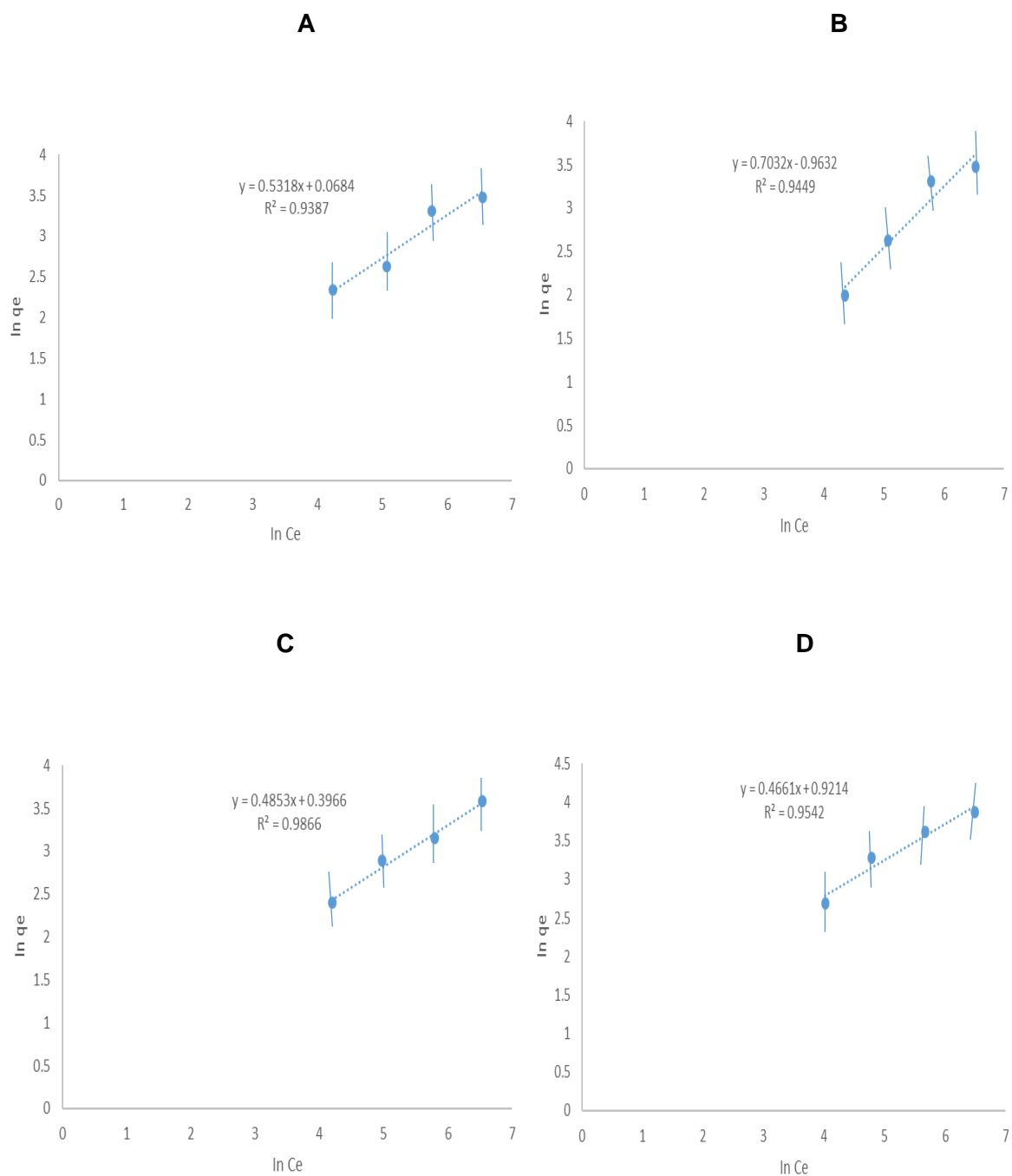


**Figure 3.6: Freundlich isotherm of various adsorbents A. Chitosan, B. Alpha cellulose, C. Banana rachis fibre, and D. Activated carbon**

The adsorption isotherm of CBB G-250 dye using various adsorbents (chitosan and activated carbon) after 50 minutes and also using various adsorbents (alpha cellulose and banana rachis fibre) after 45 minutes, 30 °C, pH 6.59 – 6.71 and 3 g/l adsorbent dosage (Figure 3.6 A to D).

The correlation coefficient was found to be 0.9387, 0.9449, 0.9866, and 0.9542 for chitosan, alpha cellulose, banana rachis fibre and activated carbon, respectively, indicating that the data was fitted well using the Freundlich model (Figure 3.6 A and B). It is observed that the banana rachis fibre Freundlich isotherm showed higher value of correlation coefficient ( $R^2 = 0.9866$ )

than that of the other three Freundlich isotherm. The intercept  $K_f$  obtained from plot of  $\log q_e$  versus  $\log C_e$  is roughly a measure of the sorption capacity and the slope ( $1/n$ ) of the sorption intensity. It was indicated magnitude of the term ( $1/n$ ) gives an indication of the favorability and capacity of the adsorbent/adsorbate systems (Annadurai *et al.*, 2002) (Figure 3.6 A to D).

The adsorbents (chitosan, alpha cellulose, banana rachis fibre, and activated carbon) calculations for Langmuir and Freundlich isotherm parameters values are as follows: The equations to calculate the Langmuir and Freundlich isotherm parameters of CBB G-250 dye at different concentrations 100, 200, 400, and 800 mg/l for the chitosan at the dosage of 3 g/l is similar to the calculations for the other adsorbents (alpha cellulose, banana rachis fibre, and activated carbon) were performed similarly as shown below.

### Isotherm calculation methodology for Chitosan

Calculations for the Langmuir isotherm of chitosan proceeded as shown below:

$$R^2 = 0.9474$$

$$Y = 0.0217x + 6.0335 \text{ (Equation chitosan (A). Figure 3.5)}$$

Where according to the Langmuir equation given in Table 2 the following holds:

For the  $q_{\max}$  value:

$$1/q_{\max} = 0.0217 \text{ and taking the inverse yields:}$$

$$q_{\max} = 46.08$$

Furthermore, from the Langmuir equation given below:

$$C_e/q_e = 1/b \cdot q_{\max} + C_{eq}/q_{\max}$$

For the b value:

$$\frac{1}{b \cdot q_{\max}} = 6.0335$$

Take the inverse:



$$b \cdot q_{\max} = 0.1657$$

$$b = 0.1657/q_{\max}$$

$$b = 0.1657/46.08$$

$$b = 3.60$$

Calculations for the Freundlich isotherm of chitosan proceeded as shown below:

$$R^2 = 0.9387$$

$$Y = 0.5318x + 0.0684 \text{ (Equation chitosan (A). Figure 3.6) Experimental data}$$

Below is given the linear form of the Freundlich equation:

$$\ln q_e = \ln K_f + (1/n) \ln C_e$$

So that  $1/n = 0.5318$  from (Equation chitosan (A). Figure 3.6), take inverse:

$$n = 1.88$$

Also:

$$\ln K_f = 0.0684$$

$$e^{0.0684} = 1.07 = K_f$$

The Langmuir and Freundlich adsorption isotherm constants for the adsorption of CBB G-250 dye on chitosan, alpha cellulose, banana rachis fibre, and activated carbon is shown in Table 3.5.

**Table 3.5: Langmuir and Freundlich isotherm constants for the adsorption of CBB G-250 dye on various adsorbents**

Equilibrium model	Adsorbents	Correlation coefficients ( $R^2$ )	Parameters	Values
Langmuir isotherm	1. Chitosan	0.9474	b (l/mg)	1. 3.60 2. 1.21 3. 3.97 4. 5.99
	2. Alpha cellulose	0.998		
	3. Banana rachis fibre	0.9661	$q_{max}$ (mg/g)	1. 46.08 2. 86.96 3. 47.39 4. 60.24
	4. Activated carbon	0.9984		
Freundlich isotherm	1. Chitosan	0.9387	$K_f$ (l/g)	1. 1.07 2. 2.62 3. 1.49 4. 2.51
	2. Alpha cellulose	0.9449		
	3. Banana rachis fibre	0.9866	N	1. 1.88 2. 1.42 3. 2.06 4. 2.15
	4. Activated carbon	0.9542		

$R^2$  Correlation coefficient

b Empirical constant, indicating the affinity of sorbent towards the sorbate

$q_{max}$  Maximum possible amount of dye that can be adsorbed per unit dry weight of sorbent.

$K_f$  Empirical constant, indicates the adsorption capacity of the sorbent

n Constant indicating the intensity of adsorption

Comparing the adsorption isotherm of banana rachis fibre with the apricot stones activated carbon, wheat bran, and the coir pith an agricultural waste products (agricultural biosorbent), can be described better by the Langmuir model and Freundlich model, correlation coefficient  $R^2$  (0.9661, 0.96, 0.9735, and 0.9080) and (0.9866, 0.99, 0.9406, and 0.9828), respectively (Prasad *et al.*, 2008; Ata *et al.*, 2012; Moussa *et al.*, 2014) (Table 3.5).

By comparing the data obtained from the two studied equilibrium models, it can be concluded that in our study the adsorption of coomassie brilliant blue onto banana rachis fibre is best described in terms of the Langmuir isotherm model followed by the Freundlich isotherm model. From the equilibrium studies, it can be concluded that the Langmuir model is the best model for describing the adsorption of Coomassie dye by banana rachis fibre. The applicability of the Langmuir model suggests that the adsorption surface is applicable to monolayer chemisorptions (Gupta *et al.*, 2011). Our results are in agreement with the results of Ata *et al.* (2012) and Moussa *et al.* (2014) who also have reported the suitability of the Langmuir model to describe the adsorption of brilliant blue dye by different adsorbents.

Evaluation by Langmuir model of activated carbon, followed by alpha cellulose, banana rachis fibre, apricot stones activated carbon, chitosan and wheat bran have been found to undergo favourable adsorption than the coir pith. Evaluation by Freundlich model of apricot stones activated carbon, followed by banana rachis fibre, coir pith, activated carbon, alpha cellulose, and wheat bran, have been found to undergo favourable adsorption than the chitosan (Moussa *et al.*, 2014; Ata *et al.*, 2012).

Based on the correlation coefficient ( $R^2$ ) shown in Table 3.5, the adsorption isotherms with activated carbon, alpha cellulose, banana rachis fibre, and chitosan can be described better by the Langmuir, correlation coefficient  $R^2$  (0.9984, 0.998, 0.9661, and 0.9474, respectively) as bigger than the Freundlich correlation coefficient  $R^2$ . Correlation coefficient  $R^2$  is the proportion of the variance in the dependent variable that is predictable from the independent variable(s). This means that Langmuir model is more applicable than Freundlich model.

Comparing alpha cellulose, activated carbon, banana rachis fibre, chitosan, coir pith, apricot stones activated carbon, and wheat bran the Langmuir plot,  $q_{\max} = 86.96, 60.24, 47.39, 46.08,$  and  $31.847, 10.09, 6.410$  mg/g respectively and for the activated carbon, chitosan, wheat bran, banana rachis fibre, alpha cellulose, and coir pith,  $b = 5.99, 3.60, 3.502, 3.97, 1.21,$  and  $0.0926$

l/mg respectively (Prasad *et al.*, 2008). The results showed that activated carbon, followed by banana rachis fibre, chitosan, and alpha cellulose were good adsorbents of the CBB G-250 dye because the value of 'n' (2.15, 2.06, 1.88, and 1.42, respectively) were greater than 1. Comparing coir pith with the banana rachis fibre, the Freundlich isotherm best fitted the data with  $n = 2.8019$  and  $2.15$  respectively and  $K_f = 6.438$  and  $1.49$  respectively (Prasad *et al.*, 2008). According to Kadirvelu and Namasivayam (2000) n values between 1 and 10 represents beneficial adsorption and thus the adsorption of dye on the adsorbents. The 'n' value is a variable whose value when greater than one indicates good adsorbance activity. It comes from  $1/n$  the exponent of non-linearity of the Freundlich adsorption isotherm (Gupta *et al.*, 2011).

### 3.5. Conclusion

1. Removal of dyes from effluents becomes environmentally important and that is where adsorption can play a role as an efficient method for the removal of dyes. Adsorption is an important technique because of its simplicity and high efficiency, as well as the availability of a wide range of adsorbents. It has proven to be an effective method for removal of different dyes from waste materials.

2. The sorption activity as determined at a low concentration of 50 mg/l CBB dye was as follows: 17.52% for alpha cellulose, 12.76% for activated carbon, 5.88% for banana rachis fibre, 0.56% for chitosan. At the higher concentration (800 mg/l), the highest was 88.60% for activated carbon, 35.71% for alpha cellulose, 17.87% for banana rachis fibre, and 8.70% for chitosan. The effect of the adsorbents dosage (1, 1.5, 2, 2.5, and 3 g/l) on decolourization of the CBB G-250 dye at the lower concentration (50 mg/l) were tested. At the adsorbents dosage of 3 g/l, the highest level was 84.4% for activated carbon, followed by 65.5% for banana rachis fibre, 56.3% for chitosan; and lastly 50% for alpha cellulose.

At the high concentration (800 mg/l), the highest activity was 79.3% for activated carbon, followed by 33.7% for chitosan, 28.1% for alpha cellulose, and lastly 19.5% for banana rachis fibre. As expected, the highest adsorption occurred with activated carbon under high loading conditions, it is used routinely for water treatment and was included in this study for benchmarking the decolourisation activities. Comparisons of the activated carbon and different adsorbents (banana rachis fibre, chitosan, and alpha cellulose) was made, the activated carbon seem to absorb the CBB G-250 dye at high concentration (800 mg/l) and the different adsorbents seem to absorb the CBB G-250 dye at initial concentration (50 mg/l).

3. The highest capacity of adsorption of CBB G-250 dye recorded using different adsorbents determined by isotherm studies at an equilibrium concentration at 30 °C and pH 6.59 - 6.71 were: chitosan 32.60 mg/g, banana rachis fibre 35.87 mg/g, alpha cellulose 39.13 mg/g, and activated carbon 48.07 mg/g. The adsorption isotherms with activated carbon, alpha cellulose, wheat bran, banana rachis fibre, apricot stones activated carbon, coir pith, and chitosan can be described better by the Langmuir model with correlation coefficients ( $R^2$ : 0.9984, 0.998, 0.9735, 0.9661, 0.96, 0.9080, and 0.9474, respectively) bigger than the corresponding

Freundlich correlation coefficients (Prasad *et al.*, 2008; Ata *et al.*, 2012; Moussa *et al.*, 2014) (Table 3.5).

By comparing the data, it can be concluded that in our study the adsorption of coomassie brilliant blue onto activated carbon is best described in terms of the Langmuir isotherm model followed by the Freundlich isotherm model. From the equilibrium studies, it can be concluded that the Langmuir model is the best model for describing the adsorption of Coomassie dye by activated carbon. This means that Langmuir model is more applicable than Freundlich model and adsorption occurred probably by CBB molecules forming a single layer of molecules on the adsorbents mentioned. The results based on Freundlich data, using the 'n' value (see page 50), showed that activated carbon, followed by banana rachis fibre, chitosan, and alpha cellulose were good adsorbents of the CBB G-250 dye. These were so because all values of 'n' obtained for the different adsorbents sighted above (2.15, 2.06, 1.88, and 1.42) were greater than 1, suggesting a good adsorption capacity.

## CHAPTER 4

### 4. Formulation and chemical analysis of composites (alpha cellulose/chitosan and banana rachis fibre/chitosan composites)

#### 4.1. Chapter Summary

Composites are defined as materials made by mixing more than two chemically and physically dissimilar components together, physically or chemically, to form one new material. Fibres from plant source are widely used in preparing polymer composites. This is because of the availability and easy of processing them. ATR-IR spectroscopy was used to identify the functional groups such as: hydroxyl (-OH), carbonyl (C=O), carboxyl (CO<sub>2</sub>H) of different adsorbents responsible for CBB sorption. Composites as well as components of composites were furthermore characterised by x-ray diffraction. The crystallinity index, x-ray diffraction (Cl<sub>XRD</sub>) percentage of chitosan, alpha cellulose/chitosan composite, alpha cellulose, chitosan, banana rachis fibre/chitosan composite, and banana rachis fibre readings values in this study range from the highest to the lowest 94.29%, 91.54%, 82.75%, 60.77%, and 37.69%. The effect of the adsorbents dosage (3 g/l) on decolourisation of the CBB G-250 dye at the initial concentration (50 mg/l) were tested. The highest levels were shown by 93.8% for banana rachis fibre/chitosan composite, followed by 84.4% for alpha cellulose/chitosan composite. At the high concentration (800 mg/l), the highest activity was 51.6% for banana rachis fibre/chitosan composite and 44.8% for alpha cellulose/chitosan composite. The adsorption isotherms with alpha cellulose/chitosan composite, and banana rachis fibre/chitosan composite can be described better by the Langmuir model. Correlation coefficient, (R<sup>2</sup>: 0.9999, and 0.994) as higher than the Freundlich correlation coefficient R<sup>2</sup>. However, banana rachis fibre/chitosan composite and alpha cellulose/chitosan composite, were also explained by the Freundlich correlation coefficients (R<sup>2</sup>: 0.9715 and 0.9635) since they did not differ much from the corresponding Langmuir values. Based on Freundlich data the 'n' value showed that banana rachis fibre/chitosan composite, and alpha cellulose/chitosan composite, respectively were good adsorbents of the CBB G-250 dye. Because all the values of n obtained for the different adsorbents sighted above (2.44 and 2.18, respectively) were greater than 1, it suggested good adsorption capacity.

*Keywords:* Composites, ATR-IR spectrometry, X- ray diffraction, Isotherms.

## 4.2. Introduction

In this chapter there was a preparation of composites (alpha cellulose/chitosan composite and banana rachis fibre/chitosan composite using *in situ* precipitation of composites. Attenuated Total Reflectance Infrared (ATR-IR) spectra were captured with a Bruker spectrometer and evaluated based on bands obtained to identify functional groups present in the various materials. X- ray diffraction measurements for alpha cellulose, chitosan, banana rachis fibre, alpha cellulose/chitosan composite and banana rachis fibre/chitosan composite powdered samples were performed.

These experiments were designed to determine the concentration of the dye, the effect of concentration of dye as well as adsorbent dosages on the adsorption process, the equilibrium time for CBB dye adsorption followed by the sorption capacity determination of the materials (banana rachis fibre/chitosan composite and alpha cellulose/chitosan composite) for the CBB G-250 dye (Bradford Protein Assay, 2018). Adsorption activity might be present in composite materials-derived from two or more original sources/materials. Adsorption interactions are the result of surface forces (hydrogen bonding, electrostatic interactions, and van der Waals forces), hence the final adsorption capacity of composite materials could almost be considered as the sum of the capacities of its origin sources (Terzopoulou *et al.*, 2015).

The effect of the different adsorbents (banana rachis fibre/chitosan composite and alpha cellulose/chitosan composite) dosages (1, 1.5, 2, 2.5, and 3 g/l) on decolourization of the CBB G-250 dye were investigated. The capacity of adsorption of CBB G-250 dye using different adsorbents (banana rachis fibre/chitosan composite and alpha cellulose/chitosan composite) were determined by isotherm studies at an equilibrium concentration. Langmuir and Freundlich adsorption isotherms were used to investigate the relationship between the concentration of sorbed species and the sorption capacity of adsorbents (banana rachis fibre/chitosan composite and alpha cellulose/chitosan composite) for CBB dye after dye adsorption equilibrium was attained.

For carbohydrates estimation, total sugar estimation of acid hydrolysates (banana rachis fibre, chitosan, alpha cellulose/chitosan and banana rachis fibre/chitosan composites) using the anthrone method. The carbohydrate content can be measured by hydrolyzing the



polysaccharides into simple sugars by acid hydrolysis and estimating the resultant monosaccharides.

Carbohydrates are first hydrolysed into simple sugars using dilute hydrochloric acid. In hot acidic medium glucose is dehydrated to hydroxymethyl furfural. This compound forms with anthrone a green colored product with an absorption maximum at 630nm (Hedge and Hofreiter, 1962). For hexosamine estimation, glucosamine estimation of the acid hydrolysates (banana rachis fibre, chitosan, alpha cellulose, alpha cellulose/chitosan and banana rachis fibre/chitosan composites) using the hexosamine method. Chitosan can be degraded to glucosamine monomer by hydrolysis. A colorimetric method depends on the acid hydrolysis of chitosan molecule by one step with sodium nitrite treatment to convert it into 2,5-anhydro-D-mannose at the new reducing end which reacts with thiobarbituric acid in basic medium to give rise very stable pink-colored solution (Mohamed, 2012).

### **4.3. Materials and Methods**

#### **4.3.1. Dissolution and regeneration of alpha cellulose and chitosan**

Phosphoric acid was cooled to 5 °C in a refrigerator. Then, 1 g of alpha cellulose and 1 g chitosan were weighed in two 150, Erlenmeyer flasks separately, wetted with 6 ml water and then mixed with 100 ml cold phosphoric acid. The obtained mixtures were incubated in a shaking bath at a temperature of 5 °C and a speed of 150 rpm for 12 hours. This was done to dissolve the alpha cellulose and chitosan completely.

Each of the mixtures were incubated at 5 °C or 50 °C for an additional 3 – 12 hours before pouring 500 ml water into the mixtures (alpha cellulose and chitosan) of the two 150, Erlenmeyer flasks separately were used in this experiment, respectively, to regenerate the alpha cellulose and chitosan (four flasks in total were used, (two with cellulose and two with chitosan). Analytical balance was used. The regenerated celluloses were centrifuged at 5000 xg for 10 minutes. The clear supernatant was discarded, and the pellets were washed with deionized water until a constant pH was obtained to completely remove the phosphoric acid. The pellets were dried at 60 °C overnight in an oven and cooled in a desiccator to room temperature and the mass was recorded after weighing on analytical balance (Hao *et al.*, 2015).

### **4.3.2. Preparation of chitosan/alpha cellulose and chitosan/banana rachis fibre composites by *in situ* precipitation**

#### **4.3.2.1. Dissolution of chitosan**

An amount of 2 g of chitosan (Sigma-Aldrich) was added into acetic acid aqueous solution with concentration of 2% (v/v) and stirred for 2 hours until the chitosan was dissolved. The procedures followed above are summarized in Figure 4.1.

#### **4.3.2.2. Immersion of alpha cellulose into chitosan solution by *In situ* precipitation**

An amounts of 0.5 g and 5 g of alpha cellulose was added separately into each 50 ml chitosan acetic acid solution, prepared as stated above, and stirred on a magnetic stirrer for 2 hours to facilitate interactions between alpha cellulose and chitosan (Wang *et al.*, 2009). The alpha cellulose/chitosan acetic acid solution was centrifuged for 10 minutes. The pellet obtained, was added to 10 ml of sodium hydroxide aqueous solution with concentration of 5% (w/v) for 2 hours. After centrifugation for 10 minutes the pellet was washed with deionized water until the pH of the washing water reached ~7 (Wang *et al.*, 2009). The gel material (pellet left after centrifugation) is made of particles dispersed in water. Alpha cellulose/chitosan gel material was air-dried in an oven at 60 °C for several hours. The weight was measured as has been reported previously. The procedures followed above are summarized in Figure 4.1.

#### **4.3.2.3. Immersion of rachis fibres into chitosan solution by *In situ* precipitation**

0.5 g and 5 g of banana rachis fibre was added, respectively into each 50 ml chitosan acetic acid solution and stirred on a magnetic stirrer for 2 hours. The banana rachis fibre/chitosan acetic acid solution was centrifuged for 10 minutes. The pellet obtained, was added to 10 ml of sodium hydroxide aqueous solution with concentration of 5% (w/v) for 2 hours. After centrifugation for 10 minutes the pellet was washed with deionized water until the pH of the washing water reached ~7 (Wang *et al.*, 2009). The gel material (pellet left after centrifugation) is made of particles dispersed in water. Banana rachis fibre/chitosan gel material was air-dried in an oven at 60 °C for several hours. The weight was measured as has been reported previously. The procedures followed above are summarized in Figure 4.1.

#### **4.3.2.4. Treatment of the clear supernatant obtained after centrifugation with sodium hydroxide aqueous solution**

To obtain material left (alpha cellulose/chitosan composite and banana rachis fibre/chitosan composite) in supernatant after the steps shown above the following procedures were followed. The clear supernatant obtained by centrifugation was added to 10 ml of sodium hydroxide aqueous solution with concentration of 5% (w/v) for 2 hours and then 20 ml of ethanol was added and left to stand for 10 hours to precipitate (Da Silva *et al.*, 2018). The precipitate was separated from the liquid phase by centrifugation for 10 minutes and the supernatant discarded, the pellet was left in the centrifuge tube. This was done to obtain or regenerate the pellet from the supernatant (Wang *et al.*, 2009).

The pellet was then added to 10 ml of sodium hydroxide aqueous solution with concentration of 5% (w/v) for 2 hours to get alpha cellulose/chitosan and banana rachis fibre/chitosan composites gel (Wang *et al.*, 2009). The gel was washed with deionized water until the pH of the washed water become ~7. Alpha cellulose/chitosan and banana rachis fibre/chitosan composites (in a gel form) was air-dried in oven at 60 °C for 2 days and then the weights were measured as has been indicated previously. The procedures followed above are summarized in Figure 4.1.

#### **4.3.2.5. Treatment of the adsorbents controls with acetic acid aqueous solution**

For the controls, the 2 g of alpha cellulose and banana rachis fibre were added separately into two aliquots each of 400 ml acetic acid aqueous solution with concentration of 2% (v/v) in glass beakers respectively and stirred for 2 hours until the alpha cellulose and banana rachis fibre were dissolved. The alpha cellulose and banana rachis fibre acetic acid solutions with concentration of 2% (v/v) were centrifuged separately for 10 minutes. The pellet in each case was added to 10 ml of sodium hydroxide with concentration of 5% (w/v) for 2 hours and then centrifuged for 10 minutes and the pellet was washed with deionized water until the pH of the washed water become ~7. The alpha cellulose and banana rachis fibre material was air-dried separately in oven at 60 °C for several hours until it is dry and then the weights were measured as indicated before. The procedures followed above are summarized in the Figure 4.1.

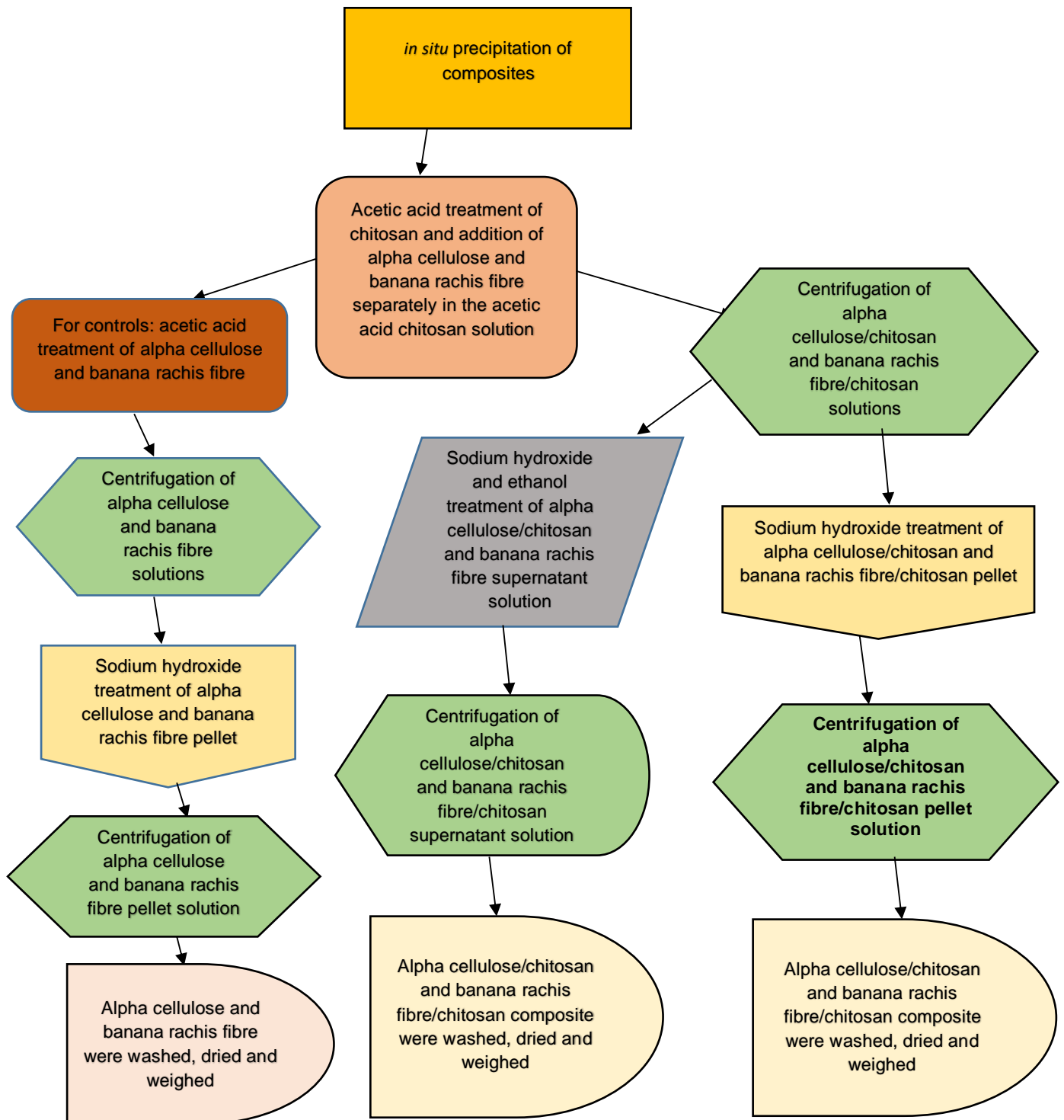


Figure 4.1: Schematic of methodology employed for the *in situ* precipitation of composites (Wang *et al.*, 2009)

### **4.3.3. Characterisation of different adsorbents using ATR-IR**

Attenuated Total Reflectance Infrared (ATR-IR) spectra were captured with a Bruker spectrometer and evaluated based on bands obtained to identify functional groups present in the various materials. Background absorption was first measured before any other analyses were performed by taking readings without any sample on the ATR crystal. Attenuated total reflectance infrared spectroscopy accessory is a sampling technique used in conjunction with infrared spectroscopy which enables samples to be examined directly in the solid or liquid state without further preparation.

Dry samples were pressed on the crystal window of the instrument by gently pressing with a stainless steel flat anvil of the attenuated total reflectance infrared accessory. The ATR-IR spectrometer was connected to a computer which captured the adsorbents absorption in the form of an absorption spectrum. The absorption spectrum was recorded over a range of 4000  $\text{cm}^{-1}$  to 400  $\text{cm}^{-1}$ . The resolution of the instrument was set to 4  $\text{cm}^{-1}$  and 24 scans were co-added to produce a single spectrum during each analysis.

### **4.3.4. Powdered X- ray diffraction analysis**

X-ray diffraction measurements were taken on a Rigaku MiniFlex II diffractometer for alpha cellulose, chitosan, banana rachis fibre, alpha cellulose/chitosan composite and banana rachis fibre/chitosan composite powdered samples were performed. The crystalline phase of all the synthesized samples (alpha cellulose, chitosan, banana rachis fibre, alpha cellulose/chitosan composite and banana rachis fibre/chitosan composite) were evaluated by XRD using Cu K  $\alpha$  radiation ( $\lambda = 1.5408 \text{ \AA}$ ) at ambient temperature (Tran *et al.*, 2013). The voltage and current from the x-ray tube were 30 kV and 15 mA, respectively. The XRD measurements of sample were collected within the  $2\theta$  angle range from  $5^\circ$  to  $50^\circ$ , the scan rate was  $5^\circ/\text{minutes}$  (Duri *et al.*, 2010).

### **4.3.5. Equilibrium and isotherm studies**

#### **4.3.5.1. Dye adsorption assessment methodology**

The percentage of decolourisation of dye on banana rachis fibre/chitosan and alpha cellulose/chitosan composites were calculated using the equation given in Section 3.3.2 (Forootanfar *et al.*, 2016).

#### **4.3.5.2. Equilibrium time sorption experiments**

The percentage of sorption activity of dye on banana rachis fibre/chitosan and alpha cellulose/chitosan composites were performed using the method given in Section 3.3.3.

#### **4.3.5.3. Adsorption Isotherm Studies**

##### **4.3.5.3.1. Equilibrium studies**

The percentage of decolourisation of dye on banana rachis fibre/chitosan and alpha cellulose composites were calculated using the equation given in Section 3.3.4.1.

##### **4.3.5.3.2. Langmuir and Freundlich isotherms**

The Langmuir and Freundlich, adsorption isotherms were constructed to investigate the relationship between the concentration of sorbed species and the sorption capacity of alpha cellulose/chitosan composite and banana rachis fibre/chitosan composite for CBB G-250 dye were performed using the method given in Section 3.3.4.2.

#### **4.3.6. Acid hydrolysis of different adsorbents**

A 2.5 N solution of hydrochloric acid was prepared and 10 mg sample of the banana rachis fibre, chitosan, alpha cellulose, banana rachis fibre/chitosan composite, and alpha cellulose/chitosan composite was boiled in separate 3 ml of the solution for 3 hours in a test tube fitted with a screw cap. After boiling the samples were cooled down to room temperature and neutralized with 2.5 N NaOH. The samples were stored overnight 4 °C. The neutralized samples were each transferred to a volumetric flask and made up to 50 ml with distilled water (Datema *et al.*, 1977). The hydrolysed samples were used to estimate the carbohydrate contents and the hexosamine contents as described below (see Section 4.3.7 and 4.3.8).

#### **4.3.7. Carbohydrates estimation**

#### **4.3.7.1. Preparation of stock and working standard glucose solution**

Standard glucose stock solution (2 mg/ml:11.1 M) was made up by dissolving 200 mg glucose in 100 ml distilled water. The working standard was prepared by transferring 10 ml of stock solution to 90 ml of distilled water in a volumetric flask. Thereafter, the stock solution was stored in a refrigerator (0 – 5 °C) after a few drops of toluene was added to minimize microbial contamination (Hofreiter, 1962).

#### **4.3.7.2. Total sugar estimation of acid hydrolysates using the Anthrone method**

Preparation of Anthrone reagent was as follows: 1 g of Anthrone was dissolved in 500 ml of ice cold 72% sulphuric acid. The reagent was prepared fresh before use. Specific volumes of the working standard solution were pipette out namely: 0.1, 0.2, and 0.5 ml into each of the test tubes, and were made up to 1 ml with distilled water. A 1 ml volume of the sample was pipetted in each of two separate tests tubes. After 4 ml of anthrone reagent was added, the contents of the tubes were mixed and placed in a water bath for 10 minutes and cooled rapidly to 0 °C on ice. Absorbencies were read at 630 nm (against water) within an hour. Standard glucose solutions (0.1, 0.2, and 0.5 mg/ml glucose) were prepared from the working standard glucose solution (see Section 4.3.7.1 above) and subsequently mixed with Anthrone reagent, treated and analyzed spectrophotometrically as described above (Sydney.edu.au/science/biology/warren/docas/spec, starch, sugars.pdf).

#### **4.3.8. Hexosamine estimation**

##### **4.3.8.1. Glucosamine estimation of the acid hydrolysis using the hexosamine method**

The hydrolysed samples were used (see Section 4.3.6). The duplicate blanks and standards containing 10, 20, 30, 40, 50, and 70 µg glucosamine, were prepared. A 1 ml acetylacetone reagent 5% (v/v) was added to all tubes. Tubes were placed in a boiling water bath for 30 minutes. The tubes were cooled in room temperature water for a minimum of 5 minutes. The tubes were left to stand up to 2 hours before the next step. 5 ml absolute ethanol was added and mixed, after which 1 ml Ehrlich reagent was added and mixed and left to stand for 25 min before absorbance readings were taken at 529 nm. The hexosamine contents of the unknowns were calculated using data obtained from the standard curve of absorbance plotted against known glucosamine amounts (Johnson, 1971).



## 4.4. Results and Discussions

### 4.4.1. Formulation of composites and chemical analysis of composites

#### 4.4.1.1. Composites preparation by *in situ* precipitation

The alpha cellulose/chitosan composite and banana rachis fibre/chitosan composite obtained after the *in situ* precipitation method (Figure 4.2 A and B).

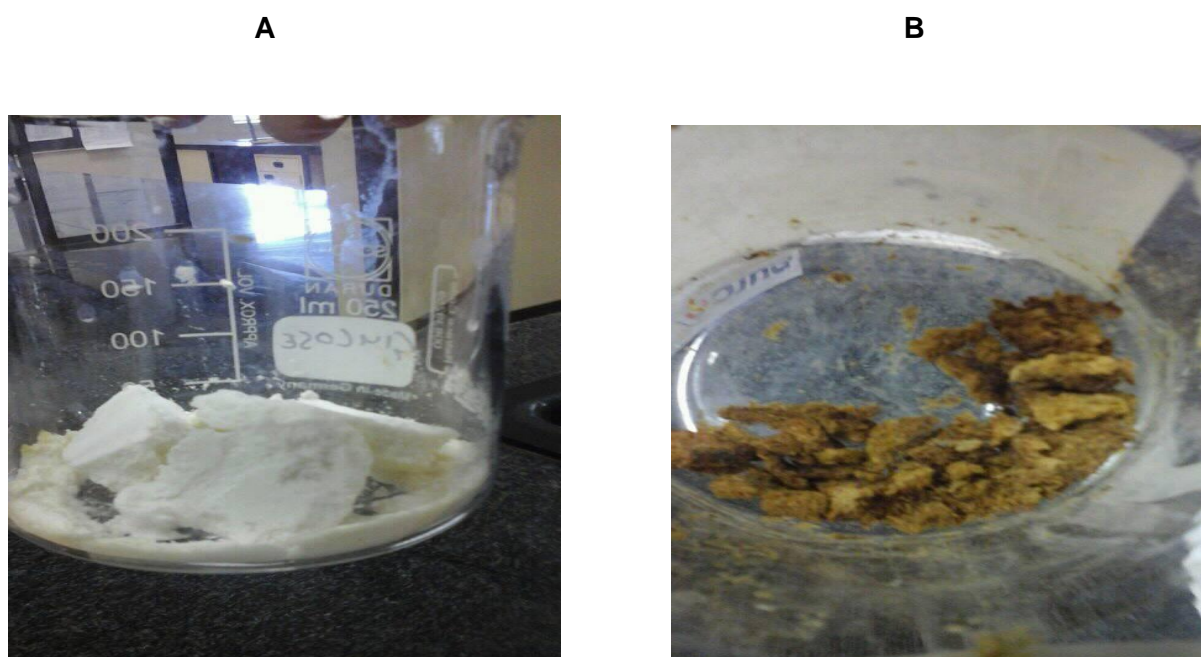


**Figure 4.2: *in situ* precipitation of the different composites preparation A. Alpha cellulose/chitosan composite (6.07 g), B. Banana rachis fibre/chitosan composite (6.18 g)**

The amount of 6.07 g was obtained from the starting materials 2 g of chitosan and 5 g of alpha cellulose for alpha cellulose/chitosan composite. Alpha cellulose/chitosan composite indicated a white colour and soft texture (Figure 4.2 A). The amount of 6.18 g was obtained from the starting materials 2 g of chitosan and 5 g of banana rachis fibre for banana rachis fibre/chitosan composite. Banana rachis fibre/chitosan composite indicated a brown colour and hard texture (Figure 4.2 B).

Cellulose have been extensively used in combination with chitosan to produce new blend materials with antibacterial activity, metal ions adsorption, odour treatment properties, improved water absorption capacity and mechanical characteristics, good antistatic and moisture absorption properties, high porosity and interconnected porous structures, self-healing characteristics, etc (Abdul *et al.*, 2016). In order to attain comprehensive improvement in electrical, physical, mechanical and thermal characteristics of chitosan-cellulose blend



materials tertiary component usually incorporate with it (Abdul *et al.*, 2016). They suggested that cellulose/chitosan blends were considerably immiscible because mechanical and dynamic mechanical thermal properties of cellulose/chitosan blends were virtually dominated by cellulose.

Liu *et al.* (2013) reported that the addition of cellulose into chitosan resulted in denser and mechanically stronger hydrogel beads. Stability of chitosan blend depends on specific interactions which may include hydrogen, ionic bonds, or dipole interference and final properties strongly depend on the miscibility of the components. Miscibility, structure and properties are critical factors in studies concerning polymer blends. Miscibility is one of the key factors affecting the structure and properties of a polymer blend which are important in applications (Abdul *et al.*, 2016). Chitosan can be modified by blending it with other polymeric materials such as cellulose because it has modifiable functional groups thus the stability of blends enhance.

Overall it can be concluded that stability of chitosan based materials can be improved by blending it with other compatible biopolymer especially cellulose. In future, research on blends should be focused on their potential use in biomedical, packaging, coatings and water treatment (Abdul *et al.*, 2016). Cellulose and chitosan are two most abundant natural polymers with promising characteristics as composite materials. However, biopolymer based materials have relatively poor mechanical, thermal and barrier properties. Addition of two or more polymers, nanomaterials can significantly increase the properties of composites. In this regards, chitosan based cellulose materials are extensively explored.

#### **4.4.2. Characterization of different adsorbents using ATR-IR**

The ATR-IR spectroscopy was conducted to identify the functional groups of rachis banana fibre, cellulose fraction extracted from banana rachis fibre, chitosan (native), alpha cellulose regenerated, holocellulose obtained from banana rachis fibre, rachis fibre control, alpha cellulose control, regenerated chitosan, banana rachis fibre/chitosan composite pellet (0.5 g), banana rachis fibre/chitosan supernatant (0.5 g), banana rachis fibre/chitosan composite pellet (5 g), banana rachis fibre/chitosan supernatant (5 g), alpha cellulose/chitosan pellet (0.5 g), alpha cellulose/chitosan composite supernatant (0.5 g), alpha cellulose/chitosan composite pellet (5 g), alpha cellulose/chitosan composite supernatant (5 g) (Figure 4.4-4.19). Identification of characteristic peaks is based on previous studies of different adsorbents.

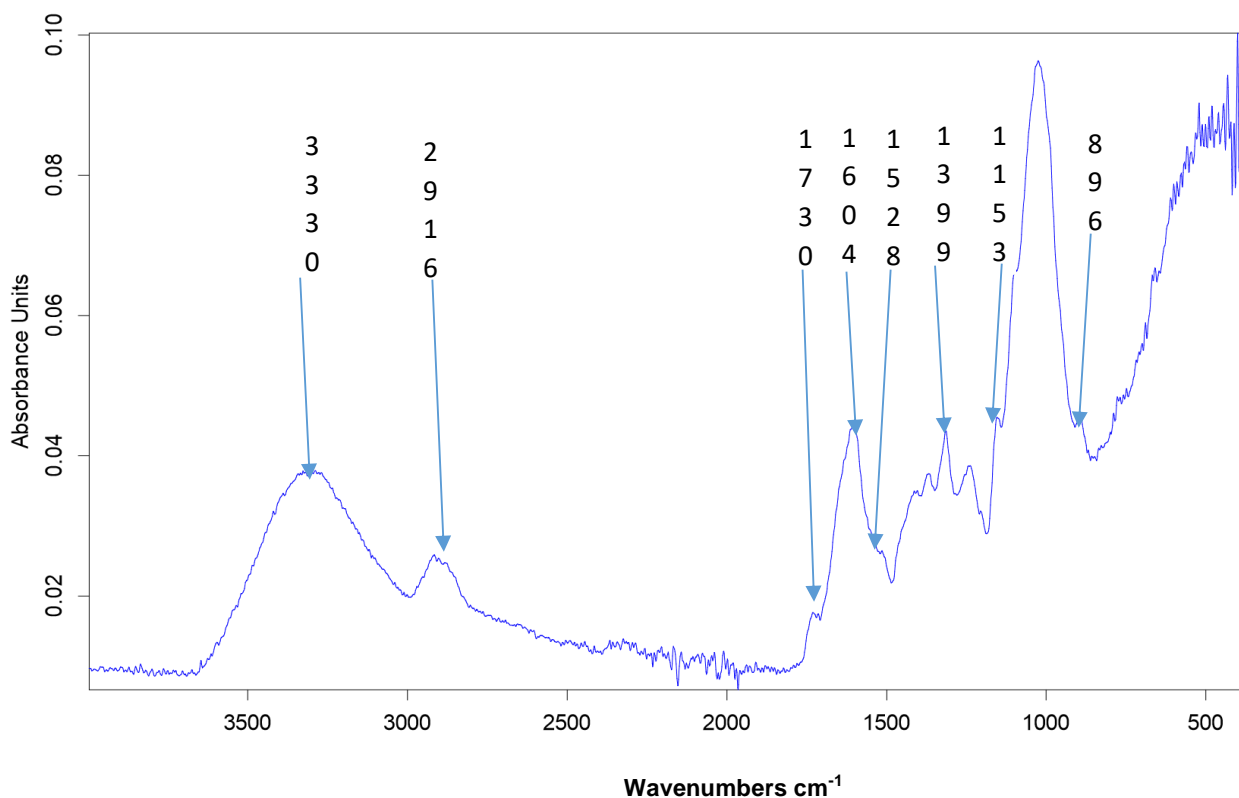


**Figure 4.3: ATR-IR spectrum of banana rachis fibre**

In the present study, the intense O-H peaks these represent stretching band of hydroxyl group at about  $3330\text{ cm}^{-1}$  and  $3350\text{ cm}^{-1}$  ( $3200 - 3650\text{ cm}^{-1}$ ) centered at about  $3000\text{ cm}^{-1}$  (Figure 4.3). The peak at  $1604\text{ cm}^{-1}$  is an indicative of water molecules and C=O bonds of hemicelluloses (Sun *et al.*, 2004c; Gañan *et al.*, 2004). The absorption at  $1730\text{ cm}^{-1}$  could correspond to the acetyl and uronic ester groups of residual hemicelluloses or to the ester linkage of carboxylic group of the ferulic and *p*-coumaric acids of lignin (Sun *et al.*, 2005a). Sun *et al.* (2005b) also reported that the absorbance at  $1528\text{ cm}^{-1}$  is associated with aromatic skeletal vibration in lignin (Sain and Panthapulakkal, 2006).

The hemicellulose, cellulose, and lignin fractions are intricately intertwined in the cell wall of lignocellulosic resources and their compositions vary distinctly from biomass to biomass type (Balogun *et al.*, 2018). The change in peak shape is a result of the different degree of hydrogen bonds present. Prominent bands of C-H asymmetric stretching ( $2923$  and  $2855\text{ cm}^{-1}$ ) which originate from aliphatic structure of extractives and lignin (Balogun *et al.*, 2015; Soria and McDonald, 2012) were also present.

The characteristic absorption bands of cellulose identified were:  $2916\text{ cm}^{-1}$  (C-H stretching),  $1425\text{ cm}^{-1}$  (C-H wagging),  $1399\text{ cm}^{-1}$  (C-H bending) (Balogun *et al.*, 2015; Telmo and

Lousada, 2011). The C-OH and O-CH<sub>3</sub> stretching vibrations associated with the sharp absorption bands at about 1030 cm<sup>-1</sup> are characteristic of lignin and cellulose constituents, while the intense band at about 1150 cm<sup>-1</sup> are indicative of cellulose C-O-C bridges of amorphous cellulose (Balogum *et al.*, 2015). The aromatic stretching and ring vibrations, which are lignin characteristic bands, were displayed between the intensity peaks of 1430 and 1600 cm<sup>-1</sup>.

The banana rachis fibre was suspected to contain starch based on several bands (1152, 1100, 1075, 1047, 1032, 990, and 925 cm<sup>-1</sup>) associated with starch (Van Soest *et al.*, 1995). The adsorption at 3200 – 3400 cm<sup>-1</sup> (3250 cm<sup>-1</sup>) which is due to stretching vibrations of O-H groups found in cellulose, hemicelluloses and lignin (C-O-C) that are present in BRF (Mokhothu, 2010) (Figure 4.4). The band at 2900 cm<sup>-1</sup> (and/or 2611 cm<sup>-1</sup>) is due to the C-H stretching of saturated carbon in cellulose and hemicellulose (Mokhothu, 2010). The band between 1917 cm<sup>-1</sup> is due to C=C stretching of fibres containing lignin. The band at 1700-1750 cm<sup>-1</sup> is due to C=O stretching vibration. The band at 1430 cm<sup>-1</sup> (1444 cm<sup>-1</sup>) is due to C-H stretching of hydrocarbon (Mokhothu, 2010) (Figure 4.3).

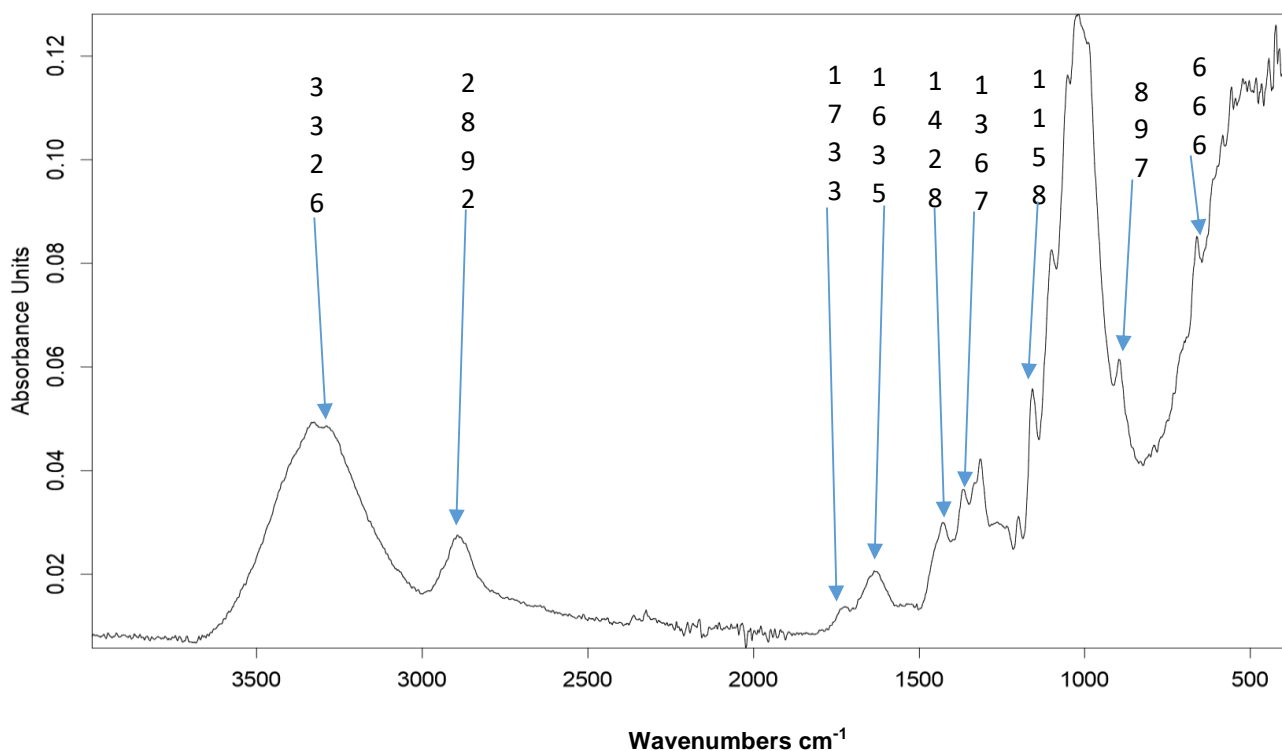


**Figure 4.4: ATR-IR spectrum of cellulose fraction extracted from banana rachis fibre**

The band at around 1430 cm<sup>-1</sup> to the scissoring motion of cellulose I and band at around 1420 cm<sup>-1</sup> to the cellulose II (Mahato *et al.*, 2013) (Figure 4.4). The band around 1313 cm<sup>-1</sup> in spectra

of cellulose can be attributed to CH<sub>2</sub> wagging vibration in cellulose and the band around 1155 cm<sup>-1</sup> was representative of anti-symmetric bridge stretching of C-O-C groups (Spiridon *et al.*, 2010). The spectra showed broad, very strong, and less intense peak O-H stretching band of hydroxyl group at about 3326 cm<sup>-1</sup> and 3350 cm<sup>-1</sup> (3200 – 3650 cm<sup>-1</sup>) centered at about 3000 cm<sup>-1</sup>, change in peak shape can indicate a different degree of hydrogen bonds. Cellulose gave spectrum around 1425 cm<sup>-1</sup> which was attributed to the CH<sub>2</sub> bending. The band at 892 (897) cm<sup>-1</sup> was referred to the glycosidic C-H rock vibration which was characteristic of cellulose structure (Li *et al.*, 2014; Penjumras *et al.*, 2014) (Figure 4.4).

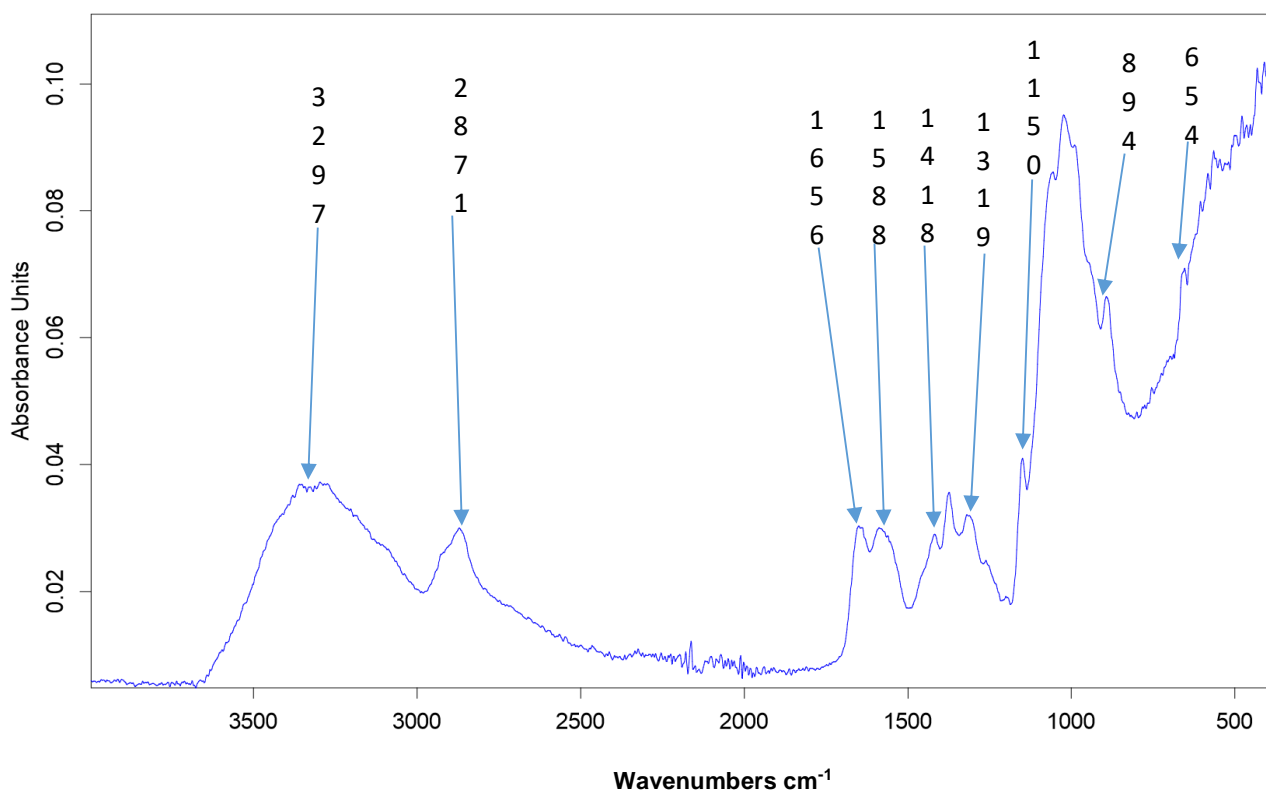


**Figure 4.5: ATR-IR spectrum of chitosan**

The hydroxyl and amino bands at wavenumber up to about 3500 cm<sup>-1</sup> (Figure 4.5). The spectra showed broad, very strong, and less intense peak O-H stretching band of hydroxyl group at about 3297 cm<sup>-1</sup> and 3350 cm<sup>-1</sup> (3200 – 3650 cm<sup>-1</sup>) centred at about 3000 cm<sup>-1</sup> and the 3263 cm<sup>-1</sup> to vibration of N-H that are present in chitosan. The vibration of C=O stretching (amide I) was detected at 1650.95 (1656) cm<sup>-1</sup> that is present in chitosan (Wanule *et al.*, 2014) (Figure 4.5). The emergence of absorption at 894 cm<sup>-1</sup> on chitosan which was the vibration of NH<sub>2</sub> after the deacetylation process (Wanule *et al.*, 2014).

As stated by Ziani *et al.* (2008), the spectrum of chitosan film prepared during my research work was similar to those previously reported in the literature. The characteristic bands of chitosan are clearly identified. The absorption band at 1592 (1588) is ascribed to the amide II band that is present in the chitosan (Figure 4.5).

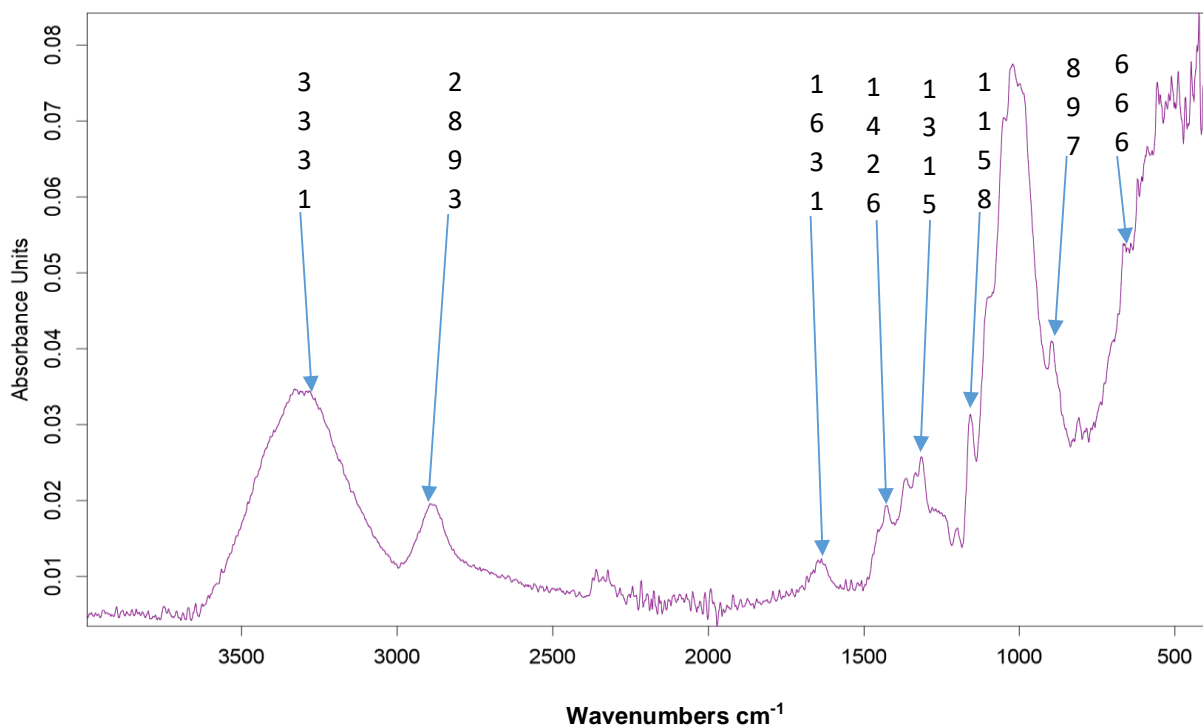


**Figure 4.6: ATR-IR spectrum of alpha cellulose regenerated**

According to Chieu *et al.* (2013), the FTIR spectrum of microcrystalline cellulose exhibits three pronounced bands at around  $3400\text{ cm}^{-1}$ ,  $2850 - 2900\text{ cm}^{-1}$  and  $890 - 1150\text{ cm}^{-1}$ . These bands can be tentatively assigned to stretching vibrations of O-H, C-H and O groups, respectively (Burns and Ciurczak., 1992; Da Roz *et al.*, 2010; Dreve *et al.*, 2009). The spectra showed broad, very strong, and less intense peak O-H stretching band of hydroxyl group at about  $3331\text{ cm}^{-1}$  and  $3350\text{ cm}^{-1}$  ( $3200 - 3650\text{ cm}^{-1}$ ) (Figure 4.6).

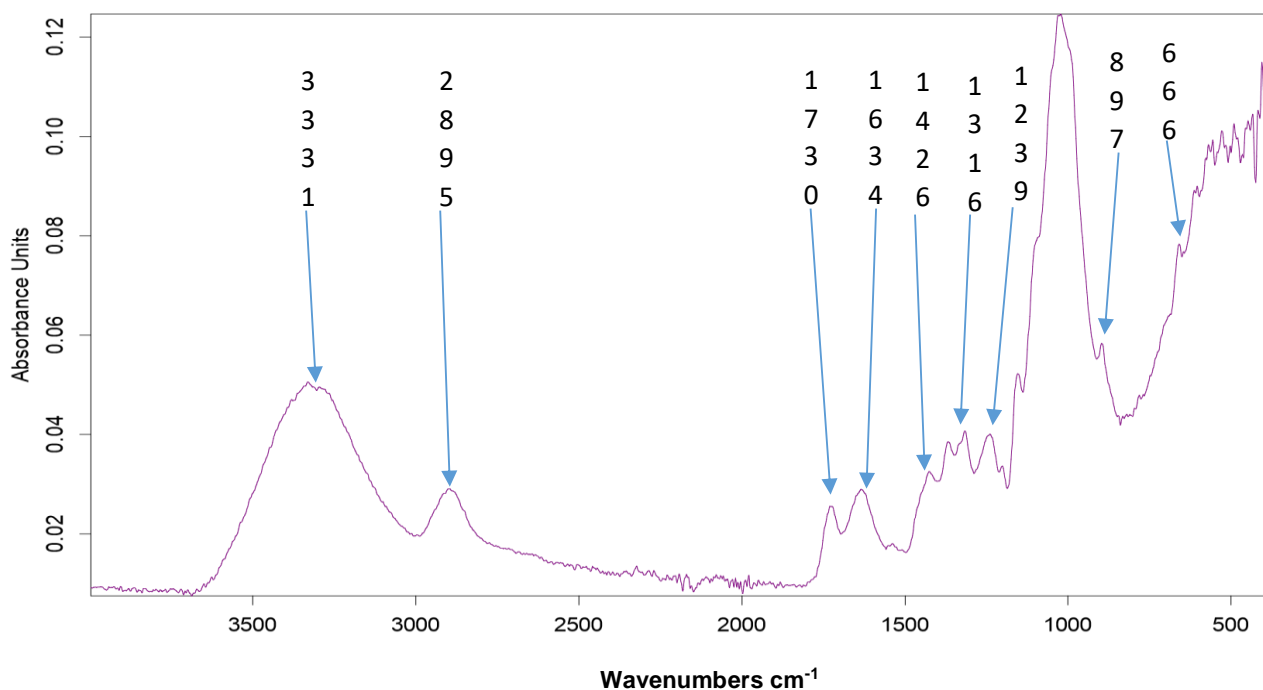


**Figure 4.7: ATR-IR spectrum of holocellulose obtained from banana rachis fibre**

The peak around  $1425\text{ cm}^{-1}$  was attributed to the  $\text{CH}_2$  bending (Li *et al.*, 2014; Penjumras *et al.*, 2014). The spectra showed broad, very strong, and less intense peak O-H stretching band of hydroxyl group at about  $3331\text{ cm}^{-1}$  and  $3350\text{ cm}^{-1}$  ( $3200 - 3650\text{ cm}^{-1}$ ) centred at about  $3000\text{ cm}^{-1}$  (Figure 4.7).

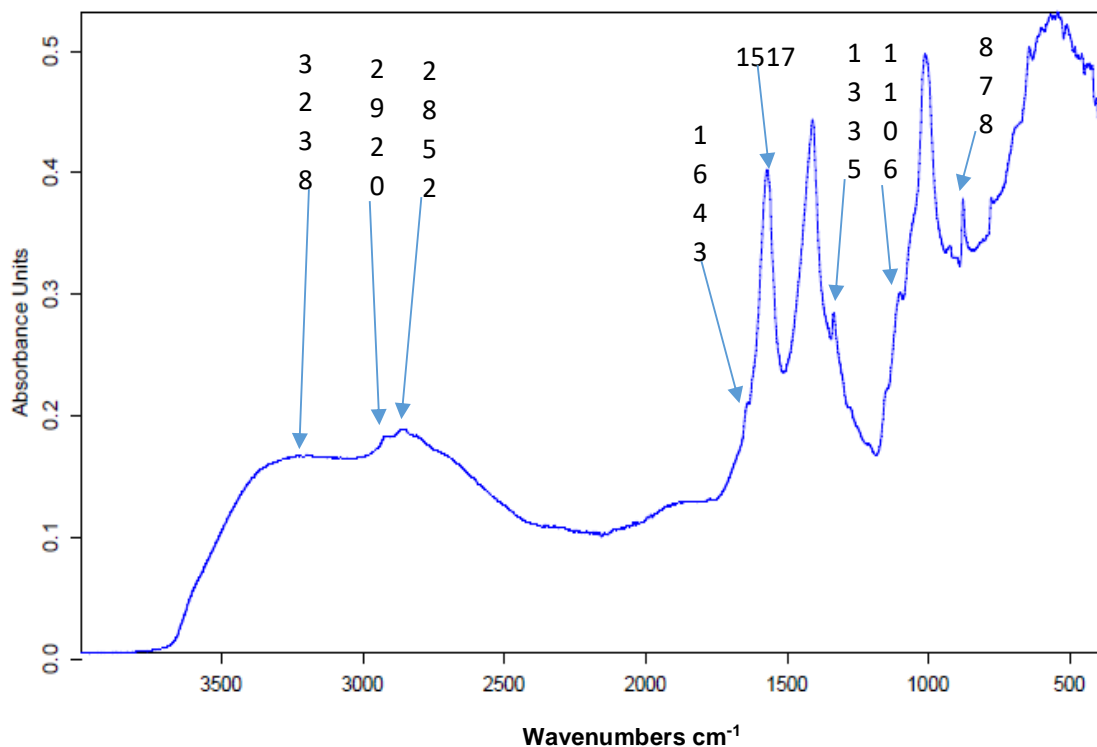


**Figure 4.8: ATR-IR spectrum of rachis fibre control**

The peaks at 3238 and 1106  $\text{cm}^{-1}$  that correspond to the stretching vibrations of O–H in cellulose and C–O in hemicelluloses and cellulose, respectively (Figure 4.9). The peak at 1643  $\text{cm}^{-1}$  is an indicative of water molecules and C=O bonds of hemicellulose (Sun *et al.*, 2004c; Gañan *et al.*, 2004). Sun *et al.*, (2005b) also reported that the absorbance at 1517  $\text{cm}^{-1}$  is associated with aromatic skeletal vibration in lignin (Sain and Panthapulakkal, 2006). The profile of the OH peak at 3238  $\text{cm}^{-1}$  has changed when compared to that of rachis fibre which indicate changes in the hydrogen bonding characteristics (Figure 4.8).

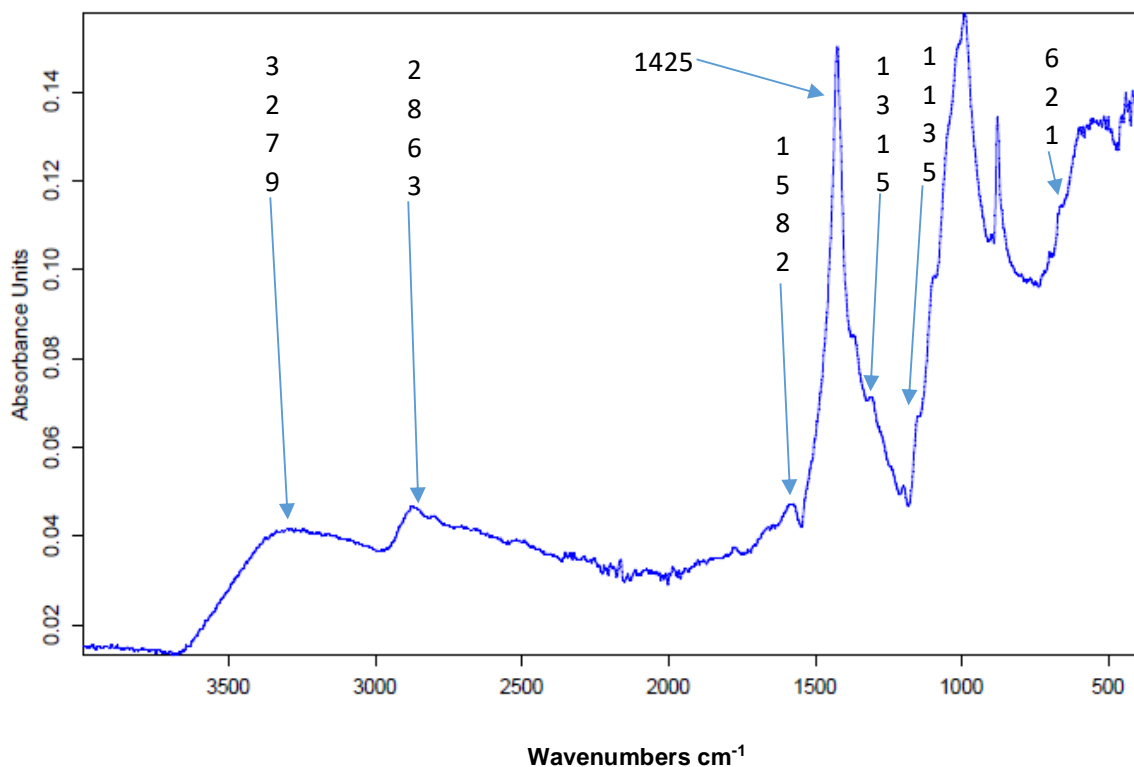


**Figure 4.9: ATR-IR spectrum of alpha cellulose control**

The cellulose control also shows a similar broadening to that observed above for the rachis fiber control (Figure 4.9). Once again the cellulose control wavenumber decreased to 3279 compared to that of cellulose which was 3331 cm<sup>-1</sup>. This is indicative of a change in the hydrogen bond pattern which could indicate a breaking of existing hydrogen bonds upon chemical treatment in the control sample (Figure 4.9).



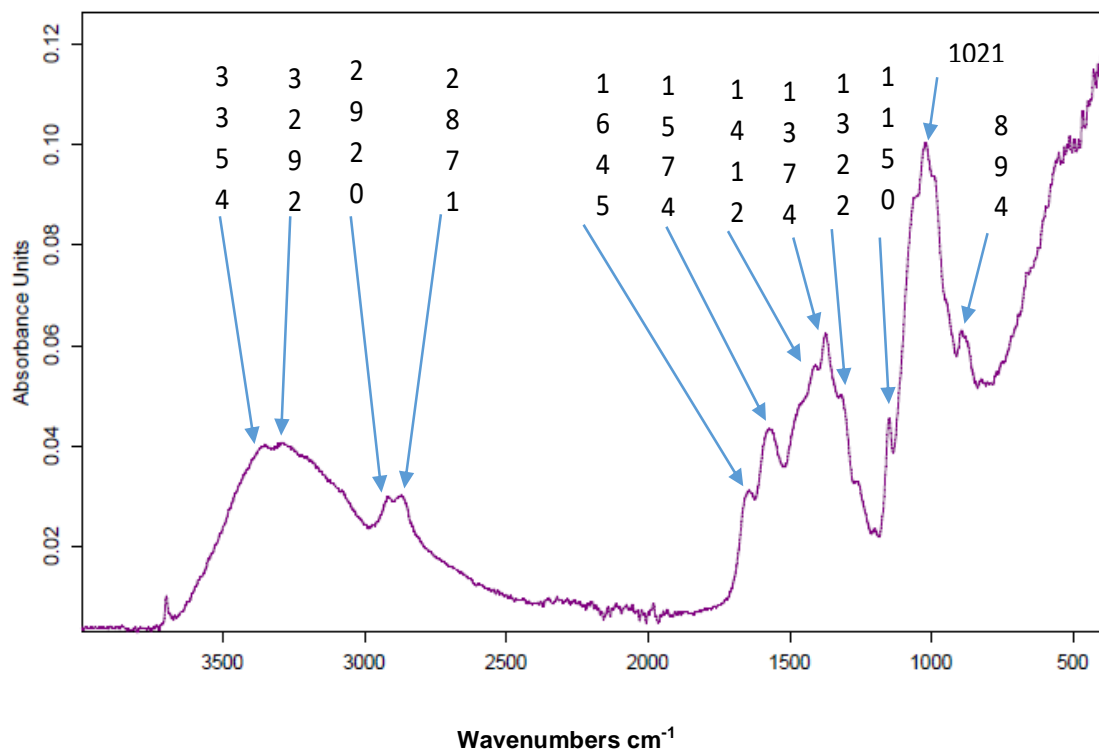


**Figure 4.10: ATR-IR spectrum of regenerated chitosan**

The identification of characteristic peaks is based on previous studies of regenerated chitosan (Figure 4.10). The adsorption at  $3292\text{ cm}^{-1}$  and  $3354\text{ cm}^{-1}$  is due to the O-H groups stretching,  $2871\text{ cm}^{-1}$  (C-H stretching) and  $2920\text{ cm}^{-1}$  (C-H stretching),  $1645\text{ cm}^{-1}$  (C-O amide I),  $1574\text{ cm}^{-1}$  (N-H deformation),  $1322\text{ cm}^{-1}$  (C-N stretching, amide III),  $894\text{ -}1150\text{ cm}^{-1}$  (ether bonding) that are present in regenerated chitosan (Figure 4.10). Regeneration of chitosan imply first dissolving the chitosan (in acetic acid) and subsequently taking it out of solution back to a solid phase by increasing the pH through addition of alkali (NaOH) (Figure 4.10).

This is usually done to increase the purity of the chitosan. Addition of NaOH is also one of the steps used in the so called *in situ* precipitation methods for composite formation used in this study. The spectra showed  $2850\text{ -}2900\text{ cm}^{-1}$  (C-H stretching),  $1657\text{ cm}^{-1}$  (C-O, amide I),  $1595\text{ cm}^{-1}$  (N-H deformation),  $1380\text{ cm}^{-1}$  ( $\text{CH}_3$  symmetrical deformation),  $1319\text{ cm}^{-1}$  (C-N stretching, amide III) and  $890\text{ -}1150\text{ cm}^{-1}$  (ether bonding) (Burns and Ciurczak., 1992; Da Roz *et al.*, 2010; Dreve *et al.*, 2009).

According to Focher *et al.*, (1992b), the FT-IR spectra of different chitosan samples though similar to each other as a whole, showed subtle differences in the absorption intensities. For instance, the chitosans show different degrees of acetylation (A - 42%, B - 28%, and C - 5%).

This indicate that wavenumber is not absolutely fixed in different chitosan samples for the same functional groups observed. Both  $\text{OH}\cdots 3$  and  $\text{CH}_2\text{OH}\cdots 6$  are involved in intra- and intermolecular hydrogen bonds. Such a band shift to a higher frequency indicated an increase in the ordered structure of a sample (Focher *et al.*, 1992b). The band at  $1412\text{ cm}^{-1}$  was assigned to ( $\text{CH}_2$  bending), due to the rearrangements of hydrogen bonds on the orientation of the primary  $-\text{OH}$  groups, at least in the amorphous regions of the polysaccharides (Focher, *et al.*, 1992a; Focher *et al.*, 1992b). The  $1598\text{ cm}^{-1}$  transmittance peak of the  $-(\text{NH}_2)$  bending vibration is sharper than the peak at  $1645\text{ cm}^{-1}$ , which shows the high degree of deacetylation of the chitosan. A shift from  $3292\text{ cm}^{-1}$  is show the peak is sharper in the regenerated chitosan, which indicates that the hydrogen bonding is enhanced (Qi *et al.*, 2004).

The intensities of the  $(\text{CO}-\text{NH}_2)$  band at  $1645\text{ cm}^{-1}$  and the  $(\text{NH}_2)$  band at  $1574\text{ cm}^{-1}$ , which can be observed clearly in pure chitosan, increase dramatically, and two new sorption bands at  $1412\text{ cm}^{-1}$  and  $1322\text{ cm}^{-1}$  appear, which show asymmetrical C-H. In this study changes in the band present at  $1656\text{ cm}^{-1}$  in chitosan shifted to  $1645\text{ cm}^{-1}$  in the regenerated chitosan. A further difference seen between regenerated and native chitosan occurred at the  $1588\text{ cm}^{-1}$  peak which is changed to  $1574\text{ cm}^{-1}$  in the regenerated sample. Therefore specific changes in the regenerated chitosan relative to native chitosan can be shown using ATR-IR (Figure 4.10 and 4.5).

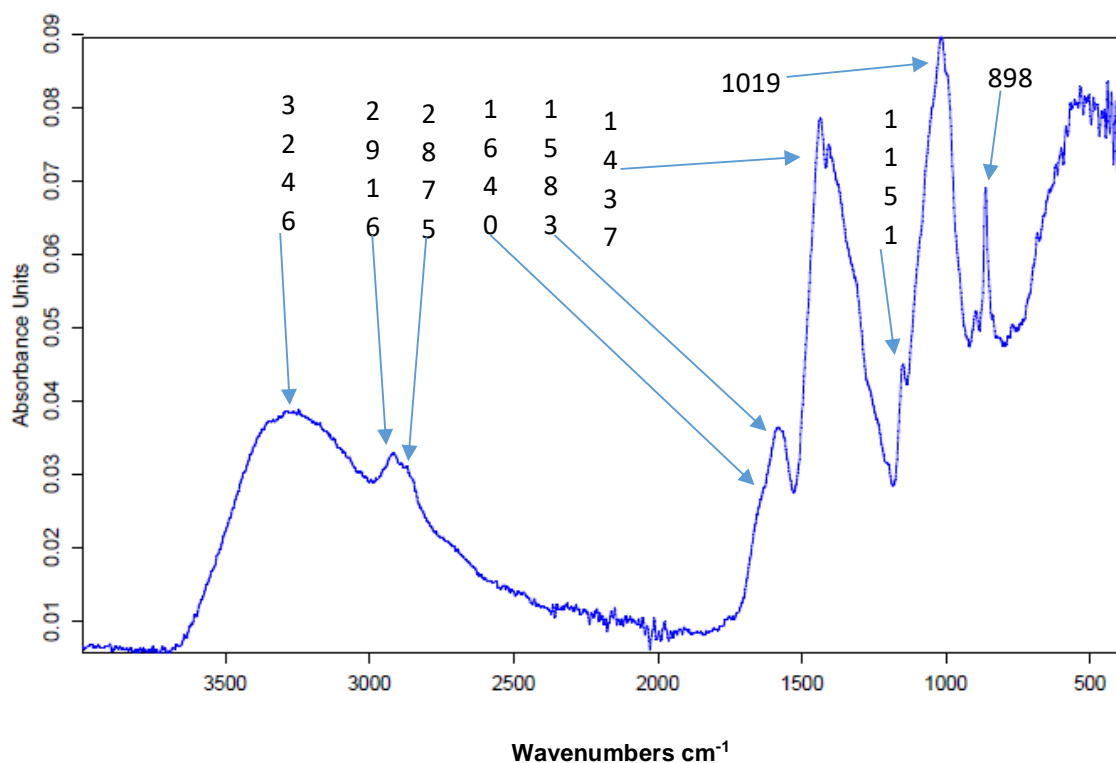


**Figure 4.11: ATR-IR spectrum of banana rachis fibre/chitosan composite pellet (0.5 g)**

The peaks at 3246 and 1019  $\text{cm}^{-1}$  that correspond to the stretching vibrations of O–H in cellulose and C–O in hemicelluloses and cellulose, respectively (Sun *et al.*, 2005) (Figure 4.11). The spectra showed broad, very strong, and less intense O–H stretching band of hydroxyl group at about 3246  $\text{cm}^{-1}$  (3200 – 3650  $\text{cm}^{-1}$ ) centered at about 3000  $\text{cm}^{-1}$ , Figure 4.11 shows the adsorption at 3200 – 3400  $\text{cm}^{-1}$  which is due to stretching vibrations of O–H groups of cellulose, hemicelluloses and lignin (C–O–C) that are present in banana rachis fibre.

The band at 2900  $\text{cm}^{-1}$  is due to the C–H stretching of saturated carbon in cellulose and hemicellulose. The bands at 1700 – 1750  $\text{cm}^{-1}$  (1750  $\text{cm}^{-1}$ ) is due to C=O stretching vibration. The band at 1430 (1437)  $\text{cm}^{-1}$  is due to C–H stretching of hydrocarbon (Mokhothu, 2010). Figure 4.11 shows hydroxyl and amino bands at the wavenumber up to 3500  $\text{cm}^{-1}$ . A broad absorption band in the range 3000 to 3500  $\text{cm}^{-1}$  was noted which is assigned to O–H stretching vibrations and the 3246  $\text{cm}^{-1}$  to vibration of N–H. The vibration of C=O stretching (amide I) at 1640  $\text{cm}^{-1}$  (Rumengan *et al.*, 2014) and 1650.95  $\text{cm}^{-1}$  (Wanule *et al.*, 2014).

The interval 3271 – 3448  $\text{cm}^{-1}$  could be connected with larger amount of N–H and O–H groups in chitosan, (Rumengan *et al.*, 2014). According to Bianchera *et al.*, (2014), ATR-FTIR analysis was performed on the chitosan powder used for scaffold preparation. Characteristic bands of chitosan were evident in the spectrum at 1640  $\text{cm}^{-1}$  (–C=O stretching), 1583  $\text{cm}^{-1}$  and 1655

$\text{cm}^{-1}$  (N–H bending vibration), and  $1380 \text{ cm}^{-1}$  (–C–O stretching of primary alcoholic group), respectively (Figure 4.11).

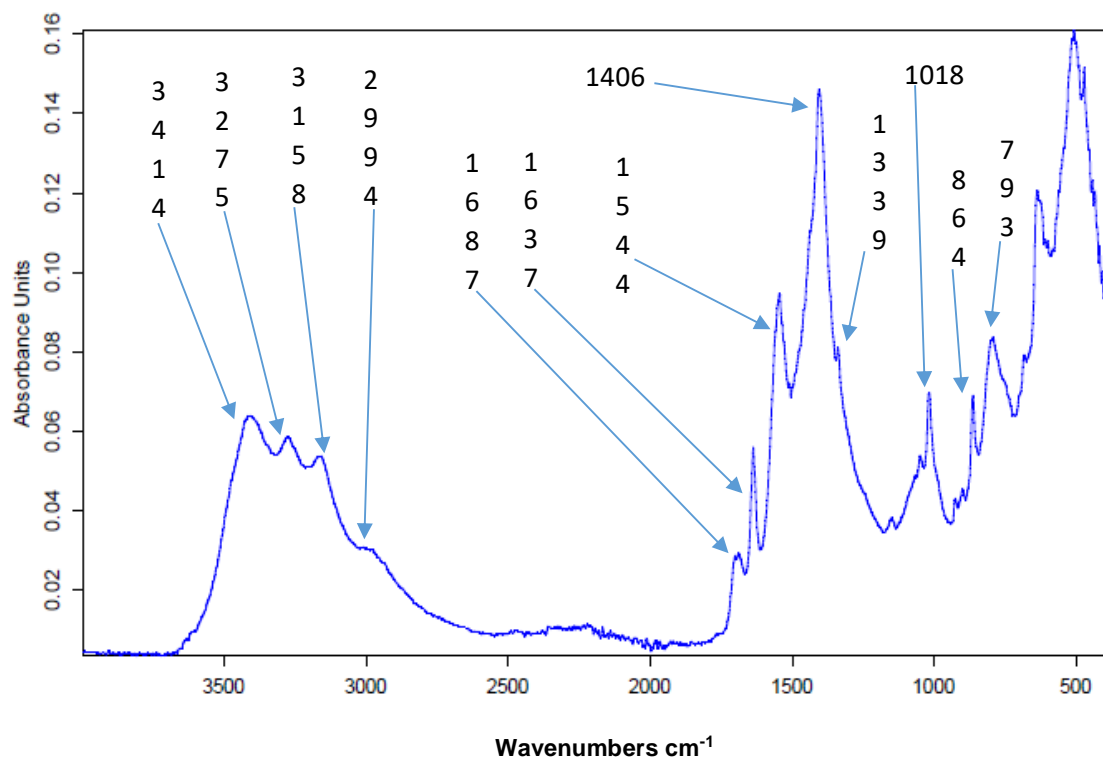


**Figure 4.12: ATR-IR spectrum of banana rachis fibre/chitosan composite supernatant (0.5 g)**

The spectra showed a broad peak with three less sharper peaks due to the O-H stretching band of hydroxyl group at about  $3158 \text{ cm}^{-1}$ ,  $3275 \text{ cm}^{-1}$ , and  $3414 \text{ cm}^{-1}$  (Mokhothu, 2010) (Figure 4.12). Figure 4.12 shows the adsorption at  $3200 - 3400 \text{ cm}^{-1}$  ( $3250 \text{ cm}^{-1}$ ) which is due to stretching vibrations of O-H groups of cellulose, hemicelluloses and lignin (C-O-C) that are present in banana rachis fibre. The band at  $2900 \text{ cm}^{-1}$  is due to the C-H stretching of saturated carbon in cellulose and hemicellulose (Figure 4.12).

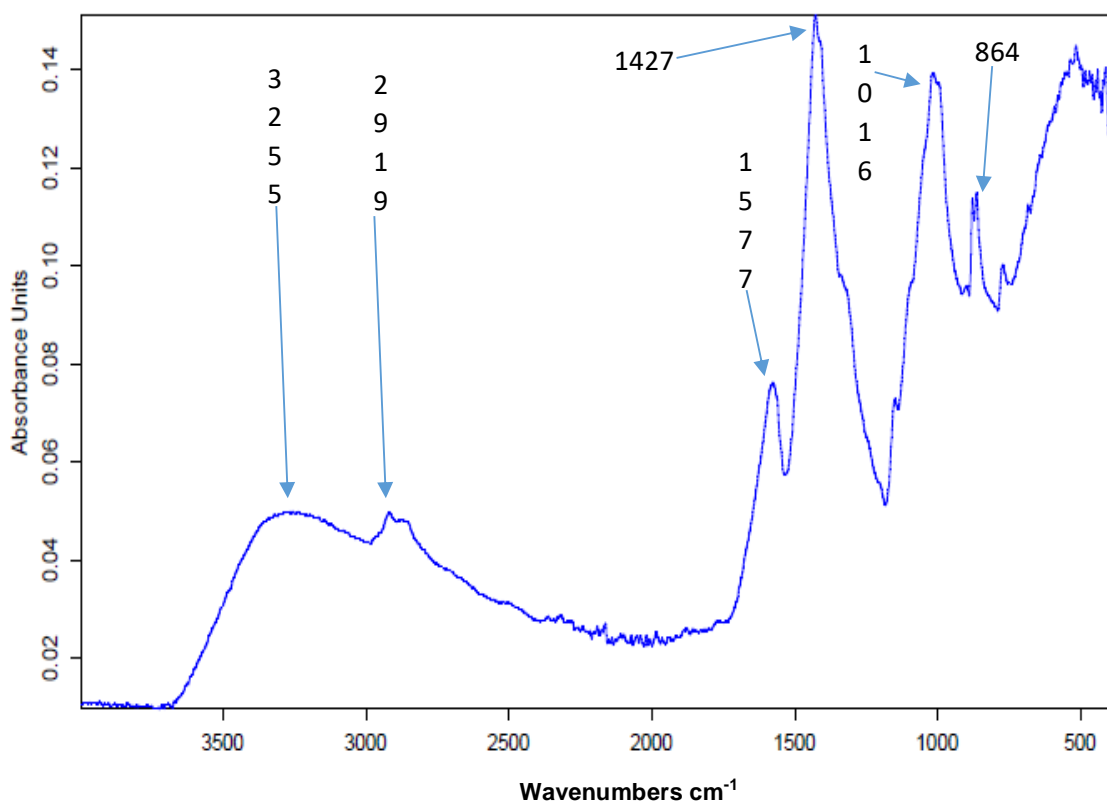


**Figure 4.13: ATR-IR spectrum of banana rachis fibre/chitosan composite pellet (5.0 g rachis fibre used during composite)**

The spectra showed broad, very strong, and less intense peak O-H stretching band of hydroxyl group at about  $3255\text{ cm}^{-1}$  ( $3200 - 3650\text{ cm}^{-1}$ ) centered at about  $3000\text{ cm}^{-1}$ , the change in peak shape is a result of the different degree of hydrogen bonds following composite formation as has also been seen in the controls (Figure 4.13). Peaks observed at  $1252\text{ cm}^{-1}$  and  $1162\text{ cm}^{-1}$  also show the presence of hemicelluloses (Sain and Panthapulakkal, 2006).

Identification of characteristic peaks is based on previous studies of fibers (Mokhothu, 2010). The band at  $2900\text{ cm}^{-1}$  ( $2611\text{ cm}^{-1}$  there is a band closer =  $2919$ ) is due to the C-H stretching of saturated carbon in cellulose and hemicellulose. This peak is broadened and show a peak at  $3255\text{ cm}^{-1}$ . As already indicated this broadening of this peak suggest that the hydrogen bond pattern has been changed during composite formation. This peak corresponded to the peak of the rachis fiber control at  $3238\text{ cm}^{-1}$ . For regenerated chitosan the peak wavenumber was  $3292\text{ cm}^{-1}$ . According to Ziani *et al.*, (2008), the broad absorption band between  $3600$  and  $3000\text{ cm}^{-1}$  could be attributed to the -OH and -NH stretching vibrations, the absorption bands at  $1660$ ,  $1592$ , and  $1385\text{ cm}^{-1}$ , respectively, ascribed to the amide I, II and III bands of chitosan. However, the composite exhibit only one band at  $1577\text{ cm}^{-1}$  in this region (Figure 4.13).

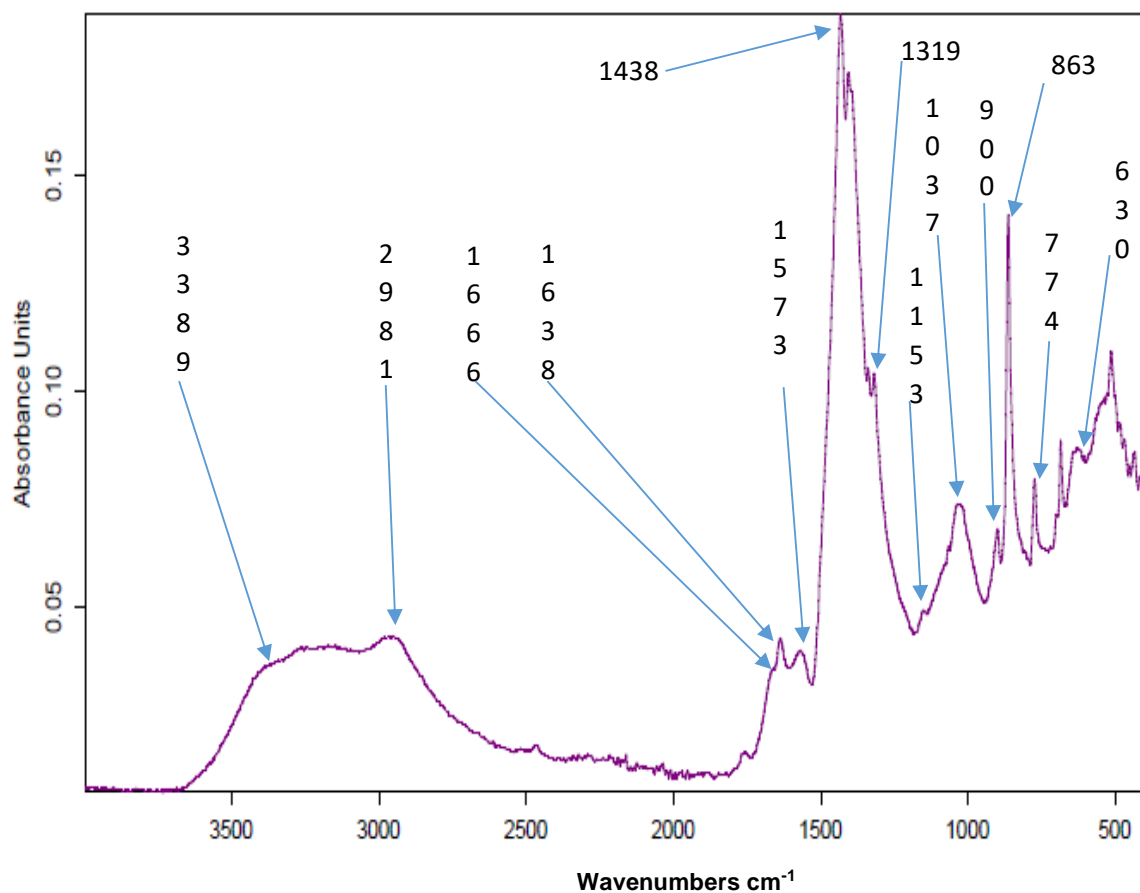


**Figure 4.14: ATR-IR spectrum of banana rachis fibre/chitosan composite supernatant (5 g)**

The identification of characteristic peaks is based on previous studies of fibres (Figure 4.14). The adsorption at 3200 – 3389  $\text{cm}^{-1}$  is due to stretching vibrations of O-H groups of cellulose, hemicelluloses and lignin (C-O-C) that are present in BRF (Figure 4.14). The band at 2981  $\text{cm}^{-1}$  is due to the C-H stretching of saturated carbon in cellulose and hemicellulose.

The infrared wavenumber of chitosan functional groups. Identification of characteristic peaks is based on previous studies of chitosan (Figure 4.14). Figure 4.14 shows hydroxyl and amino bands at the ranged spectra up to 3500  $\text{cm}^{-1}$ . A broad absorption band in the range 3000 to 3500  $\text{cm}^{-1}$  was noted which is assigned to O-H stretching vibrations and the 3263  $\text{cm}^{-1}$  to vibration of NH. It also indicates the vibration of C=O stretching (amide I) at 1627  $\text{cm}^{-1}$  (Rumengan *et al.*, 2014) and 1650.95  $\text{cm}^{-1}$  (Wanule *et al.*, 2014). Characteristic bands associated with regenerated chitosan was noticed in the supernatant these are a band at 1638  $\text{cm}^{-1}$  for the supernatant versus 1645  $\text{cm}^{-1}$  for regenerated chitosan. Also 1573  $\text{cm}^{-1}$  for the supernatant. It seems therefore that chitosan was present in the supernatant and could be retrieved to some extent from the supernatant by gel formation as was describe earlier (Figure 4.14).

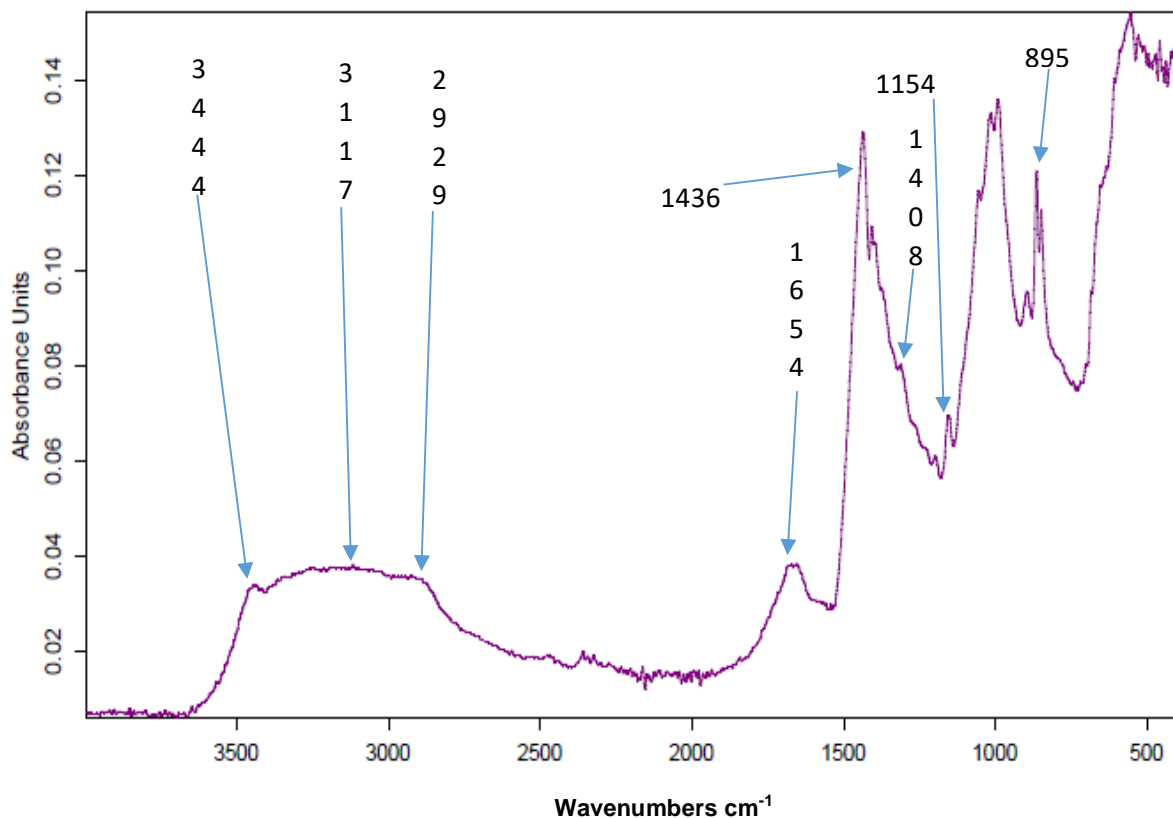


**Figure 4.15: ATR-IR spectrum of alpha cellulose/chitosan composite pellet (0.5 g)**

According to Chieu *et al.*, (2013), the regeneration of both cellulose and chitosan was confirmed by FTIR spectroscopy, the FTIR spectrum of microcrystalline cellulose exhibits three pronounced bands at around  $3400\text{ cm}^{-1}$ ,  $2850 - 2900\text{ cm}^{-1}$  and  $890 - 1150\text{ cm}^{-1}$  (Figure 4.15). These bands can be tentatively assigned to stretching vibrations of O-H, C-H and O groups, respectively (Burns and Ciurczak, 1992; Da Roz *et al.*, 2010; Dreve *et al.*, 2009).

The spectra showed broad, very strong, and less intense peak O-H stretching band of hydroxyl group at about  $3444\text{ cm}^{-1}$  ( $3200 - 3650\text{ cm}^{-1}$ ) centred at about  $3000\text{ cm}^{-1}$ , the change in peak shape is a result of the different degree of hydrogen bonds. These spectra display characteristic chitosan bands around  $3400\text{ cm}^{-1}$  (O-H stretching vibrations),  $3250 - 3350\text{ cm}^{-1}$  (symmetric and asymmetric N-H stretching),  $2850 - 2900\text{ cm}^{-1}$  (C-H stretching),  $1657\text{ cm}^{-1}$  (C-O, amide I),  $1595\text{ cm}^{-1}$  (N-H deformation),  $1380\text{ cm}^{-1}$  ( $\text{CH}_3$  symmetrical deformation),  $1319\text{ cm}^{-1}$  (C-N stretching, amide III) and  $890 - 1150\text{ cm}^{-1}$  (ether bonding) (Burns and Ciurczak., 1992; Da Roz *et al.*, 2010; Dreve *et al.*, 2009).

According to Mansur *et al.*, (2009), the spectrum of the cellulose/chitosan bead before crosslinking (CC1) was very similar to that of chitosan due to the higher content of chitosan. The strong peak at  $1654\text{ cm}^{-1}$  indicates the  $\text{-NH}$  adsorption in the  $\text{C=O}$  stretching in the amide due to partially acetylated amino groups ( $\text{-NHCOCH}_3$ ) (Mansur *et al.*, 2009). The composite exhibit a single peak at  $1654\text{ cm}^{-1}$ . The banana rachis fibre/chitosan composite also show a single peak in this region but at another wavenumber (Figure 4.15).

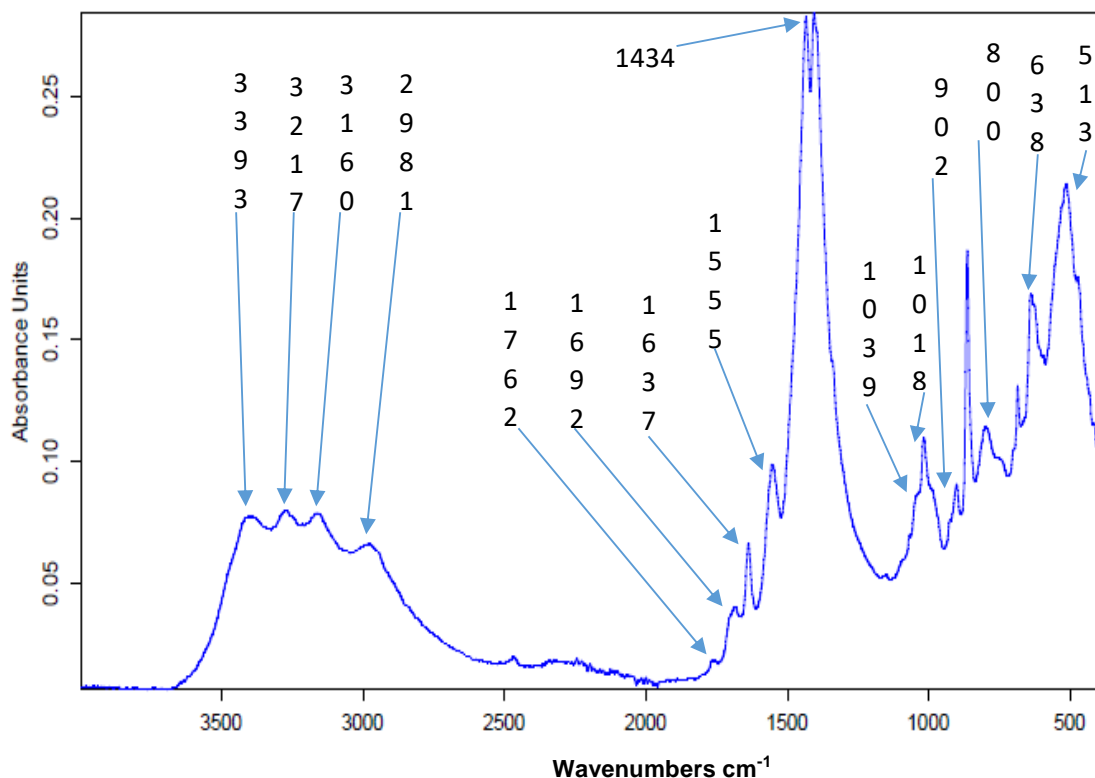


**Figure 4.16: ATR-IR spectrum of alpha cellulose/chitosan composite supernatant (0.5 g)**

The spectra showed a broad peak with three less sharper peaks due to the O-H stretching band of hydroxyl group at about  $3160\text{ cm}^{-1}$ ,  $3217\text{ cm}^{-1}$ , and  $3393\text{ cm}^{-1}$  (Figure 4.16). According to Trivedi *et al.*, (2018), the IR spectra of pristine chitosan and cellulose exhibit, broad bands which are visible in the region  $3700 - 3000\text{ cm}^{-1}$ , corresponding to O-H stretching and N-H vibrations. The presence of amide I band at  $1651\text{ cm}^{-1}$  due to the carbonyl stretching vibrations, and a bifurcated band with peaks at  $1590\text{ cm}^{-1}$  due to amide II, corresponding to N-H bending vibrations and at  $1560\text{ cm}^{-1}$ , due to free  $\text{NH}_2$  bending vibrations are present in chitosan (Larkin, 2011). A slight variation in the  $\text{CH}_x$  deformations that correspond to peaks at  $1425$  and  $1374\text{ cm}^{-1}$  can also be observed. Similarly, in the region  $3600 - 3100\text{ cm}^{-1}$  of the Raman spectra, the sharp O-H and N-H stretching vibrations in chitosan and broad O-H



stretching vibrations in cellulose are visible. In chitosan, the peak due to alkyl groups shows slight bifurcation, which is not apparent in cellulose (Trivedi *et al.*, 2018) (Figure 4.16).

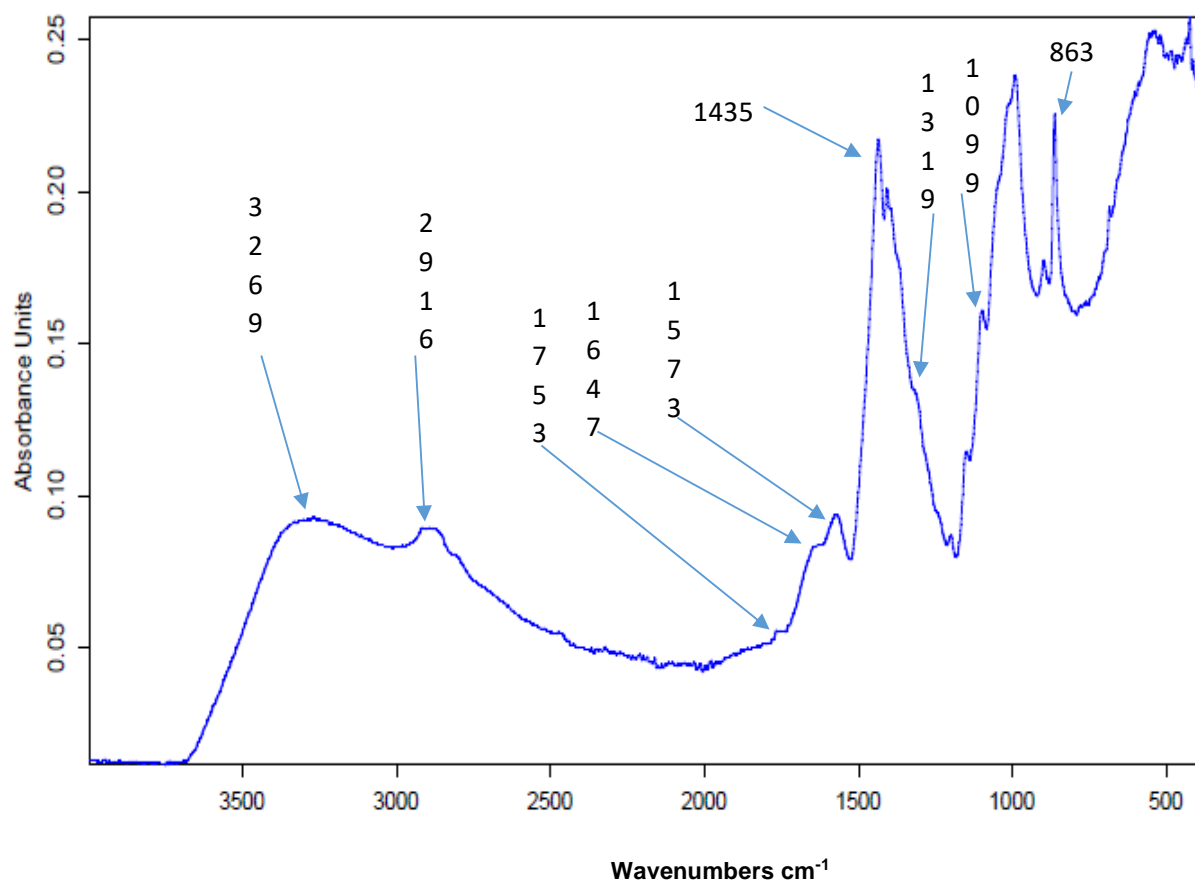


**Figure 4.17: ATR-IR spectrum of alpha cellulose/chitosan composite pellet (5 g)**

The spectra showed broad, very strong, and less intense peak O-H stretching band of hydroxyl group at about 3246 cm<sup>-1</sup> and 3269 cm<sup>-1</sup> (3200 – 3650 cm<sup>-1</sup>) centred at about 3000 cm<sup>-1</sup> is due to the O-H stretching, 2916 cm<sup>-1</sup> (C-H stretch), 1674 cm<sup>-1</sup> (C-OH stretch) the change in peak shape is a result of the different degree of hydrogen bonds that are present in alpha cellulose/chitosan composite pellet 5 g (Figure 4.17). Tanjung *et al.* (2017), presented the infrared (IR) spectra of microcrystalline cellulose (MCC), regenerated cellulose (RC) film and chitosan/regenerated cellulose (RC/Ch) film. As illustrated in the IR spectrum of the MCC, the main characteristic peaks are at approximately 3325 (O–H stretch), 2900 (C–H stretch), 1635 (C–OH stretch) and 1104 cm<sup>-1</sup> (C–O stretch). The spectrum of the cellulose/chitosan composite in this study shows a single peak at 1573 cm<sup>-1</sup>, however a shoulder appears at 1647 cm<sup>-1</sup>. This seem to indicate that the characteristic peaks of regenerated chitosan can be found in the composite. For regenerated chitosan the corresponding peaks are found at 1645 cm<sup>-1</sup> and 1574 cm<sup>-1</sup> (Figure 4.17).

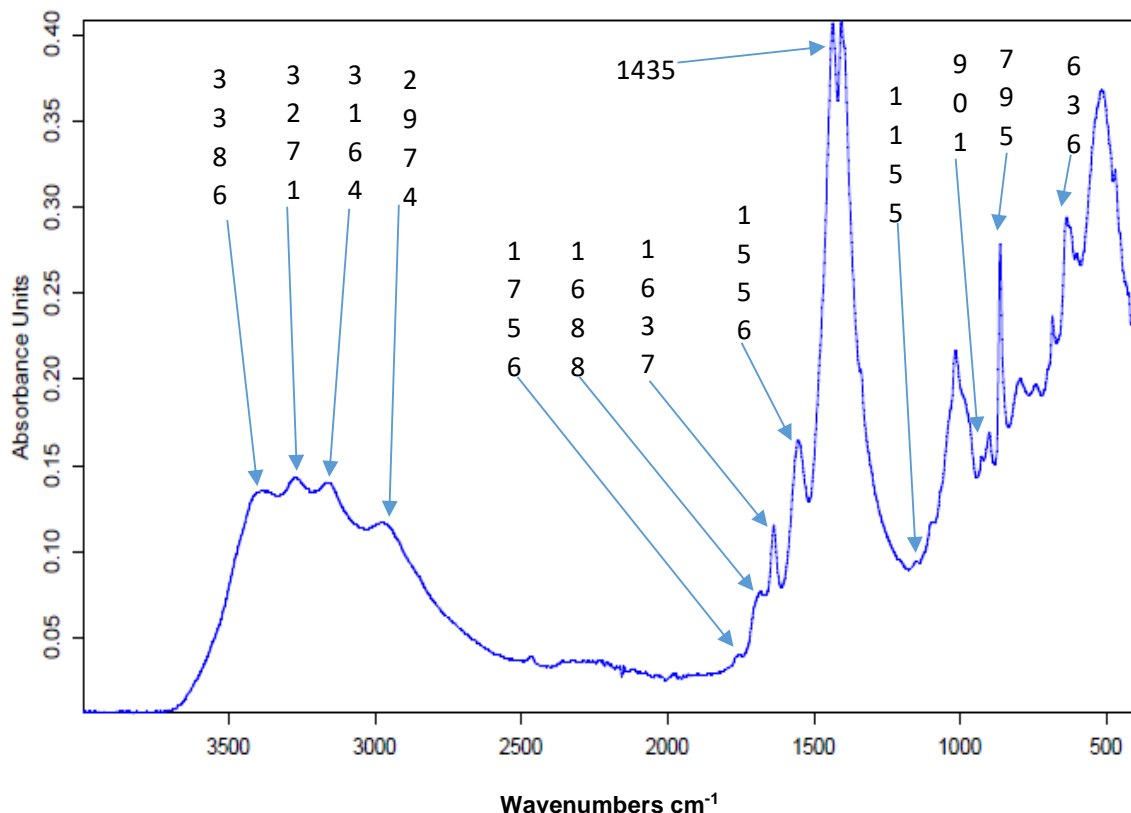


**Figure 4.18: ATR-IR spectrum of alpha cellulose/chitosan composite supernatant (5 g)**

The spectra showed a broad with three less sharper peaks due to the O-H stretching band of hydroxyl group at about  $3164\text{ cm}^{-1}$ ,  $3271\text{ cm}^{-1}$ , and  $3386\text{ cm}^{-1}$  (Figure 4.18). These spectra display characteristic chitosan bands around  $3400\text{ cm}^{-1}$  (O-H stretching vibrations),  $3250 - 3350\text{ cm}^{-1}$  (symmetric and asymmetric N-H stretching),  $2850 - 2900\text{ cm}^{-1}$  (C-H stretching),  $1657\text{ cm}^{-1}$  (C-O, amide I),  $1595\text{ cm}^{-1}$  (N-H deformation),  $1380\text{ cm}^{-1}$  ( $\text{CH}_3$  symmetrical deformation),  $1319\text{ cm}^{-1}$  (C-N stretching, amide III) and  $890 - 1150\text{ cm}^{-1}$  (ether bonding) (Burns and Ciurczak., 1992; Da Roz *et al.*, 2010; Dreve *et al.*, 2009).

The major peaks of cellulose are common to all polysaccharides, the broad regions of -OH ( $3500 - 3000\text{ cm}^{-1}$ ) and C-O (around  $1100\text{ cm}^{-1}$ ). Alternatively, chitin and chitosan share amide peaks at around  $3200$  and  $1600\text{ cm}^{-1}$  (Kumirska *et al.*, 2010). According to Riva *et al.* (2015), for pure chitosan the IR spectrum showed bands at  $3360$  and  $3265\text{ cm}^{-1}$  typical of O-H and N-H bonds respectively. The band at  $2870\text{ cm}^{-1}$  corresponds to C-H bonds and the signal at  $1650\text{ cm}^{-1}$  is commonly seen with type I amides and C=O bonds linked to acetyl and amine groups, and  $1560\text{ cm}^{-1}$  corresponds to amide groups (N-H). Finally, bands of  $1060$  and  $1030\text{ cm}^{-1}$  confirm the presence of C-O bonds. In this study in contrast to the composite there were three peaks obtained for the supernatant sample namely at  $1556$ ,  $1637$  and  $1688\text{ cm}^{-1}$ . There is therefore definite differences between these samples (supernatant and composite).

The corresponding bands in regenerated chitosan is similar but different at 1645 and 1574  $\text{cm}^{-1}$  (Figure 4.18).

The ATR-IR composites (banana rachis fibre/chitosan composite and alpha cellulose/chitosan composite) can be concluded as, the broad peak at 3286  $\text{cm}^{-1}$  due to the addition of raw banana fibres with chitosan confirmed the formation of inter molecular hydrogen bonding between chitosan and raw banana fibres. The C-O vibrations were observed from the band between 1000 and 1100  $\text{cm}^{-1}$ . These shifts in IR peaks indicated that the interfacial interaction through the formation of new bonds between chitosan and raw banana fibre. This observed shift from 3445 to 3334  $\text{cm}^{-1}$  with respect to chitosan was intense and confirmed the strong interaction between the blended components.

These shifts in IR peaks indicated that the interfacial interaction through the formation of new bonds between chitosan and banana rachis fibre which stabilized the composite. Cellulose and chitosan are similar in terms of their chemical structure. The bands for both polysaccharides are the same, expect for the presence of an amine group with chitosan. The composites (banana rachis fibre/chitosan composite and alpha cellulose/chitosan composite) are better than the banana rachis fibre, chitosan, and alpha cellulose alone because they will have a good combination of new functional groups between the two materials. The major ATR-IR bands in banana rachis fibre, alpha cellulose, chitosan, banana rachis fibre/chitosan composite, and alpha cellulose/chitosan composite (regenerated and non-regenerated samples) are shown in Table 4.1.

**Table 4.1: The major ATR-IR bands in banana rachis fibre, alpha cellulose, chitosan, banana rachis fibre/chitosan composite, and alpha cellulose/chitosan composite (regenerated and non-regenerated samples)**

Wavenumber (cm <sup>-1</sup> )	Band assignments
3750-3000	(OH) hydroxyl groups in lignin (phenolic + CH <sub>2</sub> OH), cellulose and hemicelluloses Intermolecular hydrogen-bonded H-O-H stretching
3278	06 H6...03 intermolecular hydrogen bond
3240	06 H6...03 intermolecular hydrogen bond
3000-2850	CH <sub>2</sub> and CH <sub>3</sub> in methylene and CH <sub>3</sub> , CH <sub>3</sub> in methyl groups
1732	C=O ester in acetoxy groups (H <sub>3</sub> C-(C=O)-O-) in hemicelluloses
1650	C=O in quinone or p-quinone
1595,1505	C=C skeletal vibration in phenolic ring (lignin motif type guaiacyl ie coniferyl with C-H <sub>ar</sub> out of plane deformation at 834 and 900-870 cm <sup>-1</sup> )
1462	CH <sub>2</sub> asymmetric bending (scissoring) strong in cellulose I CH <sub>3</sub> asymmetric bending in lignin (CH <sub>3</sub> -O) and hemicelluloses (CH <sub>3</sub> -(C=O)-)
1425	CH <sub>2</sub> asymmetric bending in crystallized cellulose I (strong) and amorphous cellulose (weak and shift to 1420 cm <sup>-1</sup> in cellulose II and amorphous cellulose)
1375	C-H and CH <sub>3</sub> in cellulose and hemicelluloses
1318	CH <sub>2</sub> in crystallized cellulose I (wagging)
1268	C-O guaiacyl aromatic methoxyl group in lignin and cellulose
1230	C-O syringy nuclei in lignin and hemicellulose
1163	C-O-C asymmetric stretch vibration in cellulose and hemicelluloses
1112	CH stretching vibrations in different groups of lignin and cellulose and hemicelluloses
1034	C-O-C skeletal vibration of polysaccharides ring

898	C-O-C $\beta$ -(1-4)-glycosidic linkage (weak and broad in cellulose I, strong and sharp in cellulose II)
834	C-H (2C-H adjacent) out of plane bending of 1,2,4-tetra-substituted aromatic in lignin, with contribution of the band at 900-870 $\text{cm}^{-1}$ (collapsed with C-O-C $\beta$ -(1-4)-glycosidic linkage)

#### 4.4.3. X-ray diffraction characterization

The x-ray diffraction spectra of banana rachis fibre, chitosan, alpha cellulose, banana rachis fibre/chitosan composite 5 g, and alpha cellulose/chitosan composite 5 g by x-ray diffraction analysis (Figures 4.20 - 4.24). The regions (crystalline and amorphous regions) are differentiated in this way (i.e., crystalline regions are indicated by peaks, between a-b while amorphous regions have characteristic peaks between c-d), for all the figures 4.20-4.24.

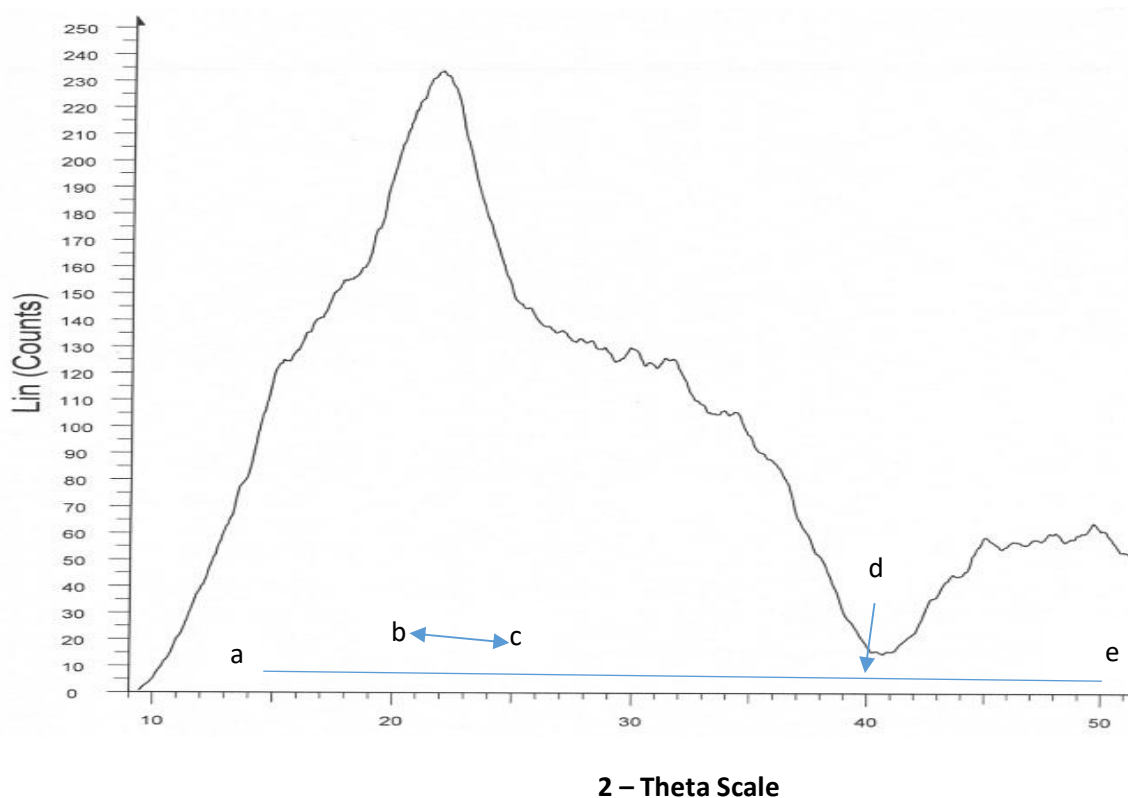


**Figure 4.19: X-ray diffraction spectra of banana rachis fibre**

The presence of both crystalline and amorphous regions (Milani et al., 2016) (Figure 4.19). Crystalline regions are indicated by peaks between b – c, while amorphous regions have characteristics peaks between a – d and d – e. The crystalline region is found where molecules

are arranged in an ordered pattern, and the amorphous region where molecules are arranged randomly (Yashoda, 2016). The banana rachis fibre spectra displayed two broad peaks and one thinner peak (crystalline). The banana rachis fibre XRD data showed broad peaks which could indicate smaller crystalline region and a larger amorphous region for the x-ray diffraction values obtained. The smaller crystalline region (lower crystallinity) of banana rachis fiber is probably due to the presence of hemicelluloses and lignin in the fibre. Broad x-ray diffraction peaks from the range of  $15^\circ$  to  $40^\circ$  and  $40^\circ$  to  $50^\circ$ . As already indicated the decrease of crystallinity of banana rachis fibre is due to the availability of hemicelluloses and lignin from the fibre, this is a large proportion of the amorphous region of lignocellulosic domains (Rosa et al., 2010) (Figure 4.19).

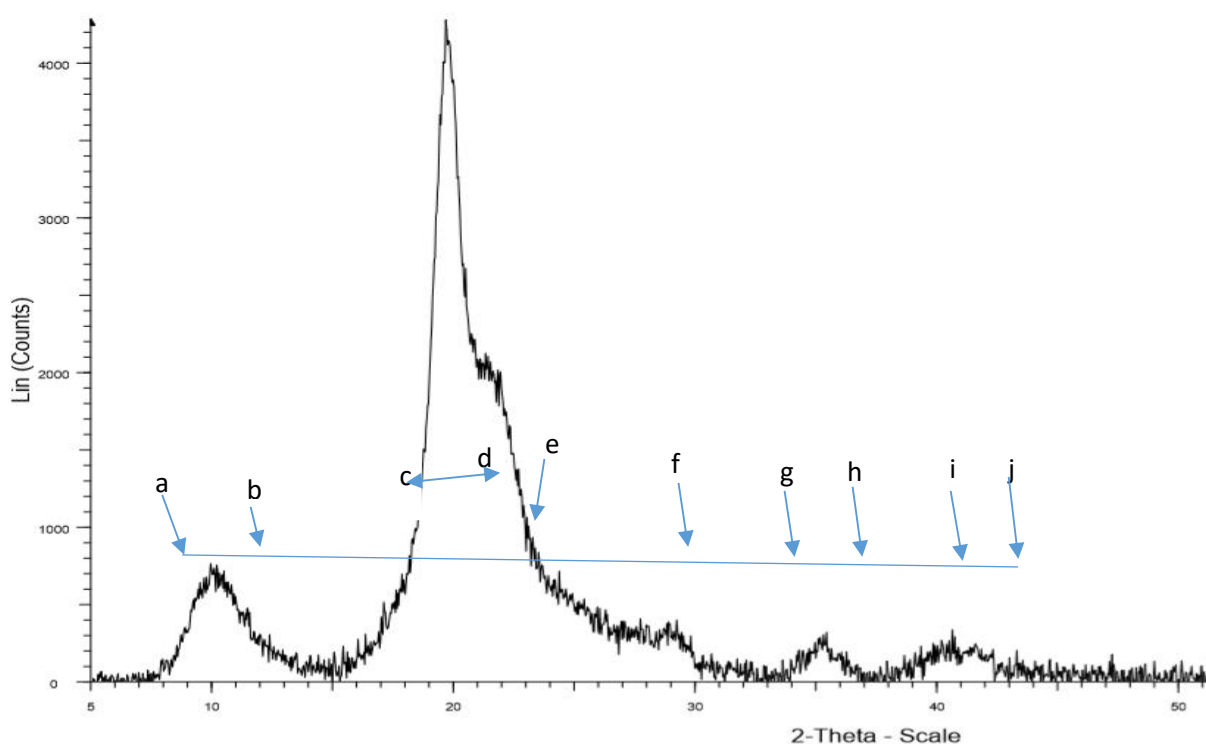


**Figure 4.20: X-ray diffraction spectra of chitosan**

The presence of both crystalline and amorphous regions (Antonino *et al.*, 2017) (Figure 4.20). The chitosan spectra displayed broad peaks of low intensity from the range of  $9^\circ$  to  $12^\circ$ ,  $23^\circ$  to  $30^\circ$ ,  $34^\circ$  to  $37^\circ$ ,  $40^\circ$  to  $42^\circ$  and one thinner peak bigger than the other (crystalline) from the range of  $18^\circ$  to  $22^\circ$ . Crystalline regions are indicated by peak between c – d, while amorphous regions have characteristics peaks between a – b, e – f, g – h, and i – j. The broader the peaks the greater the amorphous region and the thinner the peaks indicate the crystalline region (Govindan *et al.*, 2012). The crystallinity of the chitosan increases with the increase in degree

of deacetylation and is attributed to increase in intermolecular hydrogen bonding due to the presence of more free  $\text{NH}_2$  groups (higher degree of deacetylation) within the molecular structure, which in turn results in a better packing of the macromolecular polymeric chains and consequent increase in the crystallinity (de Vasconcelos *et al.*, 2007; Ray *et al.*, 2010). Deacetylation of chitosan can be facilitated under basic conditions (Yuan *et al.*, 2011) (Figure 4.20).

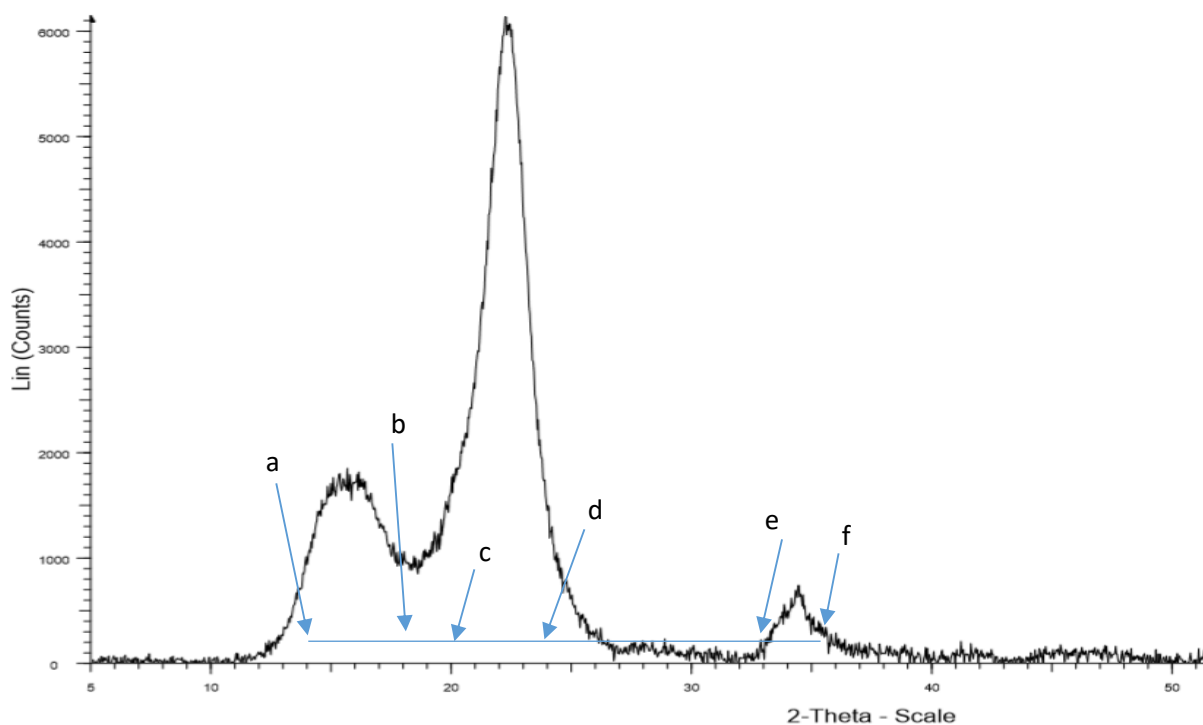


**Figure 4.21: X-ray diffraction spectra of alpha cellulose**

The presence of both crystalline and amorphous regions (Sunkyu *et al.*, 2010) (Figure 4.21). The alpha cellulose spectra displayed two broad peaks of low intensity from the range of  $14^\circ$  to  $18^\circ$ ,  $33^\circ$  to  $35^\circ$  and one thinner peak of higher intensity (crystalline) from the range of  $20^\circ$  to  $24^\circ$ . Crystalline regions are indicated by peak between c – d, while amorphous regions have characteristics peaks between a – b, e – f. An increased amorphous contribution is the main contributor to peak broadening. However, in addition to crystalline disorder (amorphous content), there are other intrinsic factors that influence peak broadening, such as crystallite size and non-uniform strain within the crystal. Samples that can be resolved into many narrow diffraction peaks over a significant range of  $2\theta$ . Unfortunately, cellulose peaks are very broad and not well resolved, with overlapping peaks. It is generally accepted in the cellulose research community that peak broadening is due to the amorphous cellulose (Sunkyu *et al.*, 2010) (Figure 4.21).

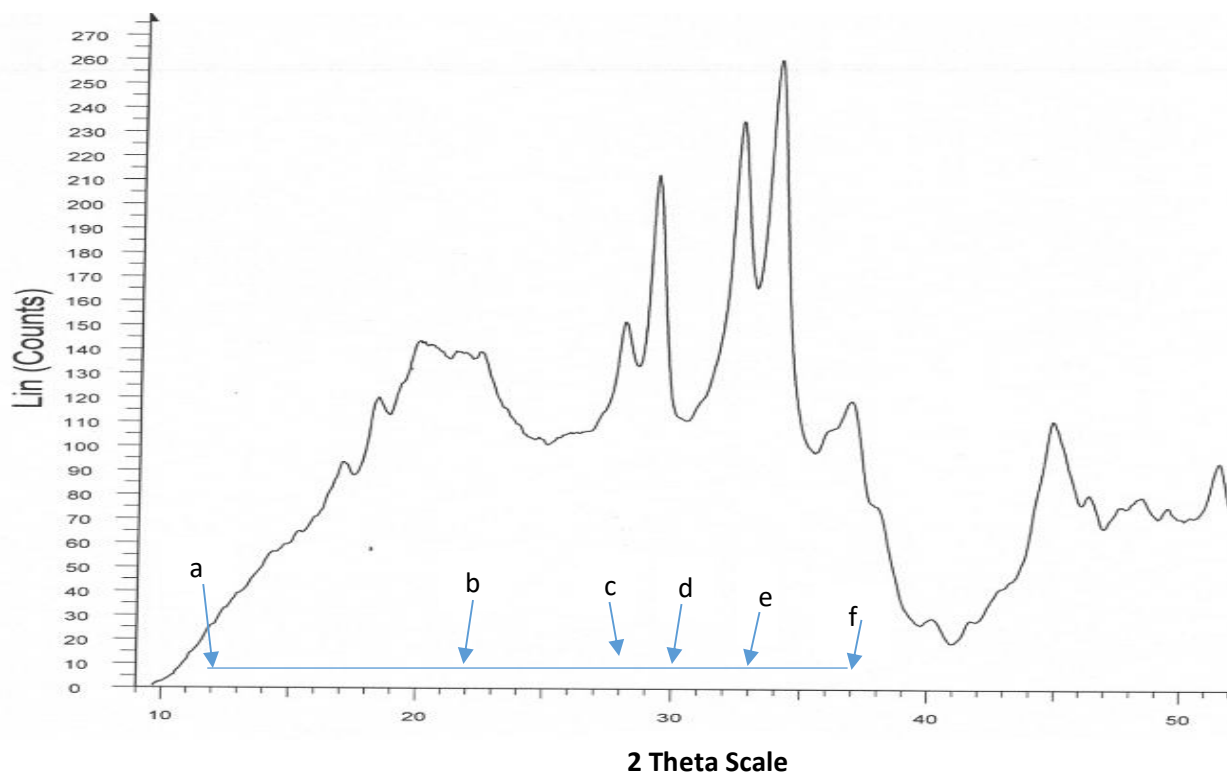


**Figure 4.22: X-ray diffraction spectra of banana rachis fibre/chitosan composite**

The banana rachis fibre/chitosan composite XRD results showed thin peaks which could indicate that an increase in crystallinity resulted composite formulation, due to the presence of highly crystalline cellulose in the composites (Figure 4.22). A further indication of this phenomenon is shown by intense x-ray diffraction peaks from the range of  $12^{\circ}$  to  $22^{\circ}$ ,  $28^{\circ}$  to  $30^{\circ}$ ,  $33^{\circ}$  to  $37^{\circ}$ , also indicating an increase in crystallinity that occurred following composite formation. Crystalline regions are indicated by c – d, e – f, while amorphous regions have characteristics peak between a – b. The increase in crystallinity is due to the increase in the rigidity of cellulose because of the hardness of the cellulose (Haafiz *et al.*, 2013). Sharpest and strongest peaks (high intensity) indicate increase in the crystallinity (Zuliahani *et al.*, 2017) (Figure 4.22).



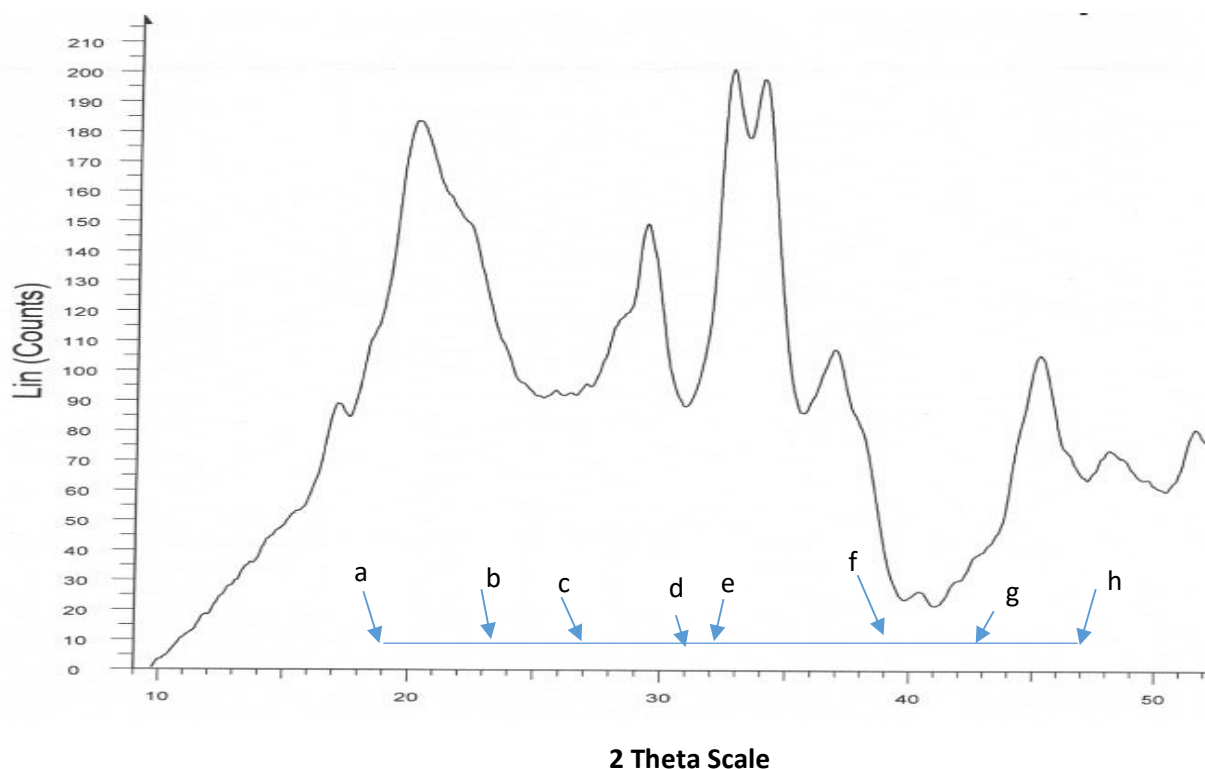


**Figure 4.23: X-ray diffraction spectra of alpha cellulose/chitosan composite**

The alpha cellulose/chitosan composite XRD results showed thin peaks which could indicate that an increase in crystallinity resulted following composite formulation, due to the presence of highly crystalline cellulose in the composites from the range of  $19^{\circ}$  to  $23^{\circ}$ ,  $28^{\circ}$  to  $31^{\circ}$ ,  $32^{\circ}$  to  $39^{\circ}$ ,  $43^{\circ}$  to  $47^{\circ}$  (Figure 4.23). Crystalline regions are indicated by peaks c – d, e – f, and g – h, while amorphous regions have characteristics peak between a – b. A further indication of this phenomenon is shown by intense x-ray diffraction peaks, also indicating an increase in crystallinity that occurred following composite formation. Sharpest and strongest peaks indicate increase in crystallinity as has already been pointed out (Zuliahani *et al.*, 2017).

The peaks located near  $2\theta = 14.9^{\circ}$ ,  $16.7^{\circ}$ ,  $22.8^{\circ}$ , and  $34.68^{\circ}$ , are the characteristics molecular planes causing 101, 101, 002, and 040 x-ray reflections to occur in banana rachis fibre, chitosan, alpha cellulose, banana rachis fibre/chitosan composite and alpha cellulose/chitosan composite (Liu *et al.*, 2012). With fiber growth, major peak intensity near 22.88 increases and its peak half-height width decreases, both of which suggest that the crystallinity and the crystallite dimension increase with secondary wall cellulose biosynthesis (Liu *et al.*, 2012) (Figure 4.23).

### Crystallinity index infrared (CI<sub>IR</sub>) measurement

It has been suggested that a so called 4-band ratio (R<sub>3</sub>) used in Eq. 5 to relate the XRD measurement to the crystalline information.

$$R_3 = (I_{22.8} + I_{20.5}) / (I_{14.9} + I_{16.5}) \quad (5)$$

where R<sub>3</sub> is indicative of XRD crystalline information and I<sub>14.9</sub>, I<sub>16.5</sub>, I<sub>20.5</sub>, and I<sub>22.8</sub> are each a three-point average of the intensity values at individual 2θ degree positions (Liu *et al.*, 2012).

Furthermore, the R<sub>3</sub> values could be converted into respective Cl<sub>XRD</sub> readings in the range of 0.0% to 100.0% by Eq. 6:

$$Cl_{XRD} (\%) = 100 \times (R_3 - 1.317) / 0.91 \quad (6)$$

The intensities of the peaks at 110 lattices (I<sub>110</sub>, at 2θ ~20° corresponding to maximum intensity) and at 2θ ~16° (amorphous diffraction) were used to calculate crystallinity index (ICR) of chitosan using Equation (7) (Al-sagheer *et al.*, 2009)

$$I_{CR} (\%) = I_{110} - I_{am} / I_{110} \times 100 \quad (7)$$

The calculations for XRD measurement to the crystalline information of the R<sub>3</sub>, and Cl<sub>XRD</sub> (%) on various samples (banana rachis fibre, alpha cellulose, banana rachis fibre/chitosan composite, alpha cellulose/chitosan composite) are shown below.

A, Banana rachis fibre

$$\begin{aligned} R_3 &= (I_{22.8} + I_{20.5}) / (I_{14.9} + I_{16.5}) \\ &= (227 + 122) / (85 + 125) \\ &= 349 / 210 \\ &= 1.66 \end{aligned}$$

$$\begin{aligned} Cl_{XRD} (\%) &= 100 \times (R_3 - 1.317) / 0.91 \\ &= 100 \times (1.66 - 1.317) / 0.91 \\ &= 100 \times 0.343 / 0.91 \\ &= 37.69\% \end{aligned}$$

B, Chitosan

$$I_{CR} (\%) = I_{110} - I_{am} / I_{110} \times 100$$

$$\begin{aligned} &= 3500 - 200/3500 \times 100 \\ &= 94.29\% \end{aligned}$$

C, Alpha cellulose

$$\begin{aligned} R_3 &= (I_{22.8} + I_{20.5}) / (I_{14.9} + I_{16.5}) \\ &= (1000 + 4800) / (1100 + 1700) \\ &= 5800/2800 \\ &= 2.07 \end{aligned}$$

$$\begin{aligned} Cl_{XRD} (\%) &= 100 \times (R_3 - 1.317) / 0.91 \\ &= 100 \times (2.07 - 1.317) / 0.91 \\ &= 100 \times 0.753/0.91 \\ &= 82.75\% \end{aligned}$$

D, Banana rachis fibre/chitosan composite

$$\begin{aligned} R_3 &= (I_{22.8} + I_{20.5}) / (I_{14.9} + I_{16.5}) \\ &= (140 + 115) / (55 + 65) \\ &= 224/120 \\ &= 1.87 \end{aligned}$$

$$\begin{aligned} Cl_{XRD} (\%) &= 100 \times (R_3 - 1.317) / 0.91 \\ &= 100 \times (1.87 - 1.317) / 0.91 \\ &= 100 \times 0.553/0.91 \\ &= 60.77\% \end{aligned}$$

E, Alpha cellulose/chitosan composite

$$\begin{aligned} R_3 &= (I_{22.8} + I_{20.5}) / (I_{14.9} + I_{16.5}) \\ &= (160 + 120) / (60 + 70) \\ &= 280/130 \\ &= 2.15 \end{aligned}$$

$$\begin{aligned} Cl_{XRD} (\%) &= 100 \times (R_3 - 1.317) / 0.91 \\ &= 100 \times (2.15 - 1.317) / 0.91 \\ &= 100 \times 0.833/0.91 \\ &= 91.54\% \end{aligned}$$

The  $CI_{XRD}$  percentage readings in this study are summarized in Table ranges from the highest to the lowest 94.29% for chitosan, 91.54% for alpha cellulose/chitosan composite, 82.75% for alpha cellulose, 60.77% for banana rachis fibre/chitosan composite and 37.69% for banana rachis fibre. According to Al-sagheer et al. (2009) obtained 33% and 37% for chitosan, which is lower than the 94.29% for chitosan obtained. Alpha cellulose/chitosan composite, alpha cellulose, and chitosan were more crystalline compared to the banana rachis fibre/chitosan composite and banana rachis fibre based on the percentage values calculated above.

The crystalline structures are highly stable to temperature variations, and their catalytic and adsorption properties render them industrial and household applications (Akhtar *et al.*, 2014). Polymers (cellulose and starch) have amorphous structure ([www.chemengonline.com](http://www.chemengonline.com)>industrial-adsorbents). Significance of the crystalline structure of the different adsorbents is to check for crystallinity of the adsorbent structure by identifying the regions (crystalline region and amorphous regions) of crystallinity. The crystallinity can impact the adsorbent nature of the different material used, because when the material is more amorphous is better for adsorption of dye than the crystalline ones.

Crystalline polymers are difficult to stain than amorphous ones because the dye molecules penetrate through amorphous regions with greater ease (Balazsy and Eastop, 1998). Other waste fibers obtained from the agroindustry, such as bleached rice husk and soy hulls, reached crystallinity index values of 57% (Johar *et al.*, 2012) and 73% (Neto *et al.*, 2013), respectively. According to Rambo and Ferreira, (2015), the rachis presented a range of 22.62%-26.79%, which is lower than the 37.69% for banana rachis fibre obtained.

On the other hand, value-added byproducts from bio-waste such as cellulose microfibrils from garlic skin and cellulose nanocrystals from garlic straw had CI values of 45% (Reddy and Rhim, 2014) and 69% (Kallel *et al.*, 2016), respectively. The amount of paracrystalline cellulose (33.1%) is almost identical to the amount of crystalline structure (31.8%) in cotton cellulose (Larsson *et al.*, 1997) and lower than the 82.75% for alpha cellulose found in this study. The absolute value of cellulosic Avicel thus obtained are extremely high (90% for cellulosic Avicel) as was indicated by Hall *et al.* (2010).

Microcrystalline cellulose (MCC) is a pure partially depolymerized cellulose synthesized from  $\alpha$ -cellulose precursor (type I $\beta$ ), obtained as a pulp from fibrous plant material, with mineral acids using hydrochloric acid to reduce the degree of polymerization. It is prepared by treating alpha cellulose with mineral acids (type I $\beta$ ). The amorphous regions are more prone to

hydrolysis by acid resulting in shorter and more crystalline fragments such as the MCC, which makes the microcrystalline cellulose easily to be compared to the composites (alpha cellulose/chitosan composite). The literature contains a wide range of reported values for cellulosic Avicel (microcrystalline cellulose) using x-ray diffraction, in the range 62 - 87.6% using the peak height method, and from 39 to 75.3% using various other methods (Hall *et al.*, 2010). It should be noted, however, that different drying methods are often being employed, which also may add to the reported variations in absolute crystallinity values. The  $CI_{XRD}$  percentage of various samples (banana rachis fibre, chitosan, alpha cellulose, banana rachis fibre/chitosan composite, and alpha cellulose/chitosan composite) are shown in Table 4.2.

**Table 4.2: The  $CI_{XRD}$  (%) of samples**

Various samples	$R^3$	$CI_{XRD}$ (%)	$I_{110}$
Banana rachis fibre	1.66	37.69	
Banana rachis fibre/chitosan composite	1.87	60.77	
Chitosan		94.29	3500
Alpha cellulose	2.07	82.75	
Alpha cellulose/chitosan composite	2.15	91.54	

#### 4.4.4. Adsorption Equilibrium and Isotherm

##### 4.4.4.1. Effect of the various adsorbents dosage on decolourization of the CBB G-250 dye

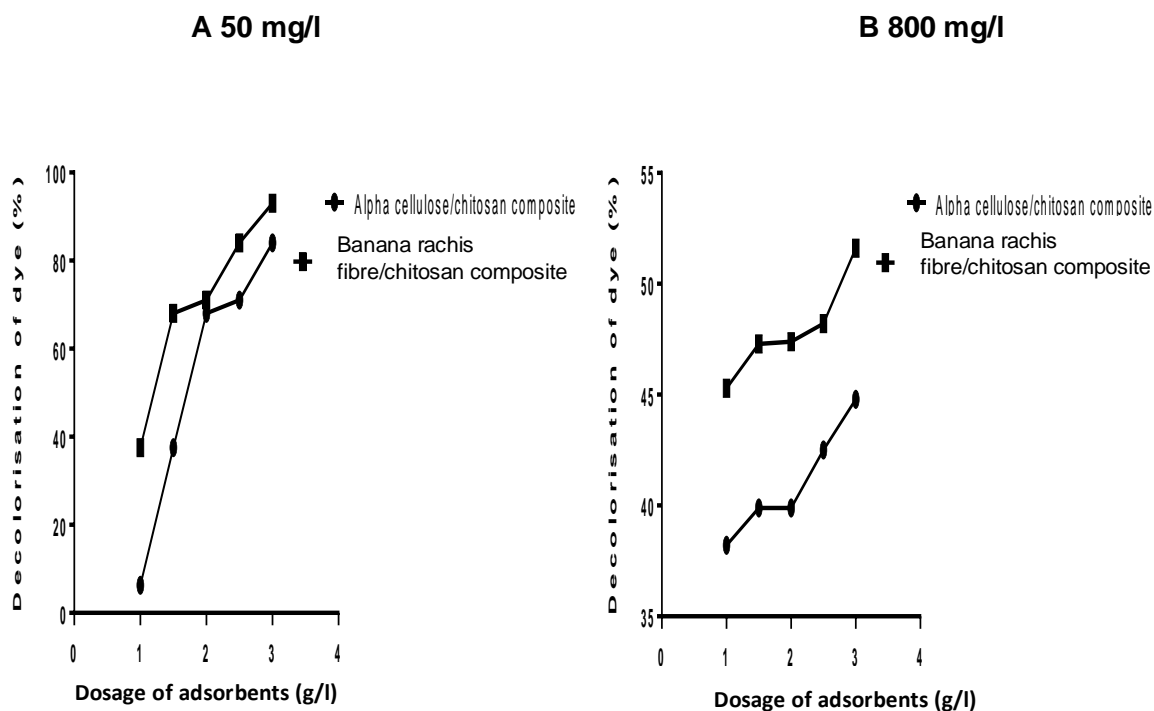


**Figure 4.24: Effect of adsorbent dosage on decolourisation of CBB G-250 dye (%) using various composites A. Alpha cellulose/chitosan composite and B. Banana rachis fibre/chitosan composite**

The effect of the various adsorbent dosage on decolourisation of CBB dye (%), Figure A. Low concentration of 50 mg/l CBB. Figure B. High concentration of 800 mg/l CBB using different adsorbents (alpha cellulose/chitosan and banana rachis fibre/chitosan composites) dosages after 80 minutes. Temperature 30 °C, pH 6.59 – 6.71 (Figure 4.24 A and B).

### Low concentration (50 mg/l) of CBB G-250 dye

#### Percentage decolourisation activity of alpha cellulose/chitosan and banana rachis fibre/chitosan composites

The equation to calculate the percentage of the decolourization of the CBB G-250 dye for the alpha cellulose at the dosages of 1, 1.5, 2, 2.5, and 3 g/l is similar to the calculations for the other adsorbents (alpha cellulose/chitosan and banana rachis fibre/chitosan composite), were performed in Section 3.4.2.

The decolourization of CBB G-250 dye by adsorption on alpha cellulose/chitosan and banana rachis fibre/chitosan composites was found to increase with time and attained at a constant value at 80 minutes. At a low concentration (50 mg/l) the percentage decolourisation increases from 6.3 to 84.4% for alpha cellulose/chitosan and then 37.5 to 93.8% for banana rachis

fibre/chitosan composites with a low concentration for CBB G-250, depending on the dosages (1, 1.5, 2, 2.5, and 3 g/l) used during adsorption.

### **High concentration (800 mg/l) of CBB G-250 dye**

#### **Percentage decolourization activity of alpha cellulose/chitosan and banana rachis fibre/chitosan composites**

The equation to calculate the percentage of the decolourisation of the CBB G-250 dye for the alpha cellulose at the dosages of 3, 2.5, 2, 1.5, and 1 g/l is similar to the calculations for the other adsorbents (alpha cellulose/chitosan and banana rachis fibre/chitosan composites) were performed similarly as in Section 3.4.2.

The decolourization of CBB G-250 dye by adsorption on alpha cellulose/chitosan and banana rachis fibre/chitosan composites was found to increase with time and attained a constant value at 80 min. At a high concentration CBB G-250 dye (800 mg/l) using a dosage of 3 g/l, the percentage decolourization at equilibrium also decreased compared to low concentration (50 mg/l) tested from 44.8% to 84.4% for alpha cellulose/chitosan composite, and 51.6% to 93.8% for banana rachis fibre/chitosan composite.

As the low concentration (50 mg/l) of Coomassie Brilliant Blue dye was increased, the absorbance efficiency was decreased (Figure 4.25 A and B). This may be due to the fact that at lower concentrations almost all the dye molecules were adsorbed very quickly on the outer surface, but further increases in dye concentrations led to fast saturation of the adsorbents (alpha cellulose/chitosan composite and banana rachis fibre/chitosan composite) surface, and thus most of the dye adsorption apparently took place slowly inside the pores (Hameed and El-Khaiary, 2008; Khaleque and Roy, 2016).

This indicate that the highest concentration performance is obtained with an adsorbent dosage of 3 g/l (Figure 4.24 A and B). It was observed that as the dosage of adsorbent was increased, the removal efficiency became higher (Figure 4.24 A and B). Increase in the removal efficiency of Coomassie brilliant blue dye with the increased amount of adsorbent dose is due to the increased surface area and the availability of additional adsorption sites (Khaleque and Roy,

2016). As the low CBB G-250 dye concentration increases from 50 to 800 mg/l the equilibrium removal of CBB G-250 dye increase from 6.3 to 84% and 38.2 to 44.8% for alpha cellulose/chitosan composite and banana rachis fibre/chitosan composite, respectively. For the batch adsorption experiments on alpha cellulose/chitosan and banana rachis fibre/chitosan composites, the effect of adsorbent dosage on the CBB G-250 dye adsorption were examined.

Significant variations in the uptake capacity and removal efficiency are observed at different adsorbent dosages (1 to 3 g/l) indicate that the highest concentration tested is obtained with an adsorbent dosage of 3 g/l (Figure 4.24 A and B) of the tested concentrations. This result was expected because the removal efficiency is generally increased by the fact that when more mass becomes available, the more the total contact surface offered for adsorption will increase.

Moreover, the higher dose of adsorbent in the solution, the greater the availability of exchangeable sites for the CBB G -250 dye, i.e. more active sites are available for binding of CBB G – 250 dye. Results based on the findings given above are qualitatively and in good agreement with those found in the literatures (Khaleque *et al.*, 2016). The percentage of decolourisation of alpha cellulose/chitosan and banana rachis fibre/chitosan composites at an initial concentration (50 mg/l) and highest concentration (800 mg/l) are shown in Table 4.3.

**Table 4.3: The percentage of decolourisation of different adsorbents at different concentrations**

Adsorbents	Percentage decolourisation (%)									
	Initial concentration (50 mg/l)					High concentration (800 mg/l)				
Dosages (g)	3	2.5	2	1.5	1	3	2.5	2	1.5	1
Alpha cellulose/chitosan composite	84.4	71.9	68.8	37.5	6.3	44.8	42.5	39.9	39.9	38.2
Banana rachis fibre/chitosan composite	93.8	84.4	71.9	68.8	37.5	51.6	48.2	47.4	47.3	45.3

#### 4.4.4.2. Equilibrium time sorption experiments



The absorbance reading over time obtained during sorption experiments at a lower and higher concentrations as indicated conducted with the sorbents (Figure 4.26 A and B).

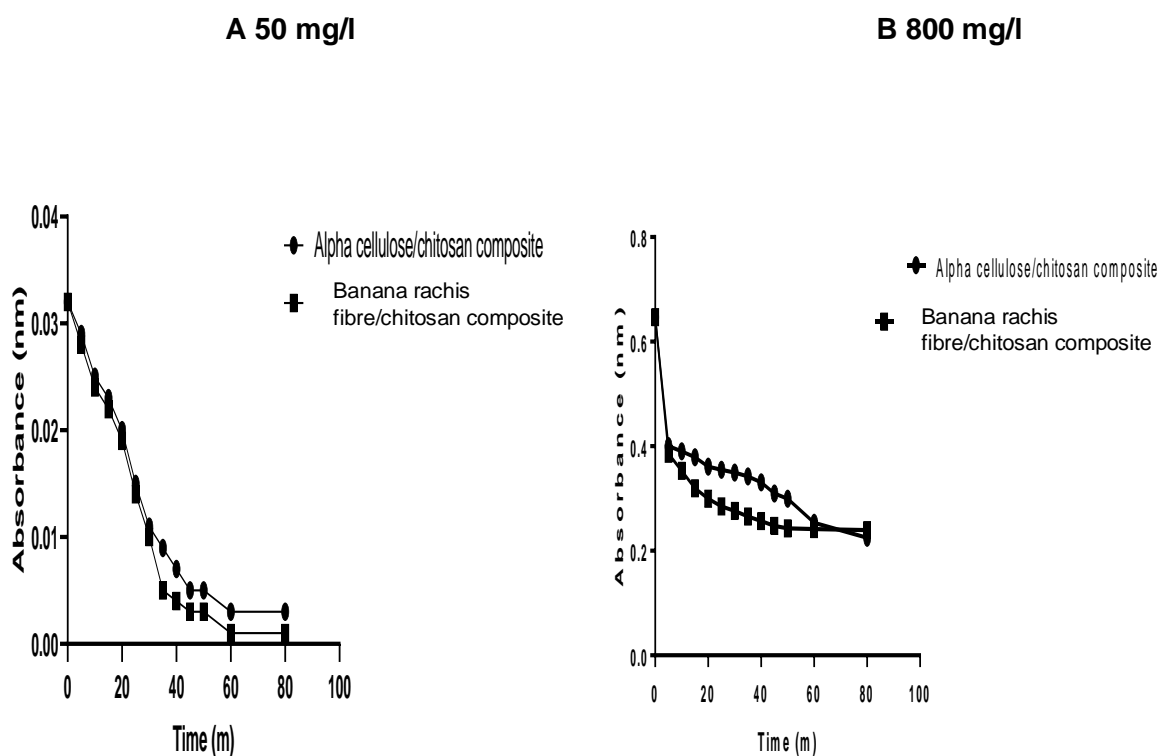


**Figure 4.25: Effect of contact time on adsorption of the CBB G-250 dye using various composites at different concentrations A. 50 mg/l and B. 800 mg/l**

The effect of contact time on adsorption, A) adsorption at an Initial concentration of 50 mg/l CBB. B) adsorption using a concentration of 800 mg/l, for various adsorbents (Alpha cellulose/chitosan composite and banana rachis fibre/chitosan composite) after 80 minutes (Figure 4.25 A and B). A temperature 30 °C was maintained and pH 6.59 – 6.71 and 3 g/l adsorbent dosage. The panel A and B above show the absorbance reading over time obtained during sorption experiments conducted with the sorbents indicated (Figure 4.25 A and B).

#### Low concentration 50 mg/l of CBB G-250 dye

The data presented in Figure 4.25 A and B shows that equilibrium was reached after 60 minutes for alpha cellulose/chitosan and banana rachis fibre/chitosan composites samples. In each case the equilibrium adsorption value was substituting in the equation derived from the CBB standard curve in order to calculate the sorption activity of the alpha cellulose/chitosan composite and banana rachis fibre/chitosan composite by first converting absorbance to concentration values.

The equation to calculate the percentage sorption activity of the alpha cellulose is similar to the calculations for the other adsorbents (alpha cellulose/chitosan and banana rachis fibre/chitosan composites), were performed in Section 3.4.3.

### **High concentration of 800 mg/l of CBB G-250 dye**

After about 60 minutes (alpha cellulose/chitosan and banana rachis fibre/chitosan composites), Figure 4.25 A and B shows that equilibrium was reached. The equation to calculate the percentage sorption activity of the activated carbon is similar to the calculations for the other adsorbents (alpha cellulose/chitosan and banana rachis fibre/chitosan composites), were performed in Section 3.4.3.

The percentage sorption activity of CBB G-250 dye increases with time and a constant value after 60 min and, it reaches a constant value indicating that no more CBB G-250 dye is removed from the solution (equilibrium has been reached). Thus changing the initial concentration of dye from 50 to 800 mg/l, the adsorbed amount increases from 63.98% to 96.22% for alpha cellulose/chitosan composite, and 68.84% to 96.68% for banana rachis fibre/chitosan composite (Figure 4.25 A and B). This may be attributed to an increase in the driving force necessary of the concentration gradient when increasing the basic dye concentration to in order to overcome the mass transfer resistance of CBB G-250 dye acting between the aqueous and solid phases (Moussa *et al.*, 2015). The percentage of sorption activity of different adsorbents at a low concentration (50 mg/l) and highest concentration (800 mg/l) are presented in Table 4.4.

**Table 4.4: Percentage of sorption activity and equilibrium concentration ( $C_e$ ) of composites observed at the lowest and highest CBB dye concentrations of CBB dye**

Adsorbents	Sorption activity (%)		Equilibrium concentration $C_e$ (mg/l)	
	Low concentration	Highest concentration	Low concentration	Highest concentration
Banana rachis fibre/chitosan composite	68.84	96.68	15.58	26.55
Alpha cellulose/chitosan composite	63.98	96.22	18.01	30.21

#### 4.4.4.3. Equilibrium studies

The capacity of adsorption of CBB G- 250 dye using alpha cellulose/chitosan and banana rachis fibre/chitosan composites were calculated as has been shown previously (Figure 4.27 A and B). Calculations for alpha cellulose/chitosan and banana rachis fibre/chitosan composites after isotherm experiments were performed: The equation to calculate the capacity of adsorption of CBB G-250 dye at different concentrations 100, 200, 400, and 800 mg/l for the chitosan at the dosage of 3 g/l is similar to the calculations for the other adsorbents(alpha cellulose/chitosan and banana rachis fibre/chitosan composites) were performed in Section 3.4.4.1.

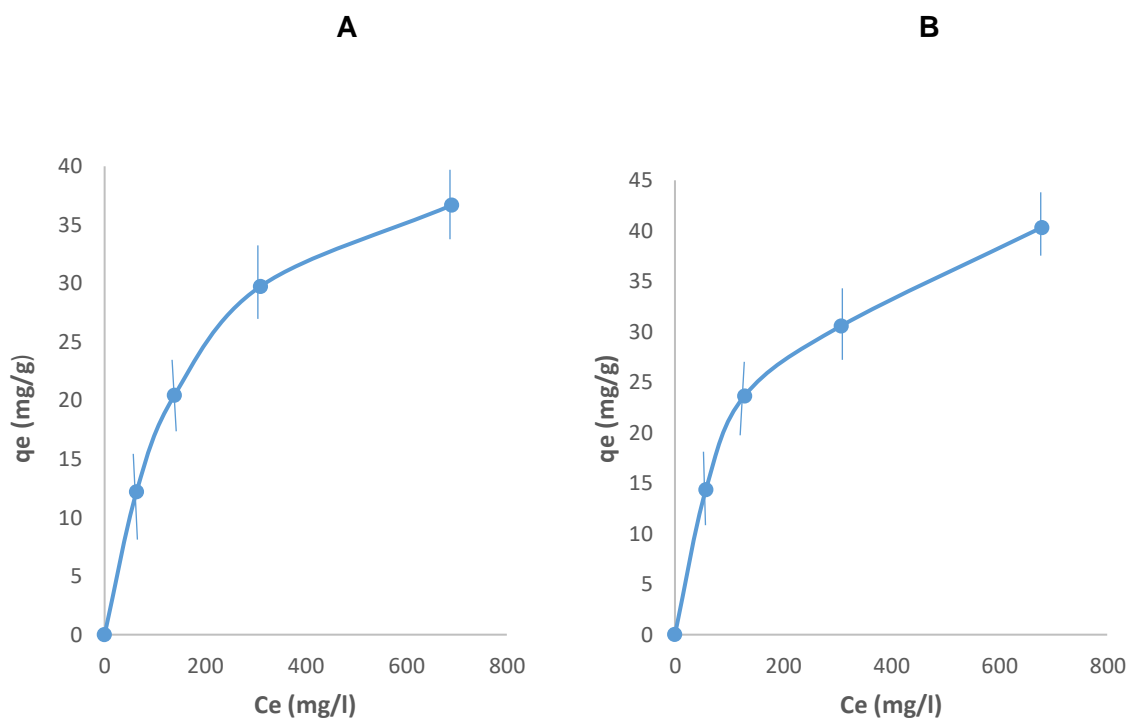


**Figure 4.26: Adsorption isotherm of CBB G-250 dye ( $q_e$  versus  $C_e$ ) using various composites A. Alpha cellulose/chitosan composite and B. Banana rachis fibre/chitosan composite**

The capacity of adsorption of CBB G-250 dye (800 mg/l) using various adsorbents (alpha cellulose/chitosan composite and banana rachis fibre/chitosan composite) after 60 minutes, 37 °C, 150 rpm, pH 6.59 – 6.71 and 3 g/l adsorbent dosage (Figure 4.26 A and B). The isotherm approaches the saturation point at 690 and 679 mg/l for alpha cellulose/chitosan composite and banana rachis fibre/chitosan composite, respectively.

At this concentration (690 and 679 mg/l) the alpha cellulose/chitosan composite and banana rachis fibre/chitosan composite, respectively,  $q_e$  values levels off and reached a saturation point where less and less CBB G-250 dye is further removed from the solution under these conditions as initial dye concentration levels increases. The capacity of adsorption of CBB G-250 dye using alpha cellulose/chitosan and banana rachis fibre/chitosan composites was found to increase with time and attained a constant value at 60 minutes (Figure 4.26 A and B).

The adsorption capacity of banana rachis fibre/chitosan composite on CBB G-250 dye is greater than that of chitosan, banana rachis fibre, alpha cellulose and alpha cellulose/chitosan composite. Banana rachis fibre used not in a composite but alone as adsorbent seems to be having a lower adsorption capacity than when it is combined with chitosan. Therefore, composite formation seems to enhance adsorption of CBB dye in the latter case. The capacity of adsorption of CBB G-250 dye using different adsorbents at an equilibrium concentration as shown in Table 4.5.

**Table 4.5: The capacity of adsorption of CBB G-250 dye using different adsorbents at an equilibrium concentration**

Adsorbents	Capacity of adsorbents of CBB G-250 (mg/g)				Equilibrium concentration (C <sub>e</sub> ) (mg/l)			
	100	200	400	800	100	200	400	800
Concentrations (mg/l)	100	200	400	800	100	200	400	800
Alpha cellulose/chitosan composite	12.20	20.43	29.77	36.67	63.4	138.7	310.7	690
Banana rachis fibre/chitosan composite	14.33	23.67	30.60	40.33	57.6	129	308.2	679

#### 4.4.4.4. Langmuir and Freundlich isotherms

Two isotherm equations (in linear format) were tested in this work. One is the Langmuir and the Freundlich equations are commonly used for the describing adsorption equilibrium of adsorbate onto the adsorbent. The Langmuir isotherm is applicable to monolayer chemisorptions while Freundlich isotherm is used to describe adsorption on surface having heterogeneous energy distribution (Gupta *et al.*, 2011).

Under this condition tested in this work the following results were obtained for the Langmuir model in batch experiments.

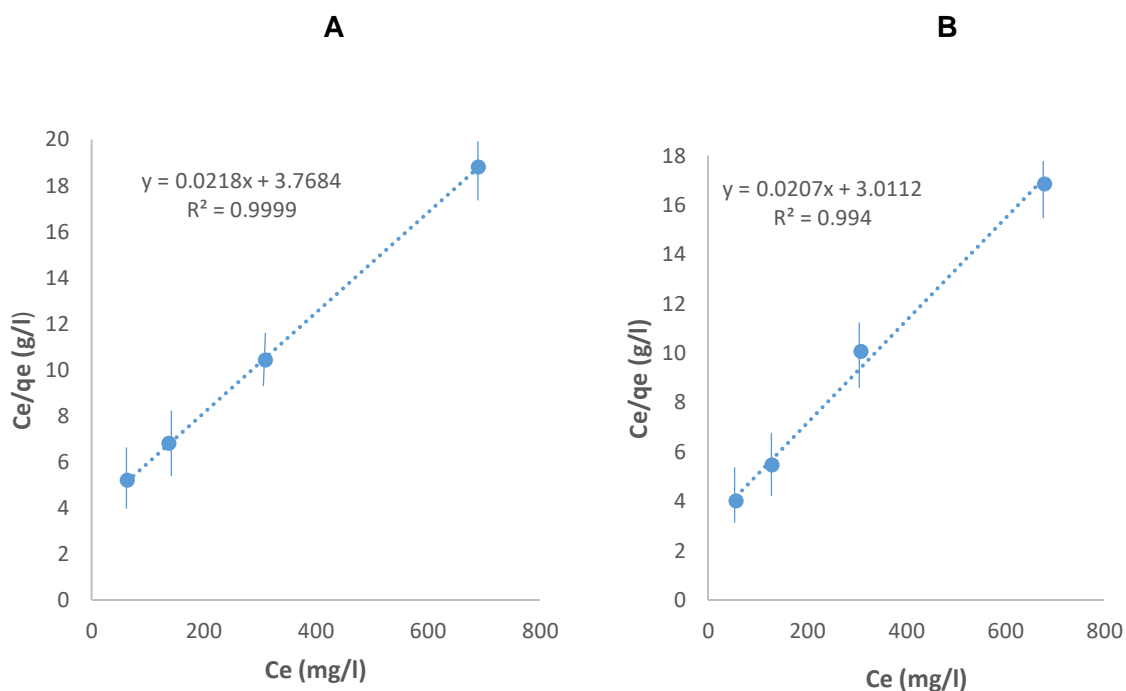


**Figure 4.27: Linearised version of Langmuir isotherm of various composites A. Alpha cellulose/chitosan composite and B. Banana rachis fibre/chitosan composite**

The adsorption of CBB G-250 dye (800 mg/l) using various adsorbents (alpha cellulose/chitosan composite and banana rachis fibre/chitosan composite) after 60 minutes, 30 °C, pH 6.59 – 6.71 and 3 g/l adsorbents dosage (Figure 4.27 A and B). The correlation coefficient was found to be 0.9999 and 0.994 for alpha cellulose/chitosan composite and banana rachis fibre/chitosan composite, respectively, indicating that the data was fitted well to the Langmuir model.

It is observed that the alpha cellulose/chitosan composite Langmuir isotherm showed higher value of correlation coefficient ( $R^2 = 0.9999$ ) than that of the banana rachis fibre/chitosan composite Langmuir isotherm. From the Langmuir plot, capacity of adsorption (36.67 and 40.33 mg/g) for alpha cellulose/chitosan composite and banana rachis fibre/chitosan composite, respectively, and equilibrium concentration (690 and 679 mg/l) for alpha cellulose/chitosan composite and banana rachis fibre/chitosan composite, respectively were obtained. The closer the value is to 1, the better the fit, or relationship, between the two factors. The goodness of fit, or the degree of linear correlation, measures the distance between a fitted line on a graph and all the data points that are scattered around the graph. A good fit has an  $R^2$  that is close to 1 ([www.investopedia.com/terms/C/coefficient-of-determination.asp](http://www.investopedia.com/terms/C/coefficient-of-determination.asp)). A plot of  $1/q_e$  versus  $1/C_e$  gives  $b$  and  $q_{max}$  if the isotherm follows the Langmuir equation (Annadurai *et al.*, 2002) (Figure 4.27 A and B).

Under this condition tested in this work the following results were obtained for the Freundlich model in batch experiments.

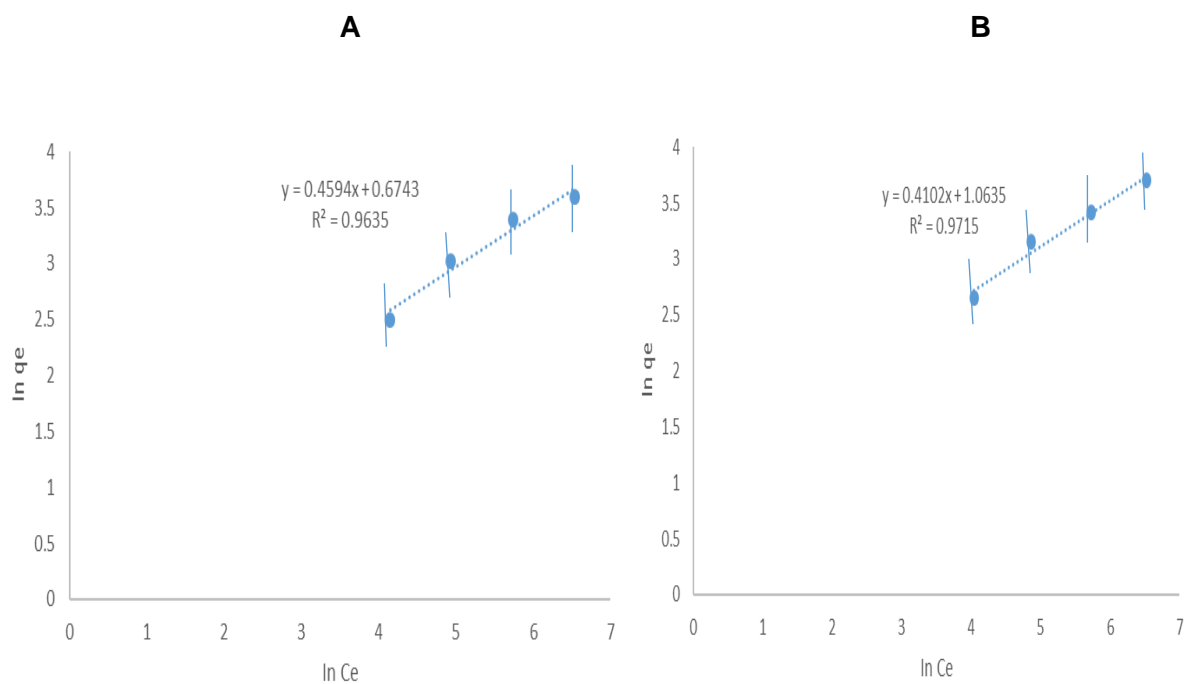


**Figure 4.28: Freundlich isotherm of various composites A. Alpha cellulose/chitosan composite and B. Banana rachis fibre/chitosan composite**

The adsorption of CBB G-250 dye (800 mg/l) using various adsorbents (alpha cellulose/chitosan composite and banana rachis fibre/chitosan composite) after 60 minutes, 30 °C, pH 6.50 – 6.71, and 3 g/l adsorbent dosage (Figure 4.28 A and B). The correlation coefficient was found to be 0.9715 and 0.9635 for banana rachis fibre/chitosan composite and alpha cellulose/chitosan composite, respectively, indicating that the data was fitted well to the Freundlich model.

It is observed that the banana rachis fibre/chitosan composite Freundlich isotherm showed higher value of correlation coefficient ( $R^2 = 0.9715$ ) than that of the other three Freundlich isotherm. The closer the value is to 1, the better the fit, or relationship, between the two factors. The goodness of fit, or the degree of linear correlation, measures the distance between a fitted line on a graph and all the data points that are scattered around the graph. A good fit has an  $R^2$  that is close to 1 ([www.investopedia.com/terms/C/coefficient-of-determination.asp](http://www.investopedia.com/terms/C/coefficient-of-determination.asp)). The intercept  $K_f$  obtained from plot of  $\log q_e$  versus  $\log C_e$  is roughly a measure of the sorption capacity and the slope ( $1/n$ ) of the sorption intensity. The magnitude of the term ( $1/n$ ) gives an indication of the favorability and capacity of the adsorbent/adsorbate systems, according to Annadurai *et al.* (2002) (Figure 4.28 A and B).

The adsorbents (alpha cellulose/chitosan composite and banana rachis fibre/chitosan composite) calculations for Langmuir and Freundlich isotherm parameters values are as follows: The equations to calculate the Langmuir and Freundlich isotherm parameters of CBB G-250 dye at different concentrations 100, 200, 400, and 800 mg/l for the chitosan at the dosage of 3 g/l is similar to the calculations for the other adsorbents (alpha cellulose/chitosan

and banana rachis fibre/chitosan composites) were calculated in Section 3.4.5 (Figure 4.27 A and B, Figure 4.28 A and B).

The Langmuir and Freundlich adsorption isotherm constants for the adsorption of CBB G-250 dye on banana rachis fibre/chitosan and alpha cellulose/chitosan composites are given in Table 4.6.

**Table 4.6: Langmuir and Freundlich isotherm constants for the adsorption of CBB G-250 dye on various composites**

Equilibrium model	Adsorbent	(Correlation coefficient) $R^2$	Parameters	Values
Langmuir isotherm	Alpha cellulose/chitosan composite	0.9999	b (l/g)	5.79
			$q_{\max}$ (mg/g)	45.87
	Banana rachis fibre/chitosan composite	0.994	b (l/g)	6.87
			$q_{\max}$ (mg/g)	48.31
Freundlich isotherm	Alpha cellulose/chitosan composite	0.9635	$K_f$ (l/g)	1.96
			n	2.18
	Banana rachis fibre/chitosan composite	0.9715	$K_f$ (l/g)	2.90
			n	2.44

$R^2$  Correlation coefficient

b Empirical constant, indicating the affinity of sorbent towards the sorbate

$q_{\max}$  Maximum possible amount of dye that can be adsorbed per unit dry weight of sorbent.

$K_f$  Empirical constant, indicates the adsorption capacity of the sorbent

n Constant indicating the intensity of adsorption



Based on the correlation coefficient ( $R^2$ ) shown in Table 4.3, the adsorption isotherms with alpha cellulose/chitosan composite, followed by banana rachis fibre/chitosan composite can be described better by the Langmuir correlation coefficient ( $R^2$ : 0.9999 and 0.994) which is bigger than the Freundlich correlation coefficient ( $R^2$ ). This means that Langmuir model is more applicable than Freundlich model. For the banana rachis fibre/chitosan composite, followed by alpha cellulose/chitosan composite can also be described by the Freundlich correlation coefficient  $R^2$  (0.9715 and 0.9635 respectively) since it ( $R^2$ ) is near to that of the Langmuir isotherm.

The results showed that banana rachis fibre/chitosan composite, and alpha cellulose/chitosan composite were good adsorbents of the CBB G-250 dye because the value of  $n$  (2.44 and 2.18) respectively were greater than 1. According to Kadirvelu and Namasivayam (2000)  $n$  values between 1 and 10 represents beneficial adsorption and thus the adsorption of dye on the adsorbents. The 'n' value is a variable whose value when greater than one indicates good adsorbance activity. The  $n$  value is a variable, from  $1/n$  the exponent of non-linearity of the Freundlich adsorption isotherm. (Gupta *et al.*, 2011).

#### **4.4.4.5. The glucose standard graph obtained using the anthrone method**

The glucose standard graph obtained using the anthrone method (Figure 4.29).

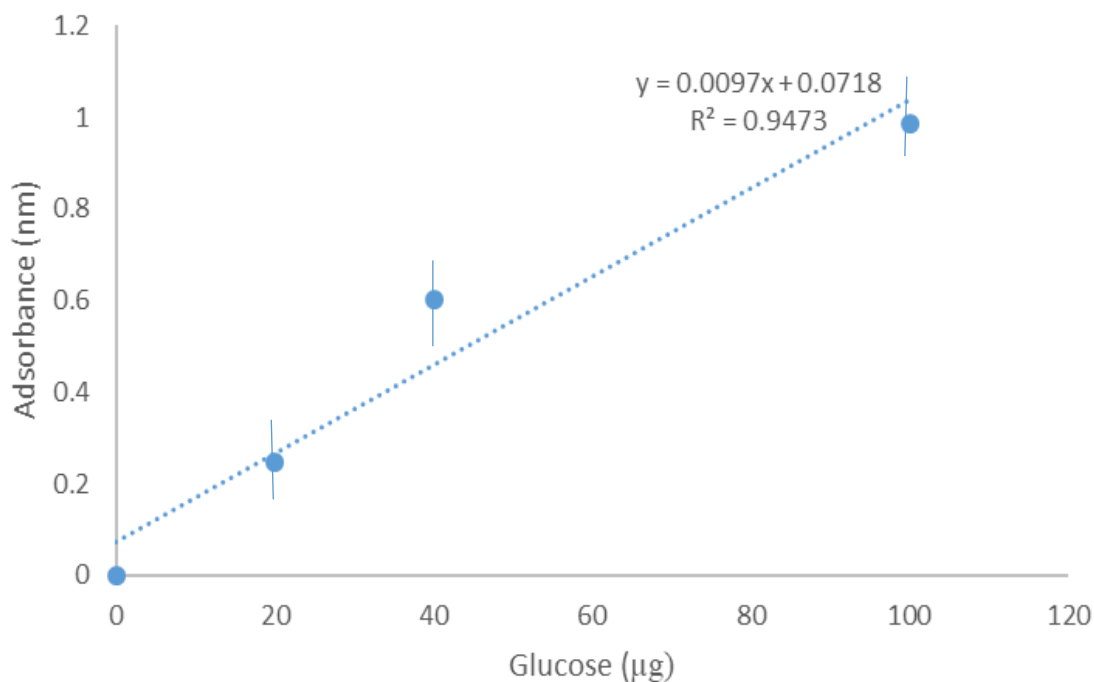


**Figure 4.29: Standard curve depicting absorbance as a function of glucose content**

The standard curve had three standards points, the fourth one is a blank (no glucose). The picture of the no glucose (blank) in the appendix (Figure 4.31).

The formula of the linear regression line obtained from Figure 4.29 was  $y = 0.0097x + 0.0718$  where  $y$  = absorbance readings at 620 nm and  $x$  = glucose level present in  $\mu\text{g}$ .

The average absorbance value of the banana rachis fiber hydrolysate samples recorded at 620 nm was 0.820.

Therefore, solving for X:

$$\begin{aligned}
 X &= \frac{(\text{Average of sample absorbance} - 0.0718)}{0.0097} \\
 &= \frac{0.820 - 0.0718}{0.0097} \\
 &= 77.13 \mu\text{g glucose.}
 \end{aligned}$$

In 0.5 ml there was  $\mu\text{g}$  glucose.

Therefore, in 50 ml (see page 62) there was X  $\mu\text{g}$  glucose.

Solving for X:

$$\begin{aligned} X &= \frac{50 \text{ ml} \times 77.13 \text{ } \mu\text{g glucose}}{0.5 \text{ ml}} \\ &= 7713 \text{ } \mu\text{g glucose} \end{aligned}$$

To convert  $\mu\text{g}$  glucose to mg glucose divide by a 1000

$$7713 \text{ } \mu\text{g} = 7.713 \text{ mg carbohydrates present in 10 mg sample 1000}$$

The % carbohydrate (expressed as glucose) present in the sample therefore was:  $(7.713 \text{ mg}/10 \text{ mg}) \times 100 = 77.13\%$ .

The equation to calculate the percentage carbohydrate of the banana rachis fibre hydrolysate is similar to the calculations for the other adsorbents (alpha cellulose hydrolysate, alpha cellulose/chitosan composite hydrolysate, banana rachis fibre/chitosan composite hydrolysate, chitosan) with an absorbance of 0.900, 0.790, 0.720, and 0 nm, respectively were performed similarly as show above.

Glucose is normally used to establish a calibration curve for the anthrone method and total sugars are expressed in terms of glucose. Under identical experimental conditions, equal quantities of adsorbents materials (banana rachis fibre, alpha cellulose, alpha cellulose/chitosan composite, banana rachis fibre/chitosan composite, and chitosan) samples showed a lighter green colour than does glucose with a darker green colour in Figure 4.31-4.36 (See appendix section) (Jutta., 1975). The absorbance or transmittance of the coloured sample is directly correlated with the presence of a certain functional groups or product in the mixture ([www.currentprotocols.onlinelibrary.wiley.com](http://www.currentprotocols.onlinelibrary.wiley.com)).

Carbohydrates, functional groups; hydroxyl group of one monosaccharides in the starch (Pomeranzy and Meloan, 1994). The significance of the carbohydrate content determinations is check for functional groups in the adsorbent which helps in the interaction between the dye and the adsorbent during the adsorption process. The increase in starch is accompanied by a parallel decrease in cellulose, hemicellulose, and pentosans. In banana rachis fibre there was a carbohydrate content of 77.13%, alpha cellulose 85.38%, alpha cellulose/chitosan composite 74.04%, banana rachis fibre/chitosan composite which are higher than 74% recorded by Debabandya *et al.* (2010). In banana rachis fibre/chitosan composite was a carbohydrate content of 66.83%, and chitosan 0% which are lower than to the 74% recorded by Debabandya *et al.* (2010) and 79.8% recorded by Baloyi (2012) for banana pseudo-stem.

The percentage of carbohydrate content present in banana rachis fibre, alpha cellulose, alpha cellulose/chitosan composite, banana rachis fibre/chitosan composite, and chitosan is given in Table 4.7.

**Table 4.7: Total carbohydrate (excluding hexosamine) content of various adsorbents as determined with the Anthrone method after acid hydrolysis**

<b>Adsorbents</b>	<b>Carbohydrate content present (%)</b>
Distilled water	0
Chitosan	0
Banana rachis fibre/chitosan composite	66.82
Alpha cellulose/chitosan composite	74.04
Banana rachis fibre	77.13
Alpha cellulose	85.38

#### **4.4.4.5. The hexosamine standard graph obtained using the modification of the method to determine hexosamine**

The hexosamine standard graph obtained using the modification of the method to determine hexosamine (Figure 4.38).

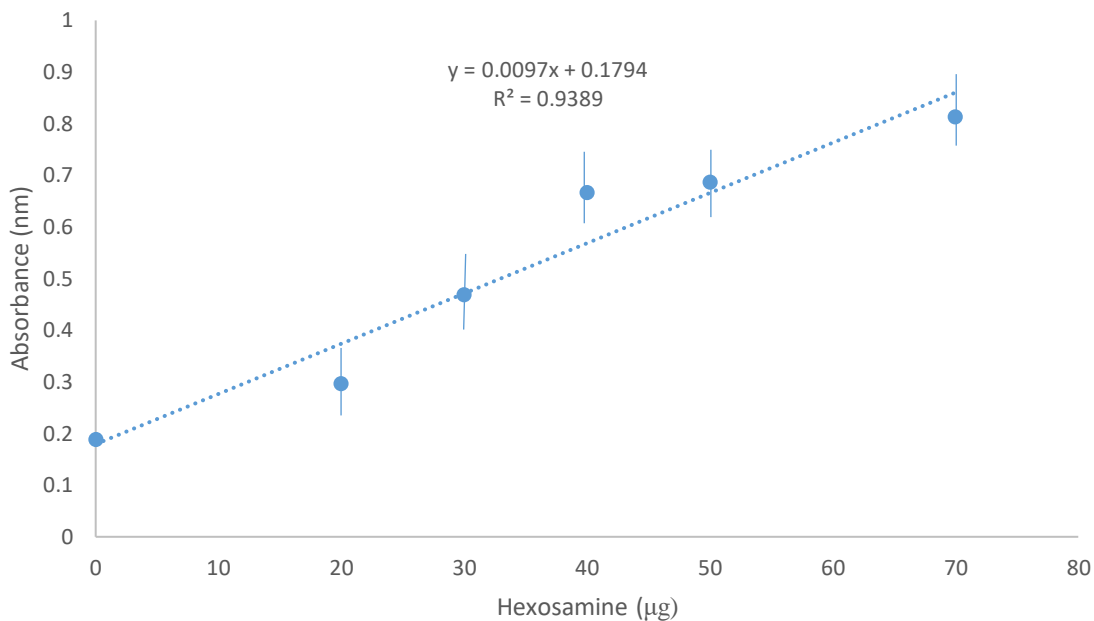


**Figure 4.37: Standard curve depicting absorbance as a function of hexosamine content**

The formula of the linear regression line obtained from figure 4.37 was  $y = 0.0097x + 0.1794$  where  $y$  = absorbance readings at 529 nm and  $x$  = hexosamine level present in  $\mu\text{g}$ .

The average absorbance value of the chitosan hydrolysate samples recorded at 529 nm was 0.663.

Therefore, solving for X:

$$\begin{aligned}
 X &= \frac{(\text{Average of sample absorbance} - 0.1794)}{0.0097} \\
 &= \frac{0.663 - 0.1794}{0.0097} \\
 &= 49.86 \mu\text{g} \\
 &\text{hexosamine.}
 \end{aligned}$$

In 40  $\mu\text{l}$  there was 49.86  $\mu\text{g}$  hexosamine.

Therefore, in 50 ml (see page 62) there was X  $\mu\text{g}$  hexosamine.

Solving for X:

$$X = \frac{49.86 \mu\text{g} \times 50 \text{ ml} \times 100 \text{ hexosamine}}{40 \mu\text{l}}$$

$$40 \mu\text{l} \\ = 6232.5 \mu\text{g hexosamine}$$

To convert  $\mu\text{g}$  hexosamine to mg hexosamine divide by a 1000

$$\underline{6232.5} \mu\text{g} = 6.2325 \text{ mg hexosamine present in } 100 \text{ mg sample } 1000$$

The % hexosamine (expressed as hexosamine) present in the sample therefore was:  
 $(6.2325\text{mg}/10 \text{ mg}) \times 100 = 62.23\%$ .

The equation to calculate the percentage hexosamine of the chitosan is similar to the calculations for the other adsorbents (banana rachis fibre/chitosan composite hydrolysate, alpha cellulose/chitosan composite hydrolysate, banana rachis fibre hydrolysate, and alpha cellulose hydrolysate) with an absorbance of 0.605, 0.550, 0.200, and 0 nm, respectively were performed similarly as shown above.

Glucosamine is part of the structure of chitosan and chitin which compose the exoskeletons of crustaceans, arthropods and fungi. (Sibi *et al.*, 2013). Under identical experimental conditions, equal quantities of adsorbents materials (banana rachis fibre, alpha cellulose, alpha cellulose/chitosan composite, banana rachis fibre/chitosan composite, and chitosan) samples showed a colourless colour and a light pink colour than does glucosamine with a pink colour in Figure 4.38- 4.43 (See appendix section). As hexosamines in polysaccharides are present in general in the form of their acetyl derivatives, the determination of hexosamine must be preceded by deacetylation.

Apart from this, complete hydrolysis of glycosidic linkages is apparently necessary for this determination. As a rule the splitting of glycosidic linkages requires longer hydrolysis than is necessary for the deacetylation. Hydrolysis of polysaccharides split off the acetyl group of glucosamine. The significance of the hexosamine content determinations is check for functional groups (acetyl group) in the adsorbent which helps in the interaction between the dye and the adsorbent during the adsorption process. The determination of hexosamines in polysaccharides requires complete hydrolysis of the polysaccharide (Dische and Borenfreund, 1950).

The hydrolysis of chitosan results in monomers of  $\beta$ -(1-4) – linked -D-glucosamine (GlcN), an amino monosaccharide with physiological importance to the human body. Glucosamine has been prepared from various crustaceans. The percentage of hexosamine content

recovered were 93% of chitosan as glucosamine (Wu *et al.*, 2004) and 85.7 – 92.4% of chitosan as glucosamine (Zamani *et al.*, 2008) higher than that of the chitosan of 62.23% obtained here. Hydrolised banana rachis fibre and alpha cellulose (2.65% and 0% respectively) samples contained the lower percentage of glucosamine when compare to the chitosan (62.23%). Banana rachis fibre/chitosan composite and alpha cellulose/chitosan composite (54.85% and 47.76%, respectively) were having a higher percentage of glucosamine obtained when comparing them with the banana rachis fibre and alpha cellulose because they contain the glucosamine from the chitosan used during composite production.

Banana rachis fibre/chitosan composite and alpha cellulose/chitosan composite were having lower percentage of glucosamine obtained when comparing them to the chitosan (62.23%). The percentage of hexosamine content present on alpha cellulose, banana rachis fibre, banana rachis fibre/chitosan composite, alpha cellulose/chitosan composite, and chitosan is given in Table 4.8.

**Table 4.8: The percentage of hexosamine present in various adsorbents after acid hydrolysis**

<b>Adsorbents</b>	<b>Hexosamine content (%)</b>
Alpha cellulose	0
Banana rachis fibre	2.65
Alpha cellulose/chitosan composite	47.76
Banana rachis fibre/chitosan composite	54.85
Chitosan	62.23

## 4.5. Conclusion

1. The composite material is a material made from two or more constituent components with significantly different physical or chemical properties that, when combined, produce a material with characteristics different from the individual components.
2. ATR-IR spectroscopy was used to identify the functional groups such as: hydroxyl (-OH), carbonyl (C=O), carboxyl (CO<sub>2</sub>H) of different adsorbents responsible for CBB sorption. Composites as well as components of composites were furthermore characterised by x-ray diffraction.
3. The crystallinity index, x-ray diffraction (CI<sub>XRD</sub>) percentage of chitosan, alpha cellulose/chitosan composite, alpha cellulose, chitosan, banana rachis fibre/chitosan composite, and banana rachis fibre readings values in this study range from the highest to the lowest 94.29%, 91.54%, 82.75%, 60.77%, and 37.69%. Alpha cellulose/chitosan composite, alpha cellulose, and chitosan seems to be having a higher percentage of crystallinity when compared with banana rachis fibre/chitosan composite, and banana rachis fibre respectively.
4. The adsorption isotherms with alpha cellulose/chitosan composite, and banana rachis fibre/chitosan composite can be described better by the Langmuir model. Correlation coefficient, ( $R^2$ : 0.9999, and 0.994) as bigger than the Freundlich correlation coefficient  $R^2$ . This means that Langmuir model is more applicable than Freundlich model and adsorption occurred by CBB molecules forming a single layer of molecules on the adsorbents mentioned.

Based on Freundlich data the 'n' value showed that banana rachis fibre/chitosan composite, and alpha cellulose/chitosan composite, respectively were good adsorbents of the CBB G-250 dye. The inverse of 'n' is a constant in Freundlich adsorption isotherm. Because all the values of n obtained for the different adsorbents sighted above (2.44 and 2.18, respectively) were greater than 1, it suggested good adsorption capacity.

5. Total sugar determination was performed after acid hydrolysates using the Anthrone method. The percentage of carbohydrate (expressed as glucose) present in different samples: 0% for chitosan hydrolysate, 66.82% for banana rachis fibre/chitosan composite hydrolysate, 74.04% for alpha cellulose/chitosan composite hydrolysate, 77.13% for banana rachis fiber hydrolysed, and 85.38% for alpha cellulose hydrolysed. The



percentage of hexosamine (expressed as glucosamine) present in different samples were: 0% for alpha cellulose hydrolysate, 2.65% for banana rachis fibre hydrolysate, 54.85% for banana rachis fibre/chitosan composite hydrolysate, 47.76% for alpha cellulose/chitosan composite hydrolysate, and 62.23% for chitosan hydrolysate.

It was worthwhile to formulate composite materials from the available raw material because based on the crystallinity index %, banana rachis fibre/chitosan composite was less crystalline followed by alpha cellulose/chitosan composite, and for the adsorption of dye to occur fast the adsorbent must be more amorphous. Based on the carbohydrate and hexosamine content determinations, alpha cellulose/chitosan composite followed by banana rachis fibre/chitosan composite showed a good percentage for both the carbohydrate and hexosamine content determination which means they were having the functional groups needed for them to be a good adsorbent in the adsorption of dye.

## Chapter 5

### Conclusion

The adsorption of Coomassie brilliant blue dye using banana rachis fibre wastes, activated carbon, alpha cellulose, chitosan, alpha cellulose/chitosan composite and banana rachis fibre/chitosan composite were investigated. It can be concluded that activated carbon, followed by banana rachis fibre/chitosan composite, alpha cellulose/chitosan composite, alpha cellulose, banana rachis fibre and chitosan were effective adsorbents for adsorption of Coomassie brilliant blue dye at high concentration (800 mg/l) of dye based on experimental evidence. Banana rachis fibre wastes is easily available, has the potential to be used for small industries that releases certain types of dye as effluent. The present work explores a new cheaper adsorbent as an alternative to costly adsorbents for the removal of CBB.

The main advantages of procedure are: cost of process, ease and simplicity of preparation of the sorbent, sensitivity and rapid attainment of phase equilibrium. ATR-IR analysis of banana rachis fibre, chitosan, alpha cellulose, and alpha cellulose/chitosan composite and banana rachis fibre/chitosan composite showed the presence of various functional groups indicating the complex nature of the adsorbents. XRD analysis of alpha cellulose/chitosan composite, banana rachis fibre/chitosan composite, banana rachis fibre, chitosan, and alpha cellulose showed that composites were more crystalline than the banana rachis fibre and alpha cellulose alone.

Chitosan seems to be more crystalline than all adsorbents. Banana rachis fibre/chitosan composite and activated carbon exhibited the highest decolourisation activities on the lowest (50 mg/l and highest (800 mg/l) concentrations of CBB tested, respectively as were indicated in experiments where the effect of the adsorbents dosages on decolourization of the CBB G-250 dye were studied. Banana rachis fibre/chitosan composite had the better capacity to adsorb CBB G-250 dye than the chitosan and banana rachis fibre separately therefore composite formation enhanced the adsorption efficiency for CBB dye.

Banana rachis fibre, alpha cellulose, activated carbon, and chitosan showed that the equilibrium can be reached quickly based on equilibrium being attained after only 45 and 50 minutes in most cases. For alpha cellulose/chitosan composite and banana rachis

fibre/chitosan composite showed that the equilibrium can be reached quickly based on equilibrium being attained after only 60 minutes. Based on Freundlich data the  $n$  value showed that banana rachis fibre/chitosan composite, followed by alpha cellulose/chitosan composite, activated carbon, banana rachis fibre, chitosan, and alpha cellulose, respectively were good adsorbents of the CBB G-250 dye. These were so because all the values of  $n$  obtained for the different adsorbents sighted above (2.44, 2.18, 2.15, 2.06, 1.88, and 1.42), respectively were greater than 1, indicating good adsorption.

Total carbohydrate present in hydrolysates alpha cellulose (as bench mark), followed by banana rachis fibre, were relatively high therefore the agricultural residues has a substantial potential to be used in biotechnology as a source of sugars. The sugars in banana rachis fibre can be accessible by effective pretreatments for lignocellulose degradation and enzymes for saccharification, chemical pretreatments for lignin degradation (organosolv based organic solvents, sodium hypochlorite, hypochlorous acid, hydrogen peroxide, alkaline hydrogen peroxide, and some combinations thereof).

Lignin oxidation have demonstrated to reach the highest delignification yield, also in terms of monosaccharides recovery. The delignified samples were then saccharified with enzymes (cellulase and beta-glucosidase) and hydrolysis efficiency was evaluated in terms of final sugars recovery. Active chlorine oxidations, hypochlorous acid in particular, were best effective for lignin removal obtaining in the meanwhile the most promising cellulose-to-glucose conversion.

The hexosamine content on the adsorbents hydrolysates present in chitosan, followed by alpha cellulose/chitosan composite, banana rachis fibre/chitosan composite were high, expect the banana rachis fibre and alpha cellulose, therefore the residues has a substantial potential to be used in biotechnology as a source of amino sugars. The information collected from this study may be informative to designing economically viable treatment process for removal of dye in effluents. This will support the technology evaluation of these new adsorbents.

The formation of unique composite material from cheap waste materials such as banana rachis could bring new opportunities for technological developments and job creation locally. More work needs to be done to elucidate the mechanisms of sorption enhancement on a

molecular level and contribute to scientific knowledge in the fields of bioremediation and biotechnology. Scientific contributions were made in the area of material sciences and particular to the relative new field of composites. Further focus has been placed on rachis as useful resource for bioremediation/ biotechnological application and innovation. The present study suggests that the banana rachis fibre combined with chitosan can be used as a sustainable adsorbent to remove Coomassie Brilliant Blue G-250 dye from the wastewater efficiently.

## References

Abdel- Ghani N. T, EL – Chaghaby G. A, Rawash EL – S. A and Lima E. C, (2017), Adsorption of Coomassie Brilliant Blue R-250 dye onto Novel Activated Carbon prepared from Nigella Sativa L. waste: Equilibrium, Kinetics and Thermodynamics Running title: Adsorption of Brilliant Blue dye onto Nigella Sativa L. waste activated carbon, *Journal of the Chilean Chemical Society*, 62, 3505 – 3511.

Abdul K.H.P.S, Saurabh C.K, Adnan A.S, Fazita M.R.N, Syakir M.I, Davoudpour Y, Rafatullah M, Addullah C.K, Haafiz M.K.M, and Dungani R, (2016), A review on chitosan-cellulose blends and nanocellulose reinforced chitosan biocomposites: properties and their applications, *Carbohydrates Polymer*, 150, 216 – 226.

Abdul K.H.P.S., Siti A.M., and Mohd O.A.K, (2006), Cell walls of tropical fibers, *BioResource*, 2, 220 - 232.

Akhtar F, Andersson L, Ogunwumi S, Hedin N, Bergstrom L, (2014), Structuring adsorbents and catalysts by processing of porous powder, *Journal of the European Ceramic Society*, 34, 1643 – 1666.

Al-sagheer F.A, Al-sagheer M.A, Muslim S, and Elsabee M.Z, (2009), Extraction and characterization of chitin and chitosan from marine sources in Arabian Gulf, *Carbohydrate Polymers*, 77, 410 – 419.

Annadurai G, Juang R, and Lee D, (2002), Use of cellulose-based wastes for adsorption of dyes from aqueous solutions, *Journal of Hazard Materials*, 92, 263 - 274.

Antonino R.S.C.M.de Q, Fook B.R.P.L, Lima V.A.de O, Rached R.I.de F, Lima E.P.N, Lima R.J.da S, Covas C.A.P, and Fook M.V.L, (2017), Preparation and characterization of chitosan obtained from shells of shrimp (*Litopenaeus vannamei* Boone), *Marine Drugs*, 14, 1-12.

Arnold E, and Larsen J, (2006), Bottled water: Pouring resources down the drain. Washington, DC. Earth policy Institute, [www.earth-policy.org/plan\\_b\\_updates/2006/update51](http://www.earth-policy.org/plan_b_updates/2006/update51), Viewed 24 July 2018.

Arsene M.A, Bilba K, Holmer S.J, Khosrow G, (2013), Treatment of non-wood plant fibres used as reinforcement in composite materials, *Materials Research*, 16, 903 - 923.

Ashik K.P, and Sharma R.S, (2015), A review on mechanical properties of natural fiber reinforced hybrid polymer composites, *Journal of Mineral and Materials Characterization and Engineering*, 3, 1 – 6.

Ata S, Din M.I, Rasool A, Qasim I, and Mohsin I.U.I, (2012), Equilibrium, Thermodynamic, and Kinetics Sorption Studies for the Removal of Coomassie Brilliant Blue on Wheat Bran as a Low-Cost Adsorbent, *Ata Journal of Analytical Methods in Chemistry*, 2012, 1 - 8.

Balazsy A.T and Eastop D, (1998), Chemical principles of textile conservation, Butterworth-Heinemann, p 11.

Baloyi S.S, (2012), Fractionation and characterization of lignocellulose from banana pseudostem, Department of Biochemistry, pp 1 – 30.

Balogun A.O., Lasode O.A., Hui L., & McDonald A.G, (2015), Fourier Transform Infrared (FTIR) study and thermal decomposition kinetics of Sorghum bicolor glume and Albizia pedicellaris residues, *Waste and Biomass Valorization*, 6, 109–116.

Balogun A.O, Lasode O.A, and McDonald A.G, (2018), Thermochemical and pyrolytic analyses of Musa spp. Residues from the rainforest belt of Nigeria, *Environmental Progress and Sustainable Energy*, p 1 - 10.

Bianchera A, Salomi E, Pezzanera M, Ruwet E, Bettini R, and Elviri L, (2014), Chitosan hydrogels for chondroitin sulphate controlled release: An analytical characterization, *Journal of Analytical Methods in Chemistry*, 2014, 1 - 8.

Bilba K, Arsene M.A, Ouensanga A (2007) Study of banana and coconut fibers: Botanical composition, thermal degradation and textural observations. *Bioresource Technology*, 98: 58 - 68.

Biochemistryquestions, Polysaccharides, The biochemistry questions site, [www.biochemistryquestions.wordpress.com](http://www.biochemistryquestions.wordpress.com), Viewed 10 September 2018.

Biologydictionary.net/chitin, Viewed 07 September 2020.

Bradford M.M, (1976), Rapid and sensitive method for the quantitation of microgram quantities of protein utilizing the principles of protein-dye binding, *Analytical Biochemistry*, 72, 248 - 254.

Bradford Protein Assay, Bio-Rad Quick Start™ Bradford Protein Assay Instructional Manual, [www.bio-rad.com/webroot/web/pdf/lsr/literature/4110065A.pdf](http://www.bio-rad.com/webroot/web/pdf/lsr/literature/4110065A.pdf).

Burns D.A, and Ciurczak E.W, (1992), Handbook of Near-Infrared Analysis, in Practical Spectroscopy Series, Marcell Dekker, New York, 13, 393 - 395.

Chiral H. J, Thomson H. B, and Splittgerber A. G, (1993), A spectral study of the charge forms of coomassie brilliant blue G-250, *Analytical Biochemistry*, 2, 258 - 266.

Cordeiro N, Belgacem M.N, Torres I.C and Moura J.C.V.P, (2004), Chemical composition and pulp of banana pseudo-stems, *Industrial Crops Production*, 19, 147 - 154.

Cordeiro N, Oliveira L, Faria H, Belgacem M.N, and Moura J.C.V.P, (2006), Surface modification of banana-based lignocellulose, *Contact Angle, Wettability and Adhesion*, 4, 1 - 19.

Crini G, (2006), Non-conventional low-cost adsorbents for dye removal: A review, *Bioresource Technology*, 97, 1061 - 1085.

Da Roz A.L, Leite F.L, Pereiro L.V, Nascente P.A.P, Zucolotto V, Oliveira O.N, and Carvalho A.J.F, (2010), Adsorption of chitosan on spin-coated cellulose films, *Carbohydrate Polymers*, 80, 65 - 70.

Da Silva S.B, Krolicka M, Broek van den L.A.M, and Frissen A.E, (2018), Water-soluble chitosan derivatives and pH-responsive hydrogels by selective C-6 oxidation mediated TEMPO-laccase redox system, *Carbohydrate Polymers*, 186, 299 - 309.

Dada A.O, Olalekan A.P, Olatunya A.M, and Dada O, (2012), Langmuir, Freundlich, Temkin and Dubinin-Radushkevich isotherm studies of equilibrium sorption  $Zn^{2+}$  unto phosphoric acid modified rice husk, *Journal of Applied Chemistry*, 3, 38 - 45.

Das S, Roy D, and Sen R, (2016), Utilization of chitinaceous wastes for the production of chitinase, *Advances in Food and Nutrition Research*, 78, 27 – 46.

Datema R, Van den Ende H and Wessels G.H, (1977), The hyphal wall of *mucor mucedo*, part 1, polyanionic polymers. *European Journal of Biochemistry*, 80, 611 – 619.

de Mesquita, J. P, Donnici, C. L, Pereira, F. V, (2010), Biobased Nanocomposites from Layer-by-Layer Assembly of Cellulose Nanowhiskers with Chitosan, *Biomacromolecules*, 11, 473 - 480.

de Vasconcelos C.L, Bezerril P.M, Dantas T.N.C, Pereira M.R, and Fonseca J.C.L, (2007), Adsorption of bovine serum albumin on template-polymerized chitosan/poly(methacrylic acid) complexes, *Langmuir*, 23, 7687 – 7694.

Department of Environmental Affairs, (2014), National Guidelines for the discharge of effluent from Land-based sources into the coastal environment, Pretoria, South Africa, RP 101/2014.

Dillon, Edward C; Wilton, John H; Barlow, Jared C; Watson and William A (1989), Large surface area activated charcoal and the inhibition of aspirin absorption, *Annals of Emergency Medicine*, 18, 547 – 552.

Dische Z, and Boenfreund E, (1950), A spectrophotometric method for the microdetermination of hexosamines, *Journal of Biology Chemistry*, 184, 517 - 522.



Dreve S, Kacso I, Bratu I, and Indrea E, (2009), Chitosan-based delivery systems for diclofenac delivery: preparation and characterization, *Journal of Physics: Conference Series*, 182, 1 – 4.

Duri S, Majoni S, Hossenlopp J.M, Tran C.D, (2010), Determination of chemical homogeneity of fire retardant polymeric nanocomposite materials by near-infrared multispectral imaging microscopy, *Analytical Letters*, 43, 1780 - 1789.

eQ Insights, (2012), Water use and treatment in the pulp and paper industry, Sappi fine paper North America, 5, 1 - 7.

Fitzer E, Kochling K. H, Boehm H. P, and Marsh, H, (1995), Recommended terminology for the description of carbon as a solid (IUPAC recommendations 1995), *Pure and Applied Chemistry*, 67, 473 - 506.

Focher B, Torri G, Cosanni A, and Terbojevich M, (1992a), Structural differences between chitin polymorphs and their precipitates from solutions—evidence from CP-MAS <sup>13</sup>C-NMR, FTIR and FT-Raman spectroscopy, *Carbohydrate Polymers*, 17, 97 - 102a.

Focher B, Torri G, Cosanni A, Terbojevich, (1992b), Chitosans from *Euphausia Superba*. 2: Characterization of solid state structure, *Carbohydrate Polymers*, 18, 43 – 49b.

Forootanfar H, Rezaei S, Zeinvand – Lorestani H, Tahmasbi H, Mogharabi M, Ameri A, and Faramarzi A.M, (2016), Studies on the laccase – mediated decolourization, kinetic, and microtoxicity of some synthesis azo dyes, *Journal of Environmental Health Science and Engineering*, 14, 1 - 9.

Fox M.R, (1987), Dye- makers of Great Britain 1856-1976: A history of chemistry companies, products and changes. Manchester: Imperical Chemical Industries, p 38.

Gabelman A.P.E, (2017), Adsorption basics: Part 1, Gabelman Process Solutions, LLC, American Institute of Chemical Engineers (AIChE), pp. 48 – 53.

Gañán P, Cruz J, Garbizu S, Arbelaiz A, Mondragon I, (2004), Stem and bunch banana fibers from cultivation wastes: Effect of treatments on physico-chemical behaviour, *Journal of Applied Polymer Science*, 94,1489 – 1495.

Gholizadeh A, Kermani M, Gholami M, and Farzaies M, (2013), Kinetic and isotherm studies of adsorption and biosorption processes in the removal of phenolic compounds from aqueous solutions: Comparative study, *Journal of Environmental Health Sciences and Engineering*, 11, 1-10.

Gong H.R, (2007), Wood characteristics and storage methods of poplar residue, *China Wood-based Panels*, 14, 29 - 30.

Gopinathan P, Subramanian K.S, Gopinathan P, and Subramanian J, (2017), Genotypic variations in characteristics of Nano-fibrillated cellulose derived from banana pseudostem, Banana pseudostem CNC, *BioResources*, 12, 6984 – 7001.

Govindan S, Nivethaa E.A.K, Saravanan R, Narayanan V, and Stephen A, (2012), Synthesis and characterization of chitosan-silver composite, *Applied Nanoscience*, 2, 299 – 303.

Gupta V.K, and Ali K, (2002), Adsorbents for water treatment: low cost alternatives to carbon, In: Hubbard A. (Ed.), *Encyclopedia of surface and colloid science*. Marcel Dekker, New York, pp. 247 - 255.

Gupta N, Kushwaha A.K, and Chattopadhyaya M.C, (2011), Adsorption of cobalt (II) from aqueous solution onto hydroxyapatite/zeolite composite, *Advance Materials Letters*, 2, 309 - 312.

Haafiz M.K, Hassan A, Zainoha Z, Inuwa I, Islam M.S, and Jawaid M.S, (2013), Properties of polylactic acid composites reinforced with oil palm biomass microcrystalline cellulose, *Carbohydrate Polymers*, 98, 139-145.

Hall M, Bansal P, Lee J.H, Realf M.J, and Bommarius A.S, (2010), Cellulose crystallinity – a key predictor of the enzymatic hydrolysis rate, *The FEBS journal*, 277, 1571 – 1582.

Hameed B.H, El-Khaiary M.I, (2008a), Removal of basic dye from aqueous medium using a novel agricultural waste material: Pumpkin seed hull, *Journal Hazard Material*, 155, 601 – 609.

Hameed B.H, Mahmoud D.K, and Ahmad A.L, (2008b), Sorption equilibrium and kinetics of basic dye from aqueous solution using banana stalk waste, *Journal of Hazardous Materials*, 158, 499 – 506.

Hao X, Shen W, Chen Z, Zhu J, Feng L, Wu Z, Wang P, Zeng X, and Wu T, (2015), Self-assembled nanostructured cellulose prepared by a dissolution and regeneration process using phosphoric acid as solvent, *Carbohydrate Polymer*, 123, 297 - 304.

Hedge J. E and Hofreiter B. T, (1962), In: *Carbohydrate Chemistry* 17 (Eds Whistler R L and Be Miller, J N), Academic Press New York.

Hubbe M.A, Orlando J.R, Fingas M, and Gupta S.B, (2013), Cellulosic substrates for removal of pollutants from aqueous systems: A review 3. Spilled oil and emulsified organic liquids, *BioResources*, 8, 3038 - 3097.

Hubbell C.A, and Ragauskas A.J, (2010), Effect of acid-chlorite delignification on cellulose degree of polymerization, *Bioresource Technology*, 101, 7410 - 7415.

Isik M, Sardon H, and Mecerreyes D, (2014), Ionic liquids and cellulose: dissolution, chemical modifications and preparation of new cellulose materials, *International Journal of Molecular Sciences*, 15, 11922 - 11940.

Jarwanto D, and S. Tachibana, (2010), Decomposition of lignin and holocellulose on acacia mangium leaves and twigs by six fungal isolates from nature, *Pakistan Journal of Biological Sciences*, 13, 604 - 610.

Jiang Y, Han S, Zhang S, Li J, Huang G, Bi Y, and Chai Q, (2014), Improved properties by hydrogen bonding interaction of poly (lactic acid)/palygorskite nanocomposites for agricultural products packaging, *Polymer Composites*, 35: 468 – 476.

Jhadhav S, (2015), Value added products from gasification – Activated carbon, The combustion, gasification and propulsion laboratory (CGPL) at the Indian Institute of Science (IISc), [Cgpl.iisc.ernet.in/site/Portals/0/Technologies/ActivatedCarbon.pdf](http://Cgpl.iisc.ernet.in/site/Portals/0/Technologies/ActivatedCarbon.pdf), Retrieved 20 - 04 - 2015.

Johar N, Ahmad I, and Dufresne A, (2012), Extraction, preparation and characterization of cellulose fibres and nanocrystals from rice husk, *Industrial Crops Products*, 37, 93 - 99.

Johnson A.R, (1971), Improved method of hexosamine determination, *Analytical Biochemistry*, 44, 628 - 635.

Jutta C-B, (1975), A note on sugar determination by the anthrone method, anthrone method, [www.aaccnet.org/publications/cc/backissues/1975/Documents/chem52\\_857.pdf](http://www.aaccnet.org/publications/cc/backissues/1975/Documents/chem52_857.pdf), Viewed on 24 October 2018.

Kadirvelu K, and Namasivayam C, (2000), Agricultural by-products as metal adsorbent: sorption of lead (II) from aqueous solutions onto coir-pith carbon, *Environmental Technology*, 21, 1091 - 1097.

Kallel F, Bettaieb F, Khiari R, García A, Bras J, and Chaabouni S.E, (2016), Isolation and structural characterization of cellulose nanocrystals extracted from garlic straw residues, *Industrial Crops Products*, 87, 287 - 296.

Kant R, (2012), Textile dyeing industry an environmental hazard, Natural Science, *Scientific Research*, 4, 22 - 26.

Khaleque A.Md, and Roy K.D, (2016), Removing reactive dyes from textile effluent using Banana fibre, *International Journal of Basic and Applied Science*, 16: 14 – 20.

Kulkarni S, and Kawave J, (2014), Regeneration and recovery in adsorption- A review, *International Journal of Innovative Science, Engineering and Technology*, 1, 61 - 64.

Kumirska J, Czerwicka M, Kaczynski Z, Bychowska A, Brzozowski K, Thoming J, and Stepnowski P, (2010), Application of spectroscopic methods for structural analysis of chitin and chitosan, *Marine Drugs*, 8, 1567 - 1636.

Kuzmina O, Heinze T, and Wawro D, (2012), Blending of cellulose ad chitosan in alkyl imidazolium ionic liquids, *ISRN Polymers Science*, 2012, 1 - 9.

Kyzas G.Z, Deliyanni E.A, Matis K.A, (2014), Graphene oxide and its application as an adsorbent for wastewater treatment, *Journal of Chemical Technology and Biotechnology*, 89, 196 - 205.

Larkin, P (2011), Infrared and Raman Spectroscopy: Principles and Spectral Interpretation; Elsevier: Amsterdam, *The Netherlands*, 2011, 110 – 130.

Larsson P.T, Wickholm K, Iversen T. A, (1997), CP/MAS C-13 NMR investigation of molecular ordering in celluloses, *Carbohydrate Research*, 302:19 – 25.

Lee H.V, Hamid S.B.A, Zain S.K, (2014), Conversion of lignocellulosic biomass to nanocellulose: Structure and Chemical Process, *The Scientific World Journal*, 2014, 1 - 20.

Li I. I, Du Y, and Xu Y, (2004), Adsorption and complexation of chitosan wet-end additives in papermaking systems, *Journal of Applied Polymer Science*, 91, 2642 - 2648.

Li K, Shiya F, Huaiya Z, Yao Z, and Lucian A.L., (2010), Analysis of the chemical composition and morphological structure of banana pseudo-stem, Banana pseudo-stem chemistry, structure, *BioResource*, 5, 576 - 585.

Li, M., Wang, L., Li, D., Cheng, Y., Adhikari, B., (2014), Preparation and characterization of cellulose nanofibers from de-pectinated sugar beet pulp, *Carbohydrate Polymers*, 102, 136 - 143.

Liu B.Y, Shi H.Q, and Xu L.Q, (2003), Analysis of lignin content in waste liquor of rice straw pulp by ultraviolet spectrophotometer, *China Pulp and Paper*, 26, 19 - 22.

Liu Y, Thibodeaux D, Gamble G, Bauer P, and VanDerveer D, (2012), Comparative investigation of fourier transform infrared (FT-IR) spectroscopy and X- ray diffraction (XRD) in the determination of cotton fiber crystallinity, *Applied Spectroscopy*, 66, 983 - 986.

Liu T., Yang X., Wang Z. L., & Yan X, (2013), Enhanced chitosan beads-supported Fe<sub>0</sub>-nanoparticles for removal of heavy metals from electroplating wastewater in permeable reactive barriers, *Water Research*, 47, 6691 - 6700.

Lowell S and Shields J.E, (1984), Powder surface area and porosity (2<sup>nd</sup> edition), Wiley, New York, pp. 11 - 13.

Madamwar D, Tiwari O, and Jain K, (2019), Mapping of research outcome on remediation of dyes, dye intermediates and textiles industrial waste, A research compendium, University Press, Ministry of Science and Technology, 1 - 234.

Mahato, D.N., Mathur, B.K., Bhattacharjee, S., (2013), DSC and IR methods for determination of accessibility of cellulosic coir fibre and thermal degradation under mercerization. *Indian Journal of Fiber and Textile Research* 38, 96 - 100.

Mansur HS, Costa-Júnior ES, Mansur AAP, Barbosa-Stancioli EF, (2009a), Cytocompatibility evaluation in cell-culture systems of chemically crosslinked chitosan/PVA hydrogels, *Materials Science and Engineering: C*, 29,1574 – 1583.

Mansur HS, Mansur AP, Curti E, De Almeida MV, (2013b), Functionalized-chitosan/quantum dot nano-hybrids for nanomedicine applications: towards biolabeling and biosorbing phosphate metabolites, *Journal of Materials Chemistry B*, 1,1696 – 1711.

Mattson, J. A., Mark, H. B., Malbin, M. D., Weber, W. J., and Crittenden, J. C, (1969), Surface chemistry of active carbon: Specific adsorption of phenols, *J. Colloid Interface Sci.*, 31, 116 - 130.

Milani M.D.Y, Samarawickrama D.S.S, Dharmasiri G.P.C.A, Kottegoda I.R.M, (2016), Study the structure, morphology, and thermal behaviour of banana fiber and its charcoal; derivate from selected banana varieties, *Journal of Natural Fibers*, 13, 332 - 342.

Mohamed E.I.B, (2012), A new rapid and sensitive spectrophotometric method for determination of a biopolymer chitosan, *International Journal of Carbohydrates Chemistry*, 2012, 1-7.

Mohanty A.K, Rout J, Misra M, Tripathy S, and Nayak S, (2001), The influence of fibre treatment on the performance of coir-polyester composites, *Composites Science and Technology*, 61, 1303 - 10.

Mokhothu T.H, (2010), Preparation and Characterization of natural fibre/co-polyester biocomposites, University of Free State, pp 46 - 49.

Morton J.F, (1987), *Fruit of warm climates*, published by Morton J.F, 20534 SW 92, Ct Miami, FL, 33189. ISBN: 0-9610184-1-0, pp 29 - 47.

Moussa A, Abdelhamid C, Samia K, Tounsia A, and Mohamed T, (2014), Kinetics equilibrium studies of Coomassie Blue G-250 adsorption on apricot stone activated carbon, *Journal of Environment & Analytical Toxicology*, 5, 1 - 8.

Mukhopadhyay S, Fanguero R, Arpac Y, and Senturk U, (2008), Banana fibers – Variability and fracture behaviour, *Journal of Engineered Fibre and Fabrics*, 3, 39.

Muzzarelli A.A.R, (2011), Potential of chitin/chitosan-bearing materials for uranium recovery: An interdisciplinary review, *Carbohydrate Polymers*, 84, 54 - 63.

Neto W. P. F, Silvério H. A, Dantas N. O, and Pasquini D, (2013), Extraction and characterization of cellulose nanocrystals from agro-industrial residue – Soy hulls, *Industrial Crops Products*, 42, 480 - 488.

Ng C, Lasso N, Marshall W.E, and Rao R.M, (2002), Freundlich adsorption isotherms of agricultural by-product-based powdered activated carbons in a geomin-water system, *Bioresource, Technology*, 85, 131 - 135.

Nishiyama Y, Langan P, and Chanzy H, (2002), Crystal structure and hydrogen-bonding system in cellulose I $\beta$  from synchrotron X-ray and neutron fiber diffraction, *Journal of the American Chemical Society*, 124, 9074 - 9082.

Penjumras P, Rahman R B.A, Talib R. A, Abdan K, (2014), Extraction and characterization of cellulose from Durian Rind, *Agriculture and Agricultural Science Procedia*, 2, 237 - 243.

Phungo M, (2014), Sorption of Coomassie brilliant blue G-250 dye using banana rachis as biosorbent in isotherm studies, Department of Biochemistry, University of Venda, pp 1 - 24.

Polysaccharides, [www.biochemistryquestions.wordpress.com](http://www.biochemistryquestions.wordpress.com), Viewed 10 September 2018.

Pomeranz Y, Meloan C.E, (1994), Carbohydrates. In: *Food Analysis*, Springer, Boston, MA, pp 625 – 677.

Pranoto Y, Rakshit S.K, and Salokhe V.M, (2005), "Enhancing antimicrobial activity of chitosan films by incorporating garlic oil, potassium sorbate and nisin," *Food Science and Technology*, 38, 859 – 865.

Prasad R.N, Viswanathan S, Devi J.R, Rajkumar J, and Parthasarathy N, (2008), Kinetics and equilibrium studies on biosorption of CBB by Coir pith, *American – Eurasian Journal of Scientific Research*, 3, 123 – 127.

Preethi P and Balakrishna M.G, (2013), Physical and chemical properties of banana fibre extracted from commercial banana cultivars grown in Tamilnadu State., *Agrotechnology*, 2013, 1 - 3.

Qi L, Xu Z, Jiang X, Hu C, and Zou X, (2004), Preparation and antibacterial activity of chitosan nanoparticles, *Carbohydrate Research*, 339, 2693 – 2700.

Properties of Activated Carbon, CPL Caron Link, accessed 2008-05-02", Archived from the original on 19 June 2012. Viewed 13 May 2018, <https://en.wikipedia.org/wiki/Activated-carbon>.

Rajagopal R, (1991), Dyes and Pigments, *Colourage*, 38, 50 - 52.

Rambo M.K.D and Ferreira M.M.C, (2015), Determination of cellulose crystallinity of banana residues using near infrared spectroscopy and multivariate analysis, *Journal of the Brazilian Chemical Society*, 26, 1 – 16.

Ray M, Pal K, Aris A, and Banthia A.K, (2010), Development and characterization of chitosan based polymeric hydrogel membranes, *Designed Monomers and Polymers*, 13, 193 – 206.

Reddy N and Yang Y, (2005), Biofibers from agricultural byproducts for industrial applications, *Trends in Biotechnology*, 23, 22 - 27.

Reddy J. P, and Rhim J.W, (2014), Isolation and characterization of cellulose nanocrystals from garlic skin, *Material Letters*, 129, 20 - 23.

Riva G.H, Estrada J.G, Vega B, Dellamary F.L, Hernandez M.E, Silva J.A, (2015), Cellulose-chitosan nanocomposites- Evaluation of physical mechanical and biological properties, *Cellulose-Fundamental Aspects and Current trends*, IntechOpen, pp 229 - 250.



Robertson E.E, and Wood R.D, (1979), 38 – Pyrolytic gasification of renewable biomass resources, *Solar Energy Conversion an introductory course*, pp 1059 – 1089.

Robinson J.C, and Galan S.V, (2010), Banana and plantations, 2<sup>th</sup> edition, Crop Production Science in Horticulture Series 19, AB International Wallingford, UK, pp 57 - 68.

Rohit K and Dixit S, (2016), A review – Future aspect of natural fiber reinforced composite, *Polymers from Renewable Resources*, 7: 43 – 59.

Rosa MF, Medeiros ES, Malmonge JA, Imam S.H, (2010), Cellulose nanowhiskers from coconut husk fibers: effect of preparation conditions on their thermal and morphological behavior. *Carbohydrate Polymer*, 81, 83 – 92.

Rowell R.M, Petterson R, and Tshabalala M.A, (2013), Cell wall chemistry, Handbook of wood chemistry and wood composites, pp 33 - 72.

Sain M, and Panthapulakkal S (2006) Bioprocess preparation of wheat straw fibers and their characterization, *Industrial Crops and Products*, 23, 1 – 8.

Santos N.B.C, Gomes R.M, Colodette J.L, Resende T.M, Lino A.G, Zanuncio A.J.V, (2011), A comparison of methods for eucalypt wood removal extractives, *5<sup>th</sup> International Colloquium on Eucalyptus Pulp*, pp. 1 - 4.

Schmitz C, Auza L.G, Koberidze D, Rasche S, Fischer F, and Bortesi L, (2019), Conversation of chitin to defined chitosan oligomers: current status and future prospects, *Marine Drugs*, 17, 452.

Shahidi F, and Synowiecki J, (1991), Isolation and Characterization of nutrients and value-added products from snow crab (*chionoecetes opilio*) and shrimp (*Pandalus borealis*) processing discards, *Journal of Agricultural and Food Chemistry*, 39: 1527 - 32.

Shoba J, (2015), Value Added Products from Gasification – Activated Carbon. The Combustion, Gasification and Propulsion Laboratory (CGPL) at the Indian Institute of Science (IISc), [https://www.pssurvival.com/PS/Charcoal/Activated\\_Carbon-2016.pdf](https://www.pssurvival.com/PS/Charcoal/Activated_Carbon-2016.pdf).

Sibi G, Dhananjaya K, Ravikumar K.R, Mallesha H, Venkakesha R.T, Trivedi D, Bhusal K.P, Neeraj, and Gowda K, (2013), Preparation of glucosamine hydrochloride from crustacean shell waste and its quantitation by RP-HPLC, *American – Eurasian Journal of Scientific Research*, 8, 63 – 67.

Sietsma, J.H. & Wessels, J. G. H. (1981). Solubility of (1 - 3)- $\beta$ -D/( 1 - 6)- $\beta$ -D-glucan in fungal walls : importance of presumed linkage between glucan and chitin, *Journal of General Microbiology*, 125, 209 - 212.

Silverio, F.O, Barbosa, L.C.A, Gomide, J.L, Reis, F.P, Pilo-Veloso, D, (2006), Methodology of extraction and determination of extractive contents in eucalypt woods. *Revista árvore, Viçosa*, 30, 1009 - 1016.

Sjostrom, E, (1993), *Wood Chemistry Fundamentals and Applications*. 2 ed. Finland: Academic Press. San Diego, p 293.

Soria, J.A., McDonald, A.G, (2012), Liquefaction of softwoods and hardwoods in supercritical methanol: A novel approach to bio-oil production. In C. Baskar, S. Baskar, R.S. Dhillon (Eds.), *Biomass conversion: The interface of biotechnology, chemistry and materials science*. pp 421 – 433.

Spiridon, I., Teacă, C., Bodîrlău, R., (2010), Structural Changes Evidenced by FTIR Spectroscopy in Cellulose Materials after Pre-Treatment with Ionic Liquid and Enzymatic Hydrolysis, *BioResources*, 6, 400 - 413.

Stamm A.J, (1964), *Wood and Cellulose science*, New York, The Ronald Press Co. pp 1-549.

Sunkyu P, Baker J.O, Himmel M.E, Parilla P.A, Johnson D.K, (2010), Cellulose crystallinity index: measurement techniques and their impact on interpreting cellulose performance, *Biotechnology for Biofuels*, 3:1-10.

Sun X.F, Xu F, Sun R.C, Fowler P, Baird M.S, (2005a), Characteristics of degraded cellulose obtained from steam-exploded wheat straw, *Carbohydrate Research*, 340, 97 – 106.

Sun X.F, Xu F, Sun X.F, Xiao B, Sun R.C, (2005b), Physico-chemical and thermal characterization of cellulose from barley straw, *Polymer Degradation and Stability*, 88, 521 – 531.

Sun X.F, Sun R.C, Fowler P, Baird M.S, (2004c), Isolation and characterization of cellulose obtained by a two-stage treatment with organosolv and cyanamide activated hydrogen peroxide from wheat straw, *Carbohydrate Polymers*, 55, 379 – 391.

Swift, M.J., Heal O.M and Anderson J.M, (1979), Decomposition in terrestrial ecosystems, *Studies in Ecology*, 5, 43 - 388.

Sydney.edu.au/science/biology/warren/docs/spec\_starch\_sugars, pdf. Analysis of starch and soluble sugars with Anthrone reagent. Viewed. 06/06/2018.

Syrovy L and Hodny Z, (1991), Staining and quantitation of proteins separated by polyacrylamide gel electrophoresis, *Journal Chromatogram*, 569, 175 - 196.

Tahir H and Alam U, (2014), Lignocellulosic: Non-conventional low cost biosorbent for the elution of coomassie brilliant blue (R-250), *International Journal of Chemistry*, 6, 56 - 72.

Tamura H, Furuike T, and New N, (2011), Production, properties, and applications of fungal cell wall polysaccharides: chitosan and glucan, *Advances in Polymer Science*, 244, 187-207.

Telmo, C., & Lousada, J, (2011), The explained variation by lignin and extractives contents on higher heating value of wood, *Biomass and Bioenergy*, 35, 1663 – 1667.

Terzopoulou Z, Kyzas G.Z, and Bikiaris D.N, (2015), Recent advances in nanocomposite materials of graphene derivatives with polysaccharides, *Materials*, 8, 652 - 683.

Tran C.D, Duri S, Delneri A, Franko M, (2013), Chitosan-cellulose composite materials: Preparation, Characterization and application for removal of microcystin, *Journal of Hazardous Materials*, 2013, 252 - 253: 355 - 366.

Tran H.N, You S.J, Nguyen T.V, and Chao H.P, (2017), Insight into the adsorption mechanism of cationic dye onto biosorbents derived from agricultural wastes, *Chemical Engineering Communications*, 204, 1020 – 1036.

Tuomela, M., Vikman M, Hatakka A and Itavaara M, (2000), Biodegradation of lignin in a compost environment: A review, *Bioresource, Technology*, 72, 169 - 183.

Uma S.K., Sathiamoorthy S, and Kumar V, (2005), Evaluation of commercial cultivars of banana (musa spp.) for their suitability for the fibre industry, *Plant Genetics Resource Newsletter*, 142, 29 - 35.

Updegraff DM, (1969), Semimicro determination of cellulose in biological materials, *Analytical Biochemistry*, 32, 420 - 424.

Van Soest, J.J.G., Tournois, H., de Wit, D., & Vliegthart, J.F.G, (1995), Short-range structure in (partially) crystalline potato starch determined with attenuated total reflectance Fourier-transform IR spectroscopy, *Carbohydrate Research*, 279, 201 – 214.

Velasquez- Arredando H.I, Ruiz-Corado A. A, and De Oliveira J. S, (2010), Ethanol production process from banana fruit and its lignocellulosic residues: Energy analysis, *Energy*, 35, 3081 - 3087.

Verma D, Jain S, Zhang X, Gope P.C, (2016), Green approaches to biocomposite materials science and engineering, *Technology and Engineering*. pp 322.

Wang Z, Hu Q, and Dai X, (2009), Preparation and characterization of cellulose fiber/chitosan composites, *Polymer Composites*, 30, 1517 - 1522.

Waranusantigui P, Pokethitiyook P, Kruatrachue M, and De Oliveira J. S, (2003), Kinetics of basic dye (methylene blue) biosorption by giant duckweed (*Spidorela polyrrhiza*), *Environmental Pollutants*, 125, 385 - 392.

Woodmansey A, (2002), Chitosan treatment of sediment Laden water-Washington state, Project. (Higher Engineer). Federal Highway administration U.S. Department of transportation. Retrieved, 1 - 90.

[www.chemengonline.com](http://www.chemengonline.com)>industrial-adsorbents, Viewed 22 January 2020.

[www.currentprotocols.onlinelibrary.Wiley.com](http://www.currentprotocols.onlinelibrary.Wiley.com), Viewed 22 January 2020.

[www.easychem.com.au/production-of-materials/biomass-research/cellulose/](http://www.easychem.com.au/production-of-materials/biomass-research/cellulose/), Viewed 11 February 2020.

[www.eclipseproject.eu/waste-based-nanofillers](http://www.eclipseproject.eu/waste-based-nanofillers), Viewed 22 January 2020.

[www.investopedia.com/terms/C/coefficient-of-determination.asp](http://www.investopedia.com/terms/C/coefficient-of-determination.asp), Viewed 20 January 2020.

[www.oxfordreference.com/view/10.1093/oi/authority.20110803095942135](http://www.oxfordreference.com/view/10.1093/oi/authority.20110803095942135), Viewed 10 May 2018.

[www.merriam-webster.com/dictionary/holocellulose](http://www.merriam-webster.com/dictionary/holocellulose), Viewed 10 May 2018.

Xie H, Zhang S, and Li S, (2005), Chitin and chitosan dissolved in ionic liquids as reversible sorbents of CO<sub>2</sub>, *Green Chemical*, 8, 630 - 633.

Yashoda, (2016), Different between amorphous and crystalline polymers, <http://pediaa.com/difference-between-amorphous-and-crystalline-polymers>, Viewed 1 October 2018.

Yuan Y, Chesnutt B.M, Haggard W.O, and Bumgardner J.D, (2011), Deacetylation of chitosan: material characterization and in vitro evaluation via albumin adsorption and pre-osteoblastic cell cultures, *Materials*, 4, 1399 - 1416.

Zamani A, Jeihanipour A, Edebo L, Niklasson C, and Taherzadeh M.J, (2008), Determination of glucosamine and N-acetyl glucosamine in fungal cell walls, *Journal of Agricultural and Food Chemistry*, 56, 8314 - 8318.

Ziani K., Oses J., Coma V., Maté J.I, (2008), Effect of the presence of glycerol and Tween 20 on the chemical and physical properties of films based on chitosan with different degree of deacetylation, *LWT – Food Science and Technology*, 41, 2159 - 2165.

Zuliahani A, Nurltanani A.S, Nurul R, Nadhirah N.B, and Hazirah A, (2017), Isolation and characterization of microcrystalline cellulose (mcc) from rice husk (rh) and kenaf. A comparison study, *Solid State Science and Technology*, 25, 96 - 102.

## Appendix

### A, Chapter 3

#### 3.4. Results and discussions

##### 3.4.2. Effect of the various adsorbent dosage on decolourization of the CBB G-250 dye

###### A, Initial concentration (50 mg/l)

###### 1. Percentage of the decolourization (chitosan)

The initial concentration represented by 50 mg/l.  $A_i$  represent the initial absorbance of the dye and  $A_t$  represent the absorbance of the dye at any interval.

Decolourization (%) =  $A_i - A_t$

$$\frac{0.032 - 0.014}{0.032} \times 100\%$$

$$= 56.3\%$$

The percentage of the decolourization for chitosan at a dosage of 3 g was 56.3%

Decolourization (%) =  $A_i - A_t$

$$\frac{0.032 - 0.017}{0.032} \times 100\%$$

$$= 46.9\%$$

The percentage of the decolourization for chitosan at dosage of 2.5 g was 46.9%

$$\text{Decolourization (\%)} = A_i - A_t$$

$$\dots\dots\dots \times 100\%$$

$$A_i$$

$$= 0.032 - 0.020$$

$$\dots\dots\dots \times 100\%$$

$$0.032$$

$$= 37.5\%$$

The percentage of the decolourization for chitosan at dosage of 2 g was 37.5%

$$\text{Decolourization (\%)} = A_i - A_t$$

$$\dots\dots\dots \times 100\%$$

$$A_i$$

$$= 0.032 - 0.025$$

$$\dots\dots\dots \times 100\%$$

$$0.032$$

$$= 21.9\%$$

The percentage of the decolourization for chitosan at dosage of 1.5 g was 21.9%

$$\text{Decolourization (\%)} = A_i - A_t$$

$$\dots\dots\dots \times 100\%$$

$$A_i$$

$$= 0.032 - 0.027$$

$$\dots\dots\dots \times 100\%$$

$$0.032$$

$$= 15.6\%$$

The percentage of the decolourization for chitosan at dosage of 1 g was 15.6%

## 2. Percentage of the decolourization (activated carbon)

The initial concentration represented by 50 mg/l.  $A_i$  represent the initial absorbance of the dye and  $A_t$  represent the absorbance of the dye at any interval.

$$\text{Decolourization (\%)} = A_i - A_t$$

$$\begin{aligned} & \dots\dots\dots \times 100\% \\ & A_i \\ & = 0.032 - 0.005 \\ & \dots\dots\dots \times 100\% \\ & 0.032 \\ & = 84.4\% \end{aligned}$$

The percentage of the decolourization for activated carbon at dosage of 3 g was 84.4%

$$\text{Decolourization (\%)} = A_i - A_t$$

$$\begin{aligned} & \dots\dots\dots \times 100\% \\ & A_i \\ & = 0.032 - 0.010 \\ & \dots\dots\dots \times 100\% \\ & 0.032 \\ & = 68.8\% \end{aligned}$$

The percentage of the decolourization for activated carbon at dosage of 2.5 g was 68.8%

$$\text{Decolourization (\%)} = A_i - A_t$$

$$\begin{aligned} & \dots\dots\dots \times 100\% \\ & A_i \\ & = 0.032 - 0.017 \end{aligned}$$



$$\begin{aligned} & \dots\dots\dots \times 100\% \\ & 0.032 \\ & = 46.9\% \end{aligned}$$

The percentage of the decolourization for activated carbon at dosage of 2 g was 46.9%

Decolourization (%) =  $A_i - A_t$

$$\begin{aligned} & \dots\dots\dots \times 100\% \\ & A_i \\ & = 0.032 - 0.019 \\ & \dots\dots\dots \\ & 0.032 \\ & = 40.6\% \end{aligned}$$

The percentage of the decolourization for activated carbon at dosage of 1.5 g was 40.6%

Decolourization (%) =  $A_i - A_t$

$$\begin{aligned} & \dots\dots\dots \times 100\% \\ & A_i \\ & = 0.032 - 0.022 \\ & \dots\dots\dots \times 100\% \\ & 0.032 \\ & = 31.3\% \end{aligned}$$

The percentage of the decolourization for activated carbon at dosage of 1 g was 31.3%.

### 3. The percentage of decolourization (Banana rachis fiber)

The initial concentration represented by 50 mg/l.  $A_i$  represent the initial absorbance of the dye and  $A_t$  represent the absorbance of the dye at any interval.

Decolourization (%) =  $A_i - A_t$

$$\dots\dots\dots \times 100\%$$

$$\begin{aligned}
 & A_i \\
 & = 0.032 - 0.011 \\
 & \dots\dots\dots \times 100\% \\
 & 0.032 \\
 & = 65.6\%
 \end{aligned}$$

The percentage of the decolourization for rachis fiber at dosage of 3 g was 65.6%

Decolourization (%) =  $A_i - A_t$

$$\begin{aligned}
 & \dots\dots\dots \\
 & A_i \\
 & = 0.032 - 0.016 \\
 & \dots\dots\dots \times 100\% \\
 & 0.032 \\
 & = 50\%
 \end{aligned}$$

The percentage of the decolourization for rachis fiber at dosage of 2.5 g was 50%

Decolourization (%) =  $A_i - A_t$

$$\begin{aligned}
 & \dots\dots\dots \\
 & A_i \\
 & = 0.032 - 0.019 \\
 & \dots\dots\dots \times 100\% \\
 & 0.032 \\
 & = 40.6\%
 \end{aligned}$$

The percentage of the decolourization for rachis fiber at dosage of 2 g was 40.6%

Decolourization (%) =  $A_i - A_t$

$$\begin{aligned}
 & \dots\dots\dots \times 100\% \\
 & A_i \\
 & = 0.032 - 0.020
 \end{aligned}$$

$$\begin{aligned} & \dots\dots\dots \times 100\% \\ & 0.032 \\ & = 37.5\% \end{aligned}$$

The percentage of the decolourization for rachis fiber at dosage of 1.5 g was 37.5%

Decolourization (%) =  $A_i - A_t$

$$\begin{aligned} & \dots\dots\dots \times 100\% \\ & A_i \\ & = 0.032 - 0.025 \\ & \dots\dots\dots \times 100\% \\ & 0.032 \\ & = 21.9\% \end{aligned}$$

The percentage of the decolourization for rachis fiber at dosage of 1 g was 21.9%.

## B, High concentration (800 mg/l)

### 1. The percentage of the decolourization (chitosan)

High concentration represented by 800 mg/l.  $A_i$  represent the initial absorbance of the dye and  $A_t$  represent the absorbance of the dye at any interval.

Decolourization (%) =  $A_i - A_t$

$$\begin{aligned} & \dots\dots\dots \times 100\% \\ & A_i \\ & = 0.647 - 0.429 \\ & \dots\dots\dots \times 100\% \\ & 0.647 \\ & = 33.7\% \end{aligned}$$

The percentage of the decolourization for chitosan at dosage of 3 g was 33.7%

Decolourization (%) =  $A_i - A_t$

$$\begin{aligned} & \dots\dots\dots \times 100\% \\ & A_i \\ & = 0.647 - 0.438 \\ & \dots\dots\dots \times 100\% \\ & 0.647 \\ & = 32.3\% \end{aligned}$$

The percentage of the decolourization for chitosan at dosage of 2.5 g was 32.3%

Decolourization (%) =  $A_i - A_t$

$$\begin{aligned} & \dots\dots\dots \times 100\% \\ & A_i \\ & = 0.647 - 0.459 \\ & \dots\dots\dots \times 100\% \\ & 0.647 \\ & = 29.1\% \end{aligned}$$

The percentage of the decolourization for chitosan at dosage of 2 g was 29.1%

Decolourization (%) =  $A_i - A_t$

$$\begin{aligned} & \dots\dots\dots \times 100\% \\ & A_i \\ & = 0.647 - 0.464 \\ & \dots\dots\dots \\ & 0.647 \\ & = 28.3\% \end{aligned}$$

The percentage of the decolourization for chitosan at dosage of 1.5 g was 28.3%

Decolourization (%) =  $A_i - A_t$

$$\dots\dots\dots \times 100\%$$

$$\begin{aligned}
 & A_i \\
 &= 0.647 - 0.511 \\
 & \dots\dots\dots \times 100\% \\
 & \quad 0.647 \\
 &= 21.0\%
 \end{aligned}$$

The percentage of the decolourization for chitosan at dosage of 1 g was 21.0%

## 2. The percentage of the decolourization (banana rachis fiber)

High concentration represented by 800 mg/l.  $A_i$  represent the initial absorbance of the dye and  $A_t$  represent the absorbance of the dye at any interval.

$$\text{Decolourization (\%)} = A_i - A_t$$

$$\begin{aligned}
 & \dots\dots\dots \times 100\% \\
 & \quad A_i \\
 & \\
 &= 0.647 - 0.521 \\
 & \dots\dots\dots \times 100\% \\
 & \quad 0.647 \\
 &= 19.5\%
 \end{aligned}$$

The percentage of the decolourization for rachis fiber at dosage of 3 g was 19.5%

$$\text{Decolourization (\%)} = A_i - A_t$$

$$\begin{aligned}
 & \dots\dots\dots \times 100\% \\
 & \quad A_i \\
 &= 0.647 - 0.536 \\
 & \dots\dots\dots \times 100\% \\
 & \quad 0.647
 \end{aligned}$$

$$= 17.2\%$$

The percentage of the decolourization for rachis fiber at dosage of 2.5 g was 17.2%

$$\text{Decolourization (\%)} = A_i - A_t$$

$$\dots\dots\dots \times 100\%$$

$$A_i$$

$$= 0.647 - 0.540$$

$$\dots\dots\dots$$

$$0.647$$

$$= 16.5\%$$

The percentage of the decolourization for rachis fiber at dosage of 2 g was 16.5%

$$\text{Decolourization (\%)} = A_i - A_t$$

$$\dots\dots\dots \times 100\%$$

$$A_i$$

$$= 0.647 - 0.565$$

$$\dots\dots\dots \times 100\%$$

$$0.647$$

$$= 12.7\%$$

The percentage of the decolourization for rachis fiber at dosage of 1.5 g was 12.7%

$$\text{Decolourization (\%)} = A_i - A_t$$

$$\dots\dots\dots \times 100\%$$

$$A_i$$

$$= 0.647 - 0.604$$

$$\dots\dots\dots \times 100\%$$

$$0.647$$

$$= 6.6\%$$

The percentage of the decolourization for rachis fiber at dosage of 1 g was 6.6%.

### 3. The percentage of the decolourization (activated carbon).

High concentration represented by 800 mg/l.  $A_i$  represent the initial absorbance of the dye and  $A_t$  represent the absorbance of the dye at any interval.

$$\text{Decolourization (\%)} = A_i - A_t$$

$$\begin{aligned} & \dots\dots\dots \times 100 \\ & A_i \\ & = 0.647 - 0.134 \\ & \dots\dots\dots \times 100\% \\ & 0.647 \\ & = 79.3\% \end{aligned}$$

The percentage of the decolourization for activated carbon at dosage of 3 g was 79.3%

$$\text{Decolourization (\%)} = A_i - A_t$$

$$\begin{aligned} & \dots\dots\dots \times 100\% \\ & A_i \\ & = 0.647 - 0.150 \\ & \dots\dots\dots \times 100\% \\ & 0.647 \\ & = 76.8\% \end{aligned}$$

The percentage of the decolourization for activated carbon at dosage of 2.5 g was 76.8%

$$\text{Decolourization (\%)} = A_i - A_t$$

$$\begin{aligned} & \dots\dots\dots \times 100\% \\ & A_i \end{aligned}$$

$$= 0.647 - 0.166$$

$$\dots\dots\dots \times 100\%$$

$$0.647$$

$$= 74.3\%$$

The percentage of the decolourization for activated carbon at dosage of 2 g was 74.3%

$$\text{Decolourization (\%)} = A_i - A_t$$

$$\dots\dots\dots \times 100\%$$

$$A_i$$

$$= 0.647 - 0.193$$

$$\dots\dots\dots \times 100\%$$

$$0.647$$

$$= 70.2\%$$

The percentage of the decolourization for activated carbon at dosage of 1.5 g was 70.2%

$$\text{Decolourization (\%)} = A_i - A_t$$

$$\dots\dots\dots \times 100\%$$

$$A_i$$

$$= 0.647 - 0.215$$

$$\dots\dots\dots \times 100\%$$

$$0.647$$

$$= 66.8\%$$

The percentage of the decolourization for activated carbon at dosage of 1 g was 66.8%.

### 3.4.3 Equilibrium time sorption experiments

#### A) Initial concentration (50 mg/l)

$$\text{Absorbance} = 0.0205x - 0.2443$$



Therefore: X (Concentration of the CBB G-250 dye) = Absorption + 0.2443

$$\begin{aligned} & \frac{\text{Absorbance}}{0.0205} \\ &= (0.026 \times 25) + 0.2443 \\ & \frac{\text{Absorbance}}{0.0205} \\ &= 43.62 \text{ mg/l} \end{aligned}$$

The concentration of dye at equilibrium ( $C_e$ ) is therefore 43.62 mg/l for the activated carbon.

The equation to calculate the percentage sorption activity of the activated carbon is:

$$\begin{aligned} \% \text{ Sorption activity} &= C_0 - C_e \\ & \frac{\text{Absorbance}}{C_0} \times 100 \end{aligned}$$

where  $C_0$  is the initial dye concentration and  $C_e$  is the dye concentration at equilibrium. Therefore,

$$\begin{aligned} \% \text{ Sorption activity} &= 50 \text{ mg/l} - 43.62 \text{ mg/l} \\ & \frac{\text{Absorbance}}{50 \text{ mg/l}} \times 100 \\ &= 12.76\% \end{aligned}$$

The percentage sorption activity of the activated carbon is therefore 12.76%.

Absorbance = 0.0205x – 0.2443

Therefore: X (Concentration of the CBB G-250 dye) = Adsorption + 0.2443

$$\begin{aligned} & \frac{\text{Absorbance}}{0.0205} \\ &= (0.028 \times 25) + 0.2443 \\ & \frac{\text{Absorbance}}{0.0205} \\ &= 46.06 \text{ mg/l} \end{aligned}$$

The concentration of dye at equilibrium ( $C_e$ ) is therefore 46.06 mg/l for the banana rachis fiber.

The equation to calculate the percentage sorption activity of the free rachis fiber is:

$$\% \text{ Sorption activity} = \frac{C_0 - C_e}{C_0} \times 100$$

where  $C_0$  is the initial dye concentration and  $C_e$  is the dye concentration at equilibrium.

Therefore,

$$\begin{aligned} \% \text{ Sorption activity} &= \frac{50 \text{ mg/l} - 47.06 \text{ mg/l}}{50 \text{ mg/l}} \times 100 \\ &= 5.88\% \end{aligned}$$

The percentage sorption activity of the banana rachis fiber is therefore 5.88%.

$$\text{Absorbance} = 0.0205x - 0.2443$$

Therefore: X (Concentration of the CBB G-250 dye) = Absorption - 0.2443

$$\begin{aligned} & \frac{0.0205}{0.0205} \\ &= \frac{(0.031 \times 25) + 0.2443}{0.0205} \\ &= 49.72 \text{ mg/l} \end{aligned}$$

The concentration of dye at equilibrium ( $C_e$ ) is therefore 49.72 mg/l for the chitosan.

The equation to calculate the percentage sorption activity of the chitosan is:

$$\% \text{ Sorption activity} = \frac{C_0 - C_e}{C_0} \times 100$$

where  $C_0$  is the initial dye concentration and  $C_e$  is the dye concentration at equilibrium.

Therefore,

$$\begin{aligned} \% \text{ Sorption activity} &= \frac{50 \text{ mg/l} - 49.72 \text{ mg/l}}{50 \text{ mg/l}} \times 100 \end{aligned}$$

$$= 0.56\%$$

The percentage sorption activity of the chitosan is therefore 0.56%.

### B, High concentration (800 mg/l)

$$\text{Absorbance} = 0.0205x - 0.2443$$

Therefore: X (Concentration of the CBB G-250 dye) = Absorption + 0.2443

$$\begin{aligned} & \frac{\text{-----}}{0.0205} \\ & = (0.434 \times 25) + 0.2443 \\ & \frac{\text{-----}}{0.0205} \\ & = 541.19 \text{ mg/l} \end{aligned}$$

The concentration of dye at equilibrium ( $C_e$ ) is therefore 541.19 mg/l for the alpha cellulose.

The equation to calculate the percentage sorption activity of alpha cellulose is:

$$\begin{aligned} \% \text{ Sorption activity} &= C_0 - C_e \\ & \frac{\text{-----}}{C_0} \times 100 \end{aligned}$$

where  $C_0$  is the initial dye concentration and  $C_e$  is the dye concentration at equilibrium.

Therefore,

$$\begin{aligned} \% \text{ sorption activity} &= 800 \text{ mg/l} - 541.19 \text{ mg/l} \\ & \frac{\text{-----}}{800 \text{ mg/l}} \times 100 \\ & = 32.35\% \end{aligned}$$

The percentage sorption activity of alpha cellulose is therefore 32.35%.

$$\text{Absorbance} = 0.0205x - 0.2443$$

Therefore: X (Concentration of the CBB G-250 dye) = Absorption + 0.2443

$$\begin{aligned} & \frac{\text{-----}}{0.0205} \\ & = (0.529 \times 25) + 0.2443 \end{aligned}$$

$$\frac{\quad}{0.0205} = 657.04 \text{ mg/l}$$

The concentration of the dye at equilibrium ( $C_e$ ) is therefore 657.04 mg/l for the banana rachis fiber. The equation to calculate the percentage sorption activity of banana rachis fiber is:

$$\% \text{ Sorption activity} = \frac{C_0 - C_e}{C_0} \times 100$$

where  $C_0$  is the initial dye concentration and  $C_e$  is the dye concentration at equilibrium. Therefore,

$$\% \text{ Sorption activity} = \frac{800 \text{ mg/l} - 657.04 \text{ mg/l}}{800 \text{ mg/l}} \times 100 = 17.87\%$$

The percentage sorption activity of banana rachis fiber is therefore 17.87%.

$$\text{Absorbance} = 0.0205x - 0.2443$$

Therefore: X (Concentration of the CBB G-250 dye) = Absorption – 0.2443

$$\frac{\quad}{0.0205} = (0.589 \times 25) + 0.2443$$

$$\frac{\quad}{0.0205} = 730.21 \text{ mg/l}$$

The concentration of dye at equilibrium ( $C_e$ ) is therefore 730.21 mg/l for the chitosan. The equation to calculate the percentage sorption activity of chitosan is:

$$\% \text{ Sorption activity} = \frac{C_0 - C_e}{C_0} \times 100$$

where  $C_0$  is the initial dye concentration and  $C_e$  is the dye concentration at equilibrium.

Therefore,

$$\begin{aligned} \% \text{ Sorption activity} &= 800 \text{ mg/l} - 730.21 \text{ mg/l} \\ &\text{-----} \times 100 \\ &800 \text{ mg/l} \\ &= 8.7\% \end{aligned}$$

The percentage sorption activity of chitosan is therefore 8.7%

#### 3.4.1.4. Equilibrium studies

A. The capacity of adsorption of CBB G-250 dye using alpha cellulose, where calculated as follows (for alpha cellulose):

1.  $q_e$  for 100 mg/l

$$\begin{aligned} q_e &= (C_0 - C_e) \times V/W \\ &= (100 - 77.8) \times (0.3333) \\ &= 7.40 \text{ mg/g} \end{aligned}$$

2.  $q_e$  for 200 mg/l

$$\begin{aligned} q_e &= (C_0 - C_e) \times V/W \\ &= (200 - 158.3) \times (0.3333) \\ &= 13.90 \text{ mg/g} \end{aligned}$$

3.  $q_e$  for 400 mg/l

$$\begin{aligned} q_e &= (C_0 - C_e) \times V/W \\ &= (400 - 325.3) \times (0.3333) \\ &= 24.90 \text{ mg/g} \end{aligned}$$

4.  $q_e$  for 800 mg/l

$$\begin{aligned} q_e &= (C_0 - C_e) \times V/W \\ &= (800 - 682.6) \times (0.3333) \\ &= 39.13 \text{ mg/g} \end{aligned}$$

B. The capacity of adsorption of CBB G-250 dye using banana rachis fiber, where calculated as follows (for banana rachis fiber):

1.  $q_e$  for 100 mg/l

$$\begin{aligned}q_e &= (C_0 - C_e) \times V/W \\&= (100 - 66.8) \times (0.3333) \\&= 11.07 \text{ mg/g}\end{aligned}$$

2.  $q_e$  for 200 mg/l

$$\begin{aligned}q_e &= (C_0 - C_e) \times V/W \\&= (200 - 146.1) \times (0.3333) \\&= 17.97 \text{ mg/g}\end{aligned}$$

3.  $q_e$  for 400 mg/l

$$\begin{aligned}q_e &= (C_0 - C_e) \times V/W \\&= (400 - 329) \times (0.3333) \\&= 23.63 \text{ mg/g}\end{aligned}$$

4.  $q_e$  for 800 mg/l

$$\begin{aligned}q_e &= (C_0 - C_e) \times V/W \\&= (800 - 692.4) \times (0.3333) \\&= 35.87 \text{ mg/g}\end{aligned}$$

C. The capacity of adsorption of CBB G-250 dye using activated carbon, where calculated as follows (for activated carbon):

1.  $q_e$  for 100 mg/l

$$\begin{aligned}q_e &= (C_0 - C_e) \times V/W \\&= (100 - 55.8) \times (0.3333) \\&= 14.73 \text{ mg/g}\end{aligned}$$

2.  $q_e$  for 200 mg/l

$$\begin{aligned}q_e &= (C_0 - C_e) \times V/W \\&= (200 - 120.5) \times (0.3333) \\&= 26.50 \text{ mg/g}\end{aligned}$$

3.  $q_e$  for 400 mg/l

$$\begin{aligned}q_e &= (C_0 - C_e) \times V/W \\&= (400 - 288.5) \times (0.3333) \\&= 37.17 \text{ mg/g}\end{aligned}$$

4.  $q_e$  for 800 mg/l

$$\begin{aligned}q_e &= (C_0 - C_e) \times V/W \\&= (800 - 655.8) \times (0.3333) \\&= 48.07 \text{ mg/g}\end{aligned}$$

## B, Chapter 4

### 4.4.4.7 Carbohydrate content of banana rachis fibre, alpha cellulose, chitosan, alpha cellulose/chitosan and banana rachis fibre/chitosan composites

Figures 4.30-4.36 shows the results of carbohydrates content tests in distilled water, chitosan, alpha cellulose, banana rachis fibre, alpha cellulose/chitosan and banana rachis/chitosan composites after adding the anthrone reagent.

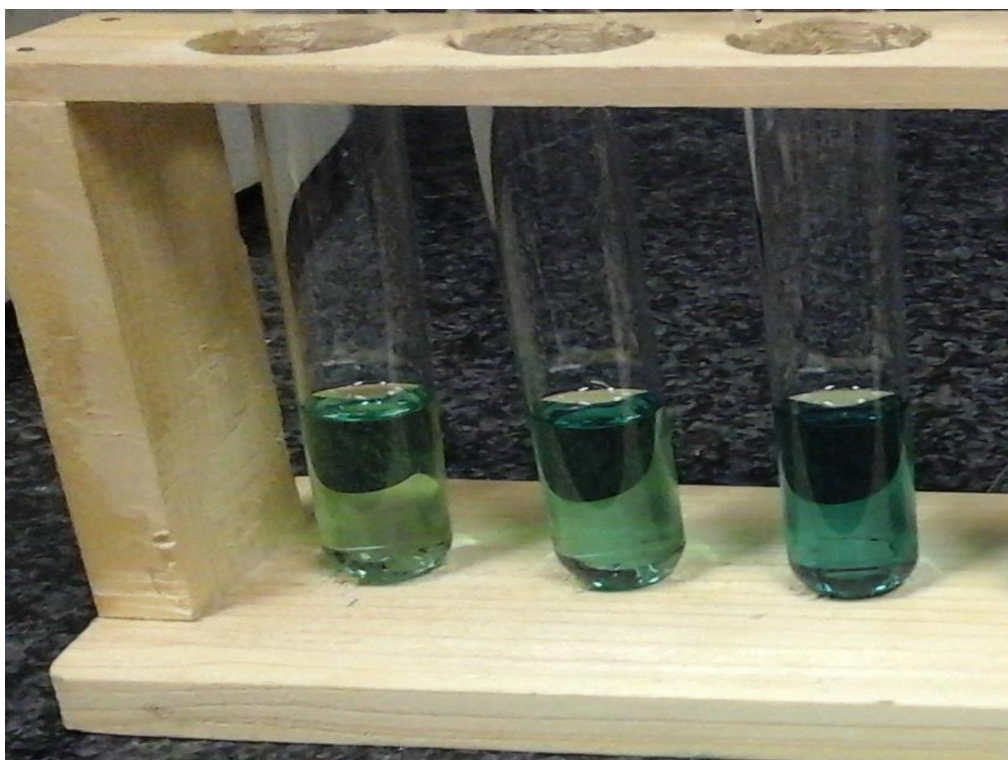


Figure 4.30: shows the different concentrations (0.1, 0.2, and 0.5 ml) of glucose solutions after the addition of anthrone reagent which was used to construct a standard curve of glucose

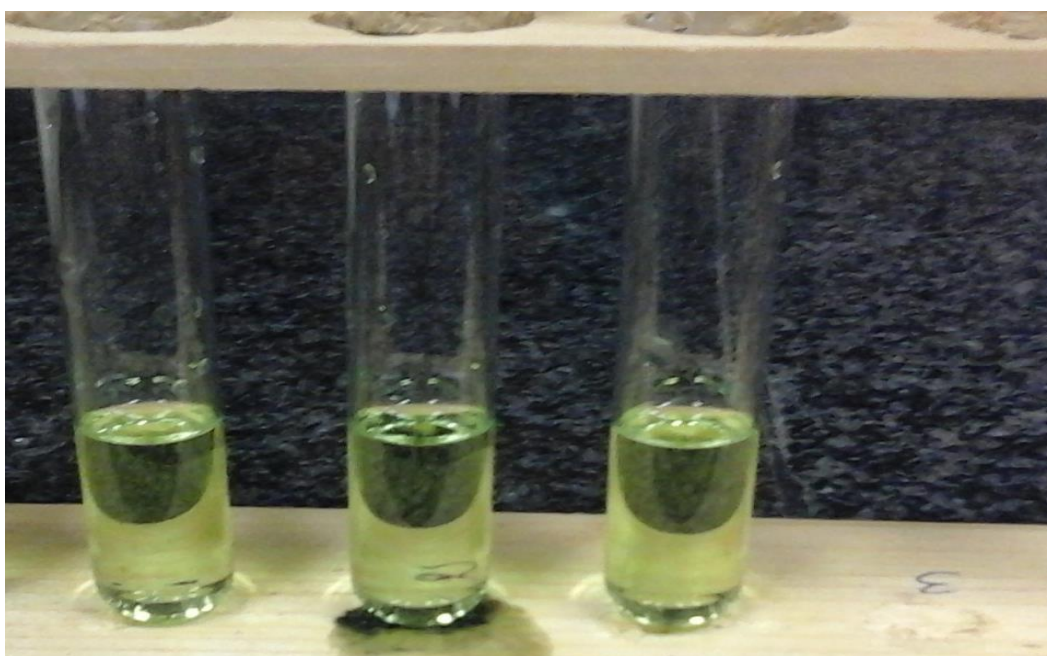
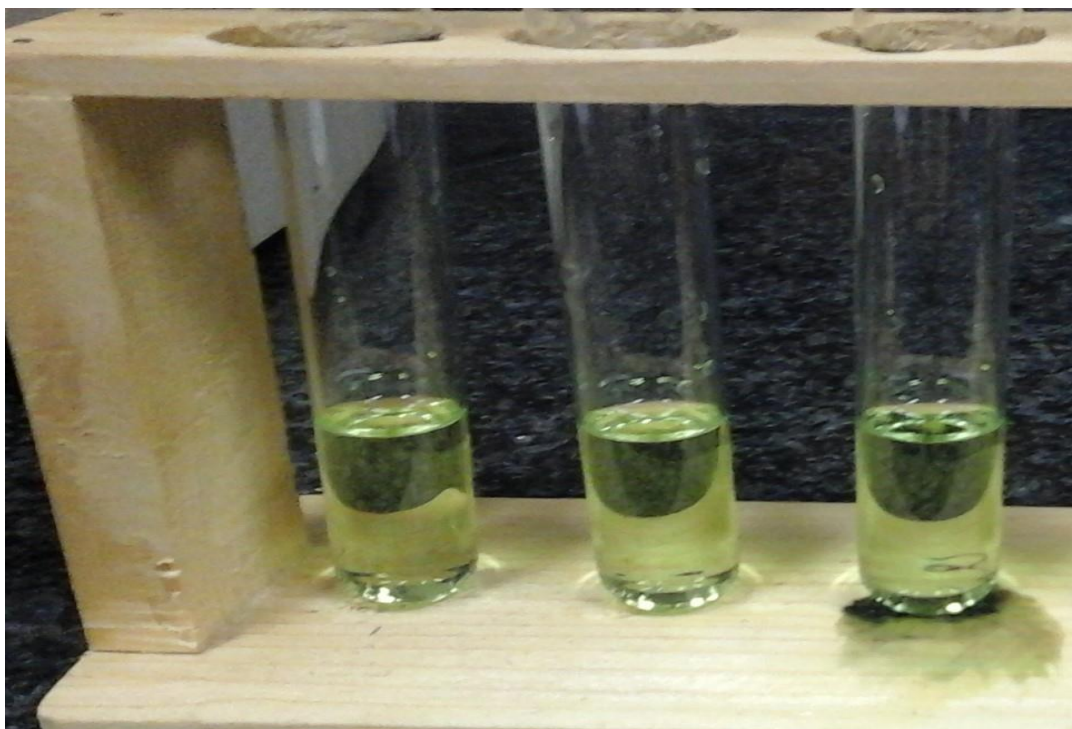
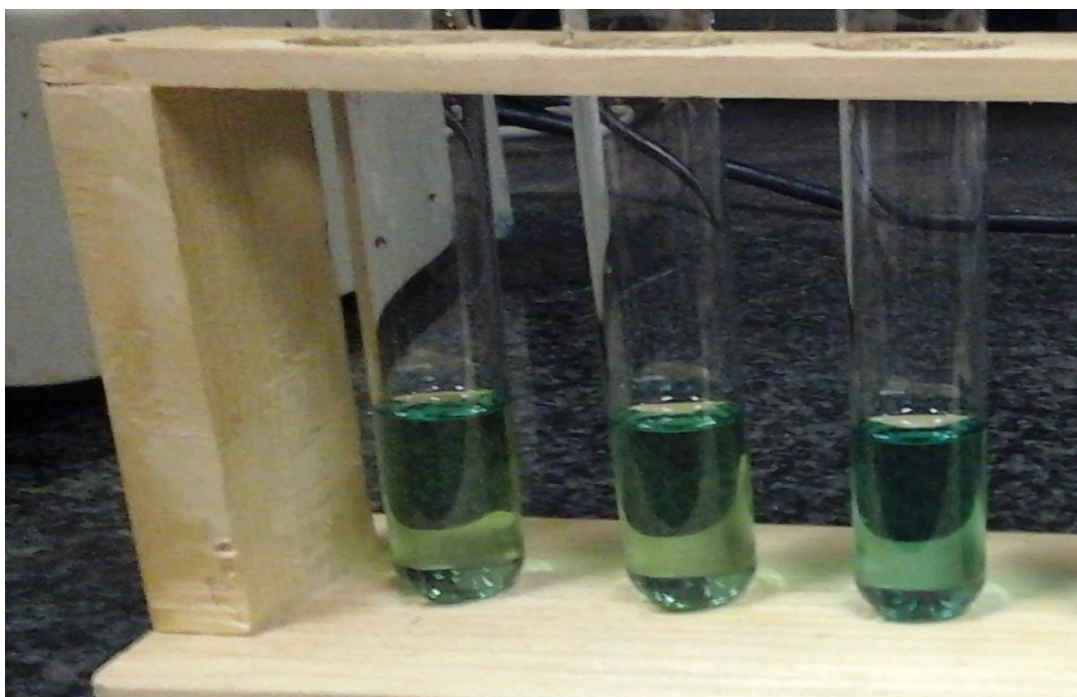


Figure 4.31: shows the different concentrations (0.1, 0.2, and 0.5 ml) of distilled water after the addition of anthrone reagent





**Figure 4.32:** shows the different concentrations (0.1, 0.2, and 0.5 ml) of chitosan hydrolysate solutions after the addition of anthrone reagent



**Figure 4.33:** shows the different concentrations (0.1, 0.2, and 0.5 ml) of alpha cellulose hydrolysate solutions after the addition of anthrone reagent



**Figure 4.34:** shows the concentrations (0.1, 0.2, and 0.5 ml) of banana rachis fibre hydrolysate solutions after the addition of anthrone reagent



**Figure 4.35:** shows the different concentrations (0.1, 0.2, and 0.5 ml) of alpha cellulose/chitosan composite hydrolysate solutions after the addition of anthrone reagent

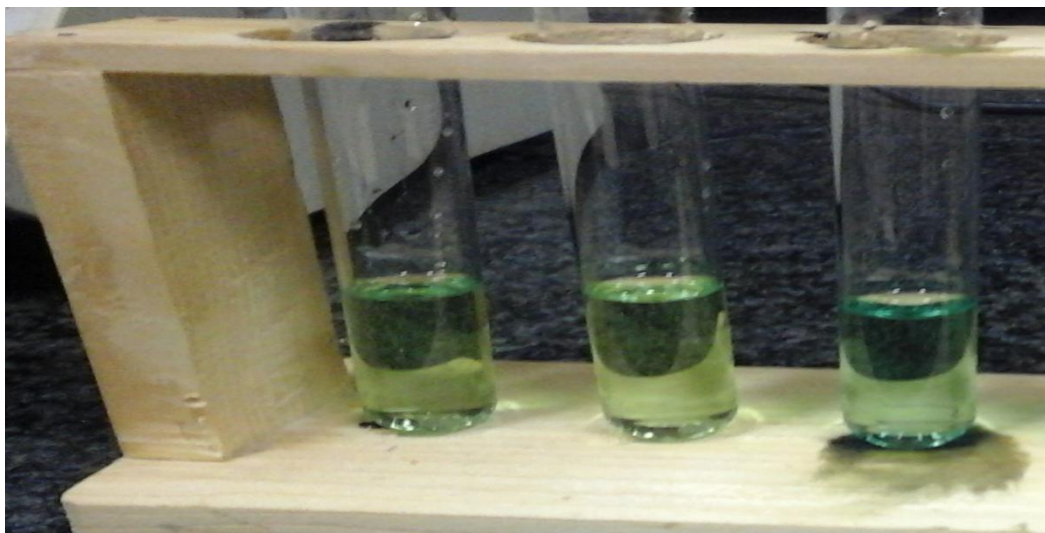


**Figure 4.36: shows the different concentrations (0.1, 0.2, and 0.5 ml) of banana rachis fibre/chitosan composite hydrolysate solutions after the addition of anthrone reagent**

The anthrone reagent was chosen since it does not react with hexosamine (Sietsma and Wessels, 1981). This is also illustrated in Figure 4.32. The colour observed in the test tubes all exhibit a yellowish colour and the intensity does not seemingly increase with an increase of hydrolysate concentrations applied (0.1 to 0.5 ml), there was no change for chitosan hydrolysate colour as it contains the hexosamine.

#### **4.4.4.8 Hexosamine content of chitosan, alpha cellulose, banana rachis fibre, alpha cellulose/chitosan and banana rachis fibre/chitosan composites**

Figures 4.38-4.43 shows the test tubes solutions used for hexosamine determination in chitosan, alpha cellulose, banana rachis fibre, alpha cellulose/chitosan and banana rachis/chitosan composites after adding the Ehrlich reagent.



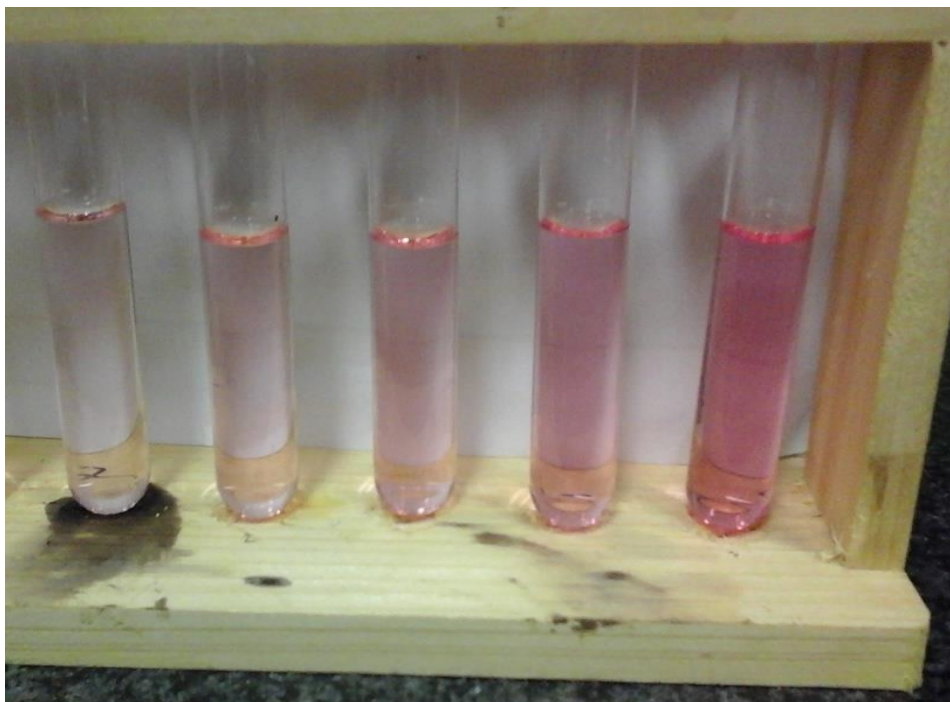


**Figure 4.38:** shows different concentrations (20, 30, 40, 50, and 70  $\mu\text{l}$ ) of glucosamine solutions after the addition of Ehrlich reagent for the standard curve of glucosamine



**Figure 4.39:** shows different concentrations (20, 30, 40, 50, and 70  $\mu\text{l}$ ) of alpha cellulose hydrolysate solutions after the addition of Ehrlich reagent



**Figure 4.40: shows different concentrations (20, 30, 40, 50, and 70  $\mu$ l) of chitosan hydrolysate solutions after the addition of Ehrlich reagent**

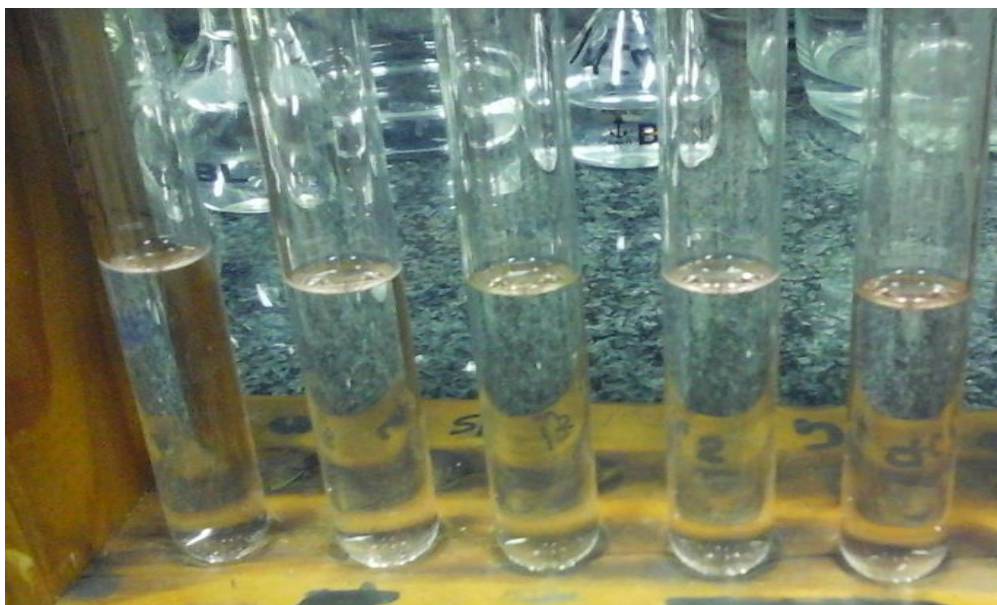


**Figure 4.41: shows different concentrations (20, 30, 40, 50, and 70  $\mu$ l) of banana rachis fibre hydrolysate solutions after the addition of Ehrlich reagent**



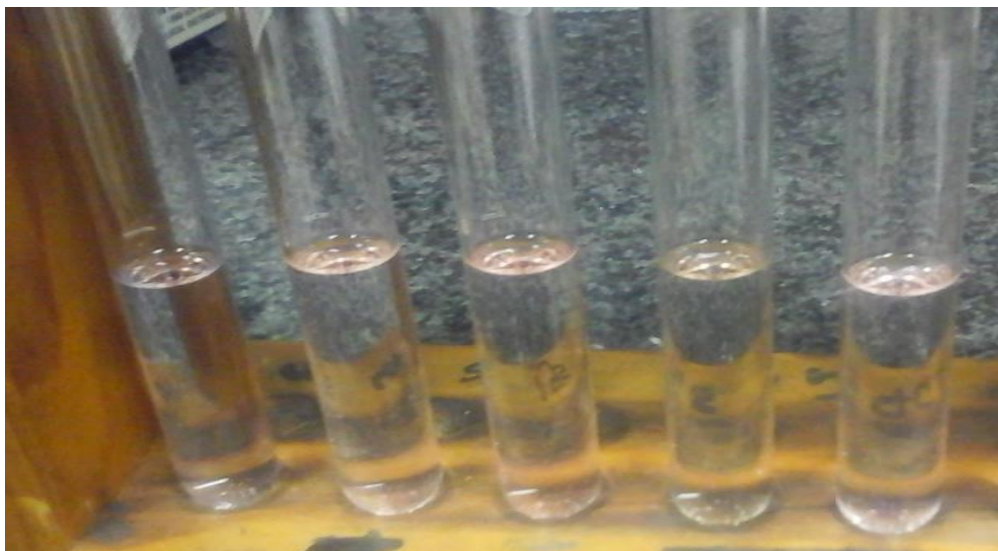


**Figure 4.42: shows different concentrations (20, 30, 40, 50, and 70  $\mu$ l) of alpha cellulose/chitosan composite hydrolysate solutions after the addition of Ehrlich reagent**

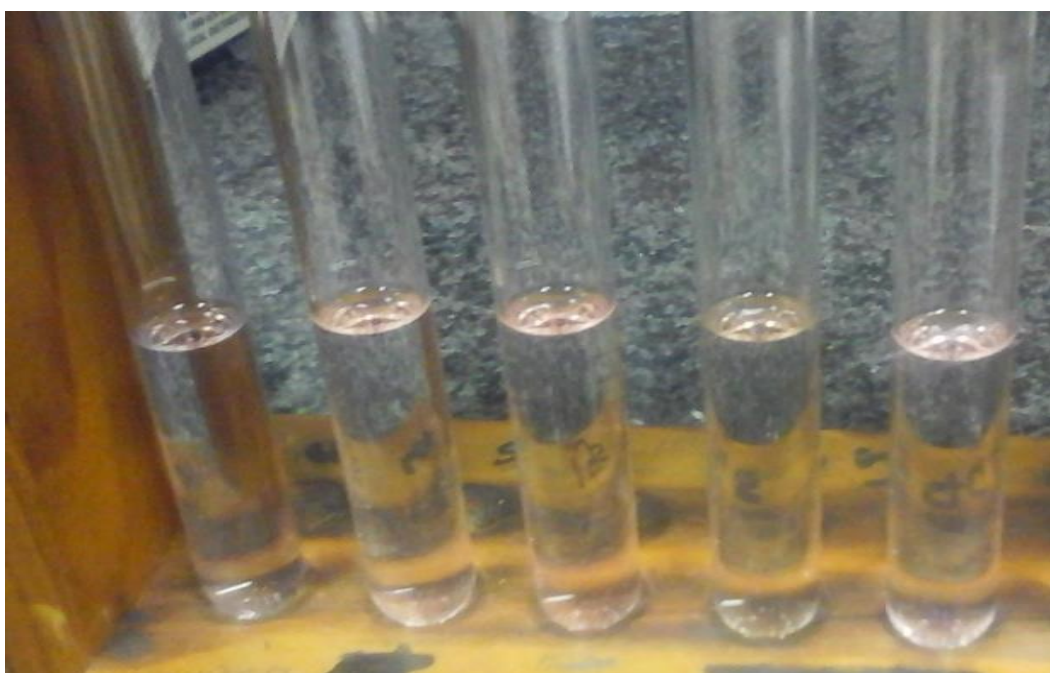


**Figure 4.43: shows different concentrations (20, 30, 40, 50, and 70  $\mu$ l) of banana rachis fibre/chitosan composite hydrolysate solutions after the addition of Ehrlich reagent**